Sensory integration through the scope of body ownership

Thesis submitted for the Degree of PhD in Cybernetics

Ioannis Dimitrios Zoulias

January 2017

Supervisory committee:
Prof. Slawomir J. Nasuto
Prof. William S. Harwin
Dr. Yoshikatsu Hayashi
Prof. Doug Saddy

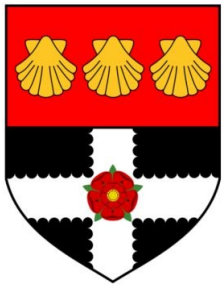

University of Reading
School of Biological Sciences

To $MW(TB)^2$

Declaration of original authorship

Declaration: I confirm that this is my own work and the use of all material from other sources has been properly and fully acknowledged.

Ioannis Dimitrios Zoulias

Contents

Nomenclature x

Abstract 1

1. Introduction 2

1.1. Overview . . . 2
1.2. Research outline . . . 3
1.2.1. Research Problem . . . 3
1.2.2. Project aim and research hypothesis . . . 4
1.2.3. Objectives . . . 5
1.3. Roadmap . . . 6

2. Sensory integration: Anatomy and mechanisms 7

2.1. Anatomy of Sensory Integration . . . 8
2.1.1. Sensory integration at the neuronal level . . . 8
2.1.2. Sensory integration at the subcortical level . . . 11
2.1.2.1. Midbrain . . . 13
2.1.2.2. Thalamus . . . 14
2.1.3. Sensory integration in the cortex . . . 15
2.1.3.1. High order association areas . . . 16
2.1.3.2. Primary sensory areas . . . 20
2.1.4. Models of sensory integration . . . 20
2.2. Measuring sensory integration I: Neural activity correlates . . . 24
2.2.1. Low level recordings: Single cell activity and local field potentials . . . 25
2.2.2. Cortical and subcortical areas: fMRI and EEG . . . 26
2.2.2.1. Functional magnetic resonance imaging . . . 26
2.2.2.2. EEG . . . 29
2.2.2.3. Brain network approaches . . . 33

2.3. Measuring sensory integration II: Behavioural and perceptional correlates . . . 34
2.3.1. Investigation for behavioural metrics through transcranial magnetic stimulation . . . 34
2.3.2. Sensory simultaneity and temporal order judgement . . . 35
2.3.3. Recalibration of senses . . . 36
2.3.4. Prior entry effect . . . 37
2.3.5. Illusions that affect perception . . . 38
2.3.5.1. Motion illusions . . . 39
2.4. Chapter conclusion . . . 42

3. The sense of self: owning and moving the body 43
3.1. The sense of self . . . 44
3.1.1. The sense of body ownership . . . 44
3.1.1.1. Embodiment and tools . . . 45
3.1.1.2. Illusory ownership . . . 46
3.1.2. Agency of motion . . . 48
3.1.2.1. Intending and imagining to move . . . 48
3.2. Neural correlates and measures of ownership . . . 49
3.2.1. Subjective and behavioural measures . . . 50
3.2.2. Neural correlates and biophysical measures . . . 53
3.2.2.1. Skin conductance response . . . 53
3.2.2.2. Brain imaging . . . 54
3.2.2.3. EEG . . . 55
3.2.3. Anatomical evidence from health conditions . . . 56
3.2.4. Models of ownership . . . 59
3.3. Manipulating body perception and SI: beyond reality . . . 62
3.3.1. Virtual reality as a platform for studying illusory ownership 62
3.3.2. Experiments on temporal stimulation incongruence . . . 64
3.4. Chapter conclusion . . . 66

4. Experimental platform and analysis tools 67
4.1. Exploration stage of platform design . . . 68
4.1.1. Scope and aims . . . 68
4.1.2. Designing the virtual avatar . . . 69
4.1.2.1. Scanning with the Kinect . . . 69
4.1.2.2. Commercially available solutions . . . 70

4.1.2.3. 3D parametric human model 70
4.1.2.4. Preparation of the model: Skeleton and insertion in a 3D environment 71
4.1.3. Presentation of avatar 73
4.1.3.1. Using Oculus Rift with EEG 74
4.1.4. Tendon vibration 75
4.1.4.1. Limitation posed by fMRI compatibility 76
4.1.4.2. Tactile stimulation systems for use inside the fMRI 77
4.1.5. Conclusions of initial platform design stage 78
4.2. Validation stage and pilot experimentation 79
4.2.1. Scope and aims 80
4.2.2. Procedure 80
4.2.3. Pilot study results 82
4.2.3.1. EEG noise due to the Rift HMD 82
4.2.3.2. Visual feedback aiding motion imagery ERD 89
4.2.4. Conclusions and next stage 90
4.3. Final experimental platform 91
4.3.1. Virtual reality: avatar, environment, and questionnaires . . . 92
4.3.2. Tactile stimulation 93
4.3.3. Biophysical measures 94
4.3.4. Minimisation of delays and device synchronisation 95
4.3.4.1. Stream synchronisation 96
4.3.4.2. Prediction of tactile cues 96
4.3.4.3. EEG delays and synchronisation 101
4.4. Chapter Summary 104

5. Threat perception under visuo-tactile stimulation 105
5.1. Aims and Hypotheses 105
5.2. Methods 106
5.2.1. Participants 106
5.2.2. Procedure 106
5.2.3. Stimuli 107
5.2.4. Data analysis 110
5.3. Results 110
5.3.1. BOI under visuo-tactile threat 110
5.3.2. Skin conductance response - measure of threat 115
5.3.3. Event related potentials - measure of threat 117

5.4. Discussion of behavioural results . . . 128
5.4.1. Multisensory threat affects ownership . . . 128
5.4.2. Questionnaires and their efficacy as measure of introspection 131
5.5. Discussion of biophysical results with respect to bodily threat and SI 131
5.5.1. SCR as a measure of threat . . . 131
5.5.2. Temporal and spatial characteristics of ERP reported threat 132
5.6. Chapter conclusion . . . 134

6. Perception of stimulus onset asynchrony and its effect on body ownership 136
6.1. Aims and Hypothesis . . . 136
6.2. Methods . . . 137
6.2.1. Participants . . . 137
6.2.2. Procedure . . . 137
6.2.3. Stimuli . . . 138
6.2.4. Data analysis . . . 142
6.3. Results . . . 142
6.3.1. Perception of visuo-tactile delays . . . 142
6.3.2. Ownership under delayed visuo-tactile cues . . . 146
6.3.2.1. Event related potentials - ownership and perception of delays . . . 150
6.4. Discussion of behavioural results . . . 154
6.4.1. Temporal order affects perception of synchrony . . . 154
6.4.2. Effect of delays on ownership . . . 155
6.4.3. Graded ownership within the philosophical framework of embodiment . . . 157
6.5. ERP as a measure of BOI . . . 159
6.6. Chapter conclusion . . . 161

7. Future experiments 163
7.1. Threat: Dissociation of empathy and bodily threat . . . 163
7.1.1. Aims and scope . . . 164
7.1.2. Procedure . . . 164
7.2. SOA outside the temporal binding window . . . 165
7.2.1. Aims and scope . . . 165
7.2.2. Procedure . . . 166
7.3. Conclusions . . . 168

8. Summary **169**

8.1. Summary of research outcomes 169

8.2. Future research avenues 171

Appendices **174**

A. Mathematical model of pneumatic vibrations 174

A.1. System model 174

A.2. Equivalent system - Boyle's law 175

A.3. Hagen - Poiseuille law 175

A.4. Compressibility correction factor 177

A.5. Energy of the air 178

A.6. Theoretical results 179

Bibliography **182**

List of Figures

2.1. Illustration of bimodal, sub-threshold and unimodal neurons 10
2.2. Illustration of the midbrain 12
2.3. The position of the thalamus within the central nervous system . . 14
2.4. Cortical areas of multisensory integration 17
2.5. Hierarchical model of sensory integration 22
2.6. A system-wide model of sensory integration 23
2.7. Possible scenarios for fMRI data indicating that an area has multisensory activity 29

3.1. Venn diagram illustrating the relationship between embodiment of tools and body ownership 45

4.1. Example of a scanned 3D human avatar - 1 72
4.2. Example of a scanned 3D human avatar - 2 72
4.3. Example of parametrically generated 3D human avatar 73
4.4. First person perspective comparison of generated avatars 74
4.5. Compatibility of the Rift HMD with simultaneous EEG recordings . 75
4.6. Pneumatic prototype for delivering vibratory stimuli in the fMRI environment 78
4.7. Experimental setup of pilot study 81
4.8. Alpha band power comparison: w/ and w/out Rift 84
4.9. Beta band power comparison: w/ and w/out Rift 85
4.10. Spectrograms during rest, and left and right arm movements for the control condition (w/out the Rift) 86
4.11. Spectrograms during rest, and left and right arm movements when wearing the Rift 87
4.12. ERD comparison between w/ and w/out the Rift 88
4.13. Spectrograms demonstrating ERD elicited by motion imagery . . . 90
4.14. Virtual reality environment and avatar created 93
4.15. Visual and tactile sensory presentation mechanisms 94

4.16. Test rig for measuring round-trip reaction time between servomotor impact and retraction . . . 97
4.17. Oscilloscope recording of circuit voltage modulated by servo impact 98
4.18. Verification of inter-stimulus delays: histograms showing visual leading and tactile leading delays . . . 100
4.19. Test rig for measuring EEG equipment delay . . . 102
4.20. EEG equipment recording delays . . . 103

5.1. Experimental setup for threat perception experiment (Experiment 1) 108
5.2. Ownership and dis-ownership, as reported in the end of block trials questions . . . 112
5.3. Reports of threat for each condition reported per trial and per block 113
5.4. Ownership (top) and dis-ownership (bottom) reports per in per trial question . . . 114
5.5. Comparison of post-stimulus SCR responce per condition . . . 116
5.6. Grand average ERP per electrode: anterior electrodes . . . 119
5.7. Grand average ERP per electrode: posterior electrodes . . . 120
5.8. Grand average ERP of all channels per condition type . . . 121
5.9. ERP component differences between the 'Hand' and 'Table' conditions 122
5.10. ERP component differences between the 'Hand & Feel' and 'Table & Feel' conditions . . . 123
5.11. ERP component differences between the 'Hand & Feel' and 'Table' conditions . . . 124
5.12. ERP component differences between the 'Table & Feel' and 'Table' conditions . . . 125
5.13. ERP component differences between the 'Hand & Feel' and 'Hand' conditions . . . 126
5.14. ERP component differences between the 'Table & Feel' and 'Hand' conditions . . . 127
5.15. Venn diagram illustrating the introduction of threat perception in embodiment . . . 128

6.1. Experimental setup for Experiment 2 . . . 139
6.2. Temporal order judgement and synchrony of stimulation . . . 144
6.3. Temporal order judgement and synchrony of stimulation II . . . 145
6.4. Ownership and dis-ownership reports . . . 148
6.5. Effect on ownership from trials with high and low perception of delays 149

6.6. Comparison of ERP data originating from a fixed-delay or random-delay block of trials 151
6.7. ERP activity comparison between trials with high and low perception of tactile delays 152
6.8. ERP activity comparison between trials where participants reported high BOI for the virtual hand versus trials with low reports of BOI 153
6.9. Venn diagram of graded ownership within the concept of embodiment 158

A.1. Schematic of the actuation system proposed to create vibration in the fMRI room. Top part is the part of the mechanism that lies outside of the shielded room and bottom part lies in the fMRI scanner. 175
A.2. Equivalent system using Boyle's law. Top left is the piston situated outside of the fMRI room. Top right shows the equivalent system when applying Boyle's law of gases. Finally bottom part of the picture illustrates the variables used for modelling. 176
A.3. Graph showing the change of the end effector vibration amplitude when using pipes of different radius. The model predicts that the greater the radius of the pipe the greater the resulting amplitude is. Pipe radius range of values is selected to reflect a realistic choice for pipes so that they can fit through the cable opening at the fMRI room wall. 179
A.4. Graph showing change of end effector amplitude with the change of input frequency of piston strokes. 180
A.5. Change of end effector amplitude as an effect of changing the length of the pipe. Pipe lengths are selected from a range of +/- 1m of the measured minimum length required to reach to the centre of the fMRI coil from the control room outside. 181

List of Tables

2.1. EEG frequency bands 32

3.1. Studies measuring the strength of BOI using questionnaires 52

4.1. Experimental design of pilot study. 82

5.1. Experiment design for Experiment 1 108
5.2. Block questionnaire for experiment 1 109
5.3. Questionnaire for experiment 1 109
5.4. Questionnaire answers 109

6.1. Experiment design for Experiment 2 140
6.2. Questionnaire for experiment 2 140
6.3. Questionnaire answers 141

7.1. Experimental design (3x4) for follow up threat experiment. 165
7.2. Experimental design (3x4) for follow up SOA experiment - Task 2. 168

Nomenclature

A1	Primary auditory cortex
BCI	Brain - Computer interface
BOI	Body ownership illusions
BOLD	Blood oxyganation level dependent
DAQ	Digital-to-analogue acquisition
DLPFC	Dorsolateral prefrontal cortex
EDA	Electrodermal activity
EEG	Electroencephalogram
ERD	Event-related desynchronisation
ERP	Event-related potential
ERS	Event-related synchronisation
ERSP	Event-related spectral perturbations
fMR-A	fMR-adaptation
fMRI	Functional magnetic resonance imaging
GSR	Galvanic skin response
HMD	Head-mounted display
IPC	Intraparietal complex
JND	Just noticable difference

LFP	Local field potential
LIP	Lateral intraparietal
LSL	Lab-streaming layer
M1	Primary motor cortex
NIRS	Near-infrared spectroscopy
NOS	Nitric oxide synthase
PET	Positron emission tomography
PFC	Prefrontal cortex
PMC	Premotor cortex
PPC	Posterior parietal cortex
PSS	Point of subjective simultaneity
RHI	Rubber hand illusion
S1	Primary somarosensory cortex
S2	Secondary somatosensory cortex
SC	Superior colliculus
SCR	Skin conductance response
SI	Sensory integration
SJ	Simultaneity judgement
SMA	Supplementary motor area
SOA	Stimulation onset asynchrony
STS	Superior temporal sulcus
TMS	Transcranial magnetic stimulation
TOJ	Temporal order judgement

TPJ	Temporo-parietal junction
V1	Primary visual cortex
VIP	Ventral intraparietal
VLPFC	Ventrolateral prefrontal cortex
VR	Virtual reality

List of Publications

1. I.D. Zoulias, Y. Hayashi, W. S. Harwin, S. J. Nasuto."Milliseconds matter: Temporal order of visuo-tactile stimulation affects the ownership of a virtual hand" Haptics: Perception, Devices, Control, and Applications: 10th International Conference, EuroHaptics 2016, London, UK, Proceedings, Part II (pp. 479–489), London: Springer International Publishing[1]. (Zoulias et al., 2016b)
2. I.D. Zoulias, Y. Hayashi, W. S. Harwin, S. J. Nasuto, "Visual Stimulation by the Oculus Rift ® HMD to detect stronger motion imagery ERD", 7th International IEEE/EMBS Conference on Neural Engineering, Montpellier, France, 2015. (Zoulias et al., 2015)
3. I.D. Zoulias, M. Wairagkar, V. Oguntosin, "Hybrid neuro-rehabilitation system using Brain Computer Interface, Virtual Reality and Soft Robotics", Eurohaptics 2016 (Zoulias et al., 2016a)
4. M. Wairagkar, I.D. Zoulias, V. Oguntosin, Y. Hayashi, S. Nasuto, "Movement Intention based Brain computer Interface for Virtual Reality and Soft Robotics Rehabilitation using novel Autocorrelation analysis of EEG", 6th International Conference on Biomedical Robotics and Biomechatronics, Singapore, 2016 (Wairagkar et al., 2016)

[1]Note: Items 1 and 2 stem from the experiments of this PhD project. Items 3 and 4 are collaborative work with M.Wairagkar and V.Oguntosin, where parts of the experimental platform developed as part of this PhD project was used.

Abstract

Sensory integration is the process by which the brain combines distinct sensory modalities, such that the merged information can be efficiently used to interact with the environment. Body ownership is an example of a subjective experience that emerges through sensory integration. The mechanisms of sensory integration are not yet fully understood. By employing illusions such as the body ownership illusion, where a person falsely perceives an artificial limb as part of their body, brain processes governing sensory integration can be investigated. In this PhD project, a virtual reality platform capable of eliciting a body ownership illusion via accurately timed visuo-tactile stimulation was developed, and used as a tool for studying sensory integration. A threat perception experiment, and an experiment inducing visuo-tactile stimulation with temporal delay were conducted using this platform. Biophysical and behavioural results from this study showed that threat perception and body ownership are not necessarily correlated, but can be viewed as parallel processes within the context of embodiment, and can be observed in distinct neural correlates of brain activity. Based on the results from these studies, it is proposed that the experience of body ownership is not an all-or-nothing, binary experience, but instead, can be considered as a graded experience and having multiple levels.

1. Introduction

1.1. Overview

The human brain receives a constant stream of sensory information originating both from the environment and from within the body. Sensory integration is the process that combines these continuous streams of information from the sensory modalities, such that the information can be efficiently used (Romo and De Lafuente, 2013). For example, the combination of visual and tactile information allows a more efficient manipulation of objects compared to using visual, or tactile sensory information alone. Although sensory integration is a profound and continuous process, finding the neural correlates and brain mechanisms that are responsible for sensory integration is a difficult task. The human brain is a complex network with an estimated 80 billion neurons and hundreds of trillions of synapses; it is a system that is constantly performing a vast number of electrochemical reactions in order to support a range of activities (Bear et al., 2001). Using brain activity recording techniques, such as functional magnetic resonance imaging (fMRI) and electroencephalograms (EEG) it is possible to capture some of the physiological parameters that are present in the brain within a single time window. Even with this simplified image of the brain's true electrochemical state, the task of identifying the regions and mechanisms of the brain involved in sens-

ory integration and excluding those areas and mechanisms not involved remains a complex and challenging endeavour.

The first step in isolating the brain activity due to sensory integration, from the non-related brain activity, is to study the sense of body ownership. Body ownership is the sense of experiencing ownership of one's limbs (Tsakiris, 2011), and is strongly coupled with sensory integration. Visual information about a limb's shape and appearance are integrated with proprioceptive information of the limb's position, and tactile information received from that limb, in order to elicit the sense of ownership over that limb (Ehrsson, 2012). By manipulating this sensory convergence, it is possible to expand the sense of ownership to include fake / artificial limbs. This is the illusion of body ownership and is a commonly used tool to study sensory integration (Botvinick and Cohen, 1998).

By developing a platform that can induce and extinguish the illusion of body ownership using visuo-tactile stimulation, while simultaneously recording brain activity and other biophysical signals, the underlying brain mechanisms of sensory integration can be studied. Examining the differences in the brain activity between the duration for which the illusion is active, and the time during which the illusion is extinguished, can provide evidence of the brain regions and cognitive mechanisms that are involved in sensory integration.

1.2. Research outline

1.2.1. Research Problem

Sensory integration is an important process that allows humans and animals to interact fluently with their environment, however, as yet the brain mechanisms that are responsible for sensory integration are not well defined. Although pre-

vious studies have employed body ownership illusions as a tool for investigating sensory integration in humans, there is no universal and objective measure of body ownership itself. Furthermore, the precise temporal and spatial characteristics of the brain mechanisms of body ownership are not thoroughly understood. Uncovering the brain mechanisms of body ownership is an important step for defining the underlying mechanism of sensory integration in humans. Identifying and understanding the neural mechanisms of sensory integration will further the understanding of health conditions such as phantom limb pain and somatoparaphrenia, and will aid the development of therapies to treat such conditions.

1.2.2. Project aim and research hypothesis

This project aims to identify temporal and spatial neural correlates of sensory integration through experiments using a body ownership illusion. In detail, this project aims to study the effect of visuo-tactile integration on the sense of illusory ownership, by measuring biophysical responses and subjective self-reports from participants experiencing illusory body ownership. Furthermore, it aims to provide the framework for an objective method of measuring the strength of an illusory body ownership.

The research hypothesis proposes that changes in the applied visuo-tactile stimulation will result in a change in the perceived strength of the body ownership illusion, and that measurable changes in the biophysical signals will correlate with the participant's perception of the illusion. Visuo-tactile stimulation congruence is hypothesised to increase the illusory ownership and the perception of threat towards the fake body. Moreover, small temporal discrepancies between the visuo-tactile stimulation are proposed to result in a gradual change in the strength of the illusory body ownership, and the observed correlated biophysical differences are proposed to identify the brain mechanism of sensory integration.

To summarise, this project aims to make a novel contribution to science by investigating the effect of small delays in the perception of body ownership, which have not been previously reported. In addition, it aims to expand previous research on the effect of stimulation on bodily threat perception by expanding the threatening stimuli from visual-only cues, to visuo-tactile. Through these contributions it aims to inform and expand existing models of body ownership and sensory integration.

1.2.3. Objectives

To achieve the project aims and to conduct studies for testing the hypothesis outlined above, it is necessary to develop an experimental platform able to elicit body ownership and simultaneously record brain activity. To this effect, this project can be broken down into stages addressing the following objectives:

- To create tools that deliver appropriate visual and tactile stimuli with high accuracy of the visuo-tactile inter-stimulus delays.
- To develop a virtual reality platform that is capable of eliciting a body ownership illusion, and merges the visuo-tactile stimulation tools with EEG recording, other biophysical signals, and subjective self-reports from participants.
- To design and conduct experiments using the novel VR platform and to test the research hypotheses.
- To analyse the experimental data within the context of existing models of body ownership and sensory integration mechanisms.

1.3. Roadmap

Chapter 2 provides a detailed introduction on the anatomical and functional correlates of sensory integration. In Chapter 3, the research on the sense of body ownership is reviewed, along with the current experimental platforms employed for body ownership illusions. Chapter 4 describes the virtual reality platform developed, and outlines the methods and procedures throughout all design stages, to the final platform created. Chapter 5 presents and discusses the experiment on threat perception and its relation to SI, through behavioural results and biophysical data. Chapter 6 describes the second experiments which focused on the timing element of the BOI through small temporal discrepancies in visuo-tactile feedback. In Chapter 7 a plan of follow-up experiments is detailed, drawing from the discussion of the experimental outcomes. To conclude, Chapter 8 summarises the work of this project and discusses possible future directions from the research finding presented herein.

2. Sensory integration: Anatomy and mechanisms

The physical world is an environment rich in sensory cues. To process information and perform actions, animals and humans must utilise an array of senses to perceive multiple environmental stimuli. Sensory integration (SI) is the cognitive process of combining signals from different sensory modalities to allow a fluid interaction with the external world. In addition, the combination of multiple sensory streams leads to high-level cognitive behaviours such as the perception of one's self (covered in detail in Chapter 3) Blanke (2012); Ehrsson et al. (2005a).

This chapter introduces both the underlying brain mechanisms, and the cognitive processes, of sensory integration. The chapter starts by reviewing the anatomical structures responsible for integrating the senses, ranging from the single neuron to system-wide networks, and outlines the brain regions and the neural activity correlates identified as playing a significant role in SI. The experimental techniques used to measure and identify neural signatures for SI are reviewed. The interplay between the sensory modalities, and the effects of temporal delays between the sensory streams on the perception of the senses are examined. To conclude, this chapter introduces the use of illusions as a tool for studying SI mechanisms.

2.1. Anatomy of Sensory Integration

This section discusses the evidence and theories on how sensory integration is achieved in the human brain, starting at the lowest level, i.e. the single neuronal activation, and moving through to the highest level, i.e. brain-wide networks of activity and large-scale, multi-cortical interactions (Cappe et al., 2012; Clemo et al., 2012; Ghazanfar and Schroeder, 2006; Klemen and Chambers, 2012). It provides an overview of the anatomical structures upon which theories and models of how SI is achieved in the human brain are based.

2.1.1. Sensory integration at the neuronal level

At the lowest level of sensory interaction lies the single neuron. A neuron that produces an action potential when stimulated by input from only one sensory modality is a unimodal neuron. Therefore, a multimodal neuron (e.g. bimodal or trimodal) is a neuron that produces an action potential upon receiving stimulatory input from any one sensory modality, from a given group of sensory modalities. For example, an auditory-visual bimodal neuron will fire if either a visual or an auditory input is received. Bimodal neurons are extensively studied for their sensory integration properties (Horn and Hill, 1966; Meredith and Stein, 1986; Wallace and Stein, 1997) and their presence is a classifying feature that identifies a brain region as a centre of SI (Clemo et al., 2012; Klemen and Chambers, 2012; Stein and Stanford, 2008; Wallace, 2004). Recent studies by Allman et al. (2009); Carriere et al. (2007); Kayser et al. (2008); Lakatos et al. (2007) have characterised new types of neurons with presynaptic input from sensory sources of multiple modalities. These unimodal neurons do not exhibit strictly multimodal behaviour; instead, these 'sub-threshold neurons' have their activity (e.g. mean spiking) modulated when stimulated by two modalities simultaneously (see Angelaki et al.

(2009); Clemo et al. (2012); Klemen and Chambers (2012); Stevenson et al. (2014) for review).

Furthermore, Allman et al. (2008) have shown that some populations of sub-threshold neurons exhibit unimodal behaviour until their inhibitory GABA receptors are chemically knocked out, at which point these neuronal populations exhibit bimodal behaviour. These results suggest a more subtle mode of multisensory integration in neurons, with a spectrum of behaviours from unimodal to multimodal, and with a wide range of configurations depending on the additive strengths of the sensory modalities providing input to a single neuron (see Figure 2.1) (Angelaki et al., 2009; Clemo et al., 2012; Stein and Stanford, 2008; Stevenson et al., 2014). Studies have shown that bimodal neurons found in different brain regions have different properties (Clemo et al., 2012; Klemen and Chambers, 2012; Stein and Stanford, 2008), further supporting the theory that SI at the neuronal level has a variety of strengths that cannot be explained by the traditional classification into unimodal, bimodal and n-modal neurons.

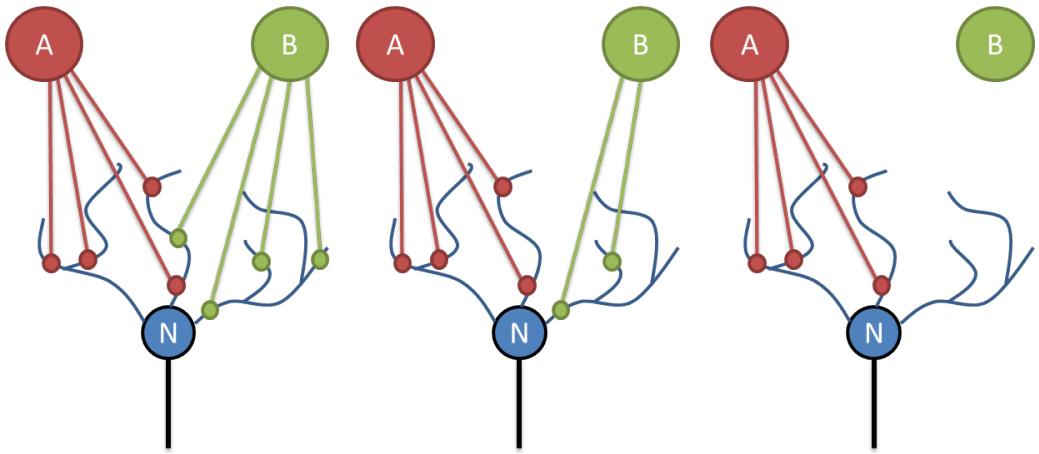

Figure 2.1.: *Illustration of bimodal, sub-threshold and unimodal neurons (N): (left) A bimodal neuron fires when receiving input from sensory modality A or B, (centre) A sub-threshold neuron will not fire when receiving input from B only, however, input from B facilitates firing when simultaneous with input from A. (right) A uni-sensory neuron only fires when receiving input from sensory modality A, and inputs from B have no effect on firing. Figure adapted from Allman et al. (2009); Clemo et al. (2012).*

2.1.2. Sensory integration at the subcortical level

Having explained the contribution of individual neurons to sensory integration, the next step for investigating the anatomy of SI is to define brain regions that process multiple sensory modalities. In the subcortical structures this is achieved by identifying the regions receiving input from multiple cortical areas responsible for a given set of sensory modalities (Cappe et al., 2012; Stevenson et al., 2014; Wallace, 2004). Additionally, a brain area populated by multimodal neurons can be inherently defined as a multisensory area. Using techniques such as electrophysiological recordings and anatomical traces of neurons, the neuronal composition of brain areas can be characterised. Thus, by characterising a brain region's composition of unimodal, bimodal and/or other neurons, and its input and output signalling pathways between sensory processing brain regions, multisensory centres can be identified (Cappe et al., 2010). The following paragraphs review the integrative roles of structures within the midbrain and the thalamus, concentrating on sub-cortical multisensory areas.

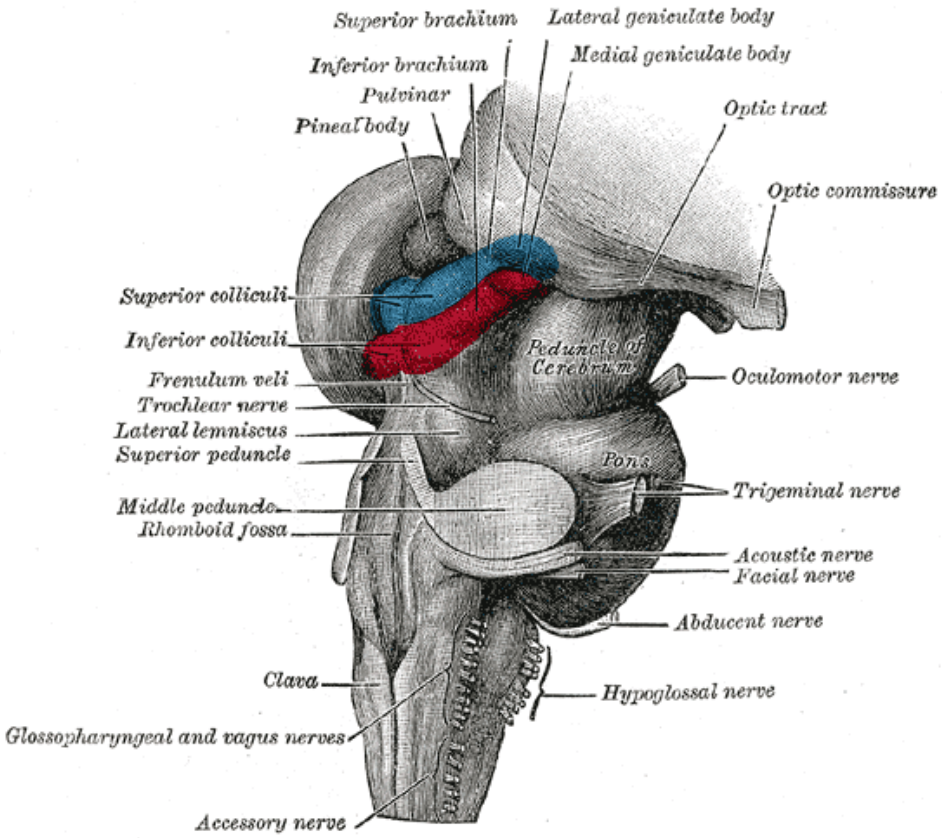

Figure 2.2.: *Illustration of the midbrain. The superior colliculus is highlighted in blue. Image reproduced from Gray (1918).*

2.1.2.1. Midbrain

A prominent subcortical area identified for its multisensory architecture is the midbrain (see Figure 2.2). The midbrain comprises a majority of multimodal neurons, at 63% of its total neuronal population (Wallace and Stein, 1997). Within the dorsal midbrain lies the superior colliculus (SC, see Figure 2.2), an area widely investigated for its multisensory properties (Wallace, 2004; Wallace and Stein, 1997). The SC is composed of two types of neurons that have been shown to activate in a multimodal fashion: i) large tectospinal and tectoreticulospinal neurons, and ii) nitric oxide synthase (NOS)-positive interneurons (Fuentes-Santamaria et al., 2008; Meredith and Stein, 1986). Both types of neurons receive input from visual and auditory modalities, and the tectospinal and tectoreticulospinal neurons also receive somatosensory input. Input in the SC is spatially mapped into receptive fields, and the spatial characteristics are shared between modalities. An auditory and a visual cue that are produced at the same spatial location generate input at the same region within the SC. Given this neural organisation, the sensory integration functions of the SC are proposed to be the enhancement of signals from sensory cues co-located in space, and the downregulation of the response when sensory cues are spatially separated (Clemo et al., 2012; Holmes and Spence, 2005; Klemen and Chambers, 2012; Miller, 2005; Stein and Stanford, 2008). A temporal element comes into play when activity from different modalities arrives in the SC and affects the strength of the response. Signals arriving within a small time window result in a stronger output compared to signals arriving with a longer delay between them (Felch et al., 2016; Meredith et al., 1987). An important feature of the SC is that it can update the mapping of sensory inputs to reflect the ocular position, in order to compensate for the movement of individual sensory organs (Jay and Sparks, 1984). That is, the function of the SC in multisensory processing

is the coordination of movement between the auditory and visual organs and the head, to aid the gaze tracking of an object moving within the visual field.

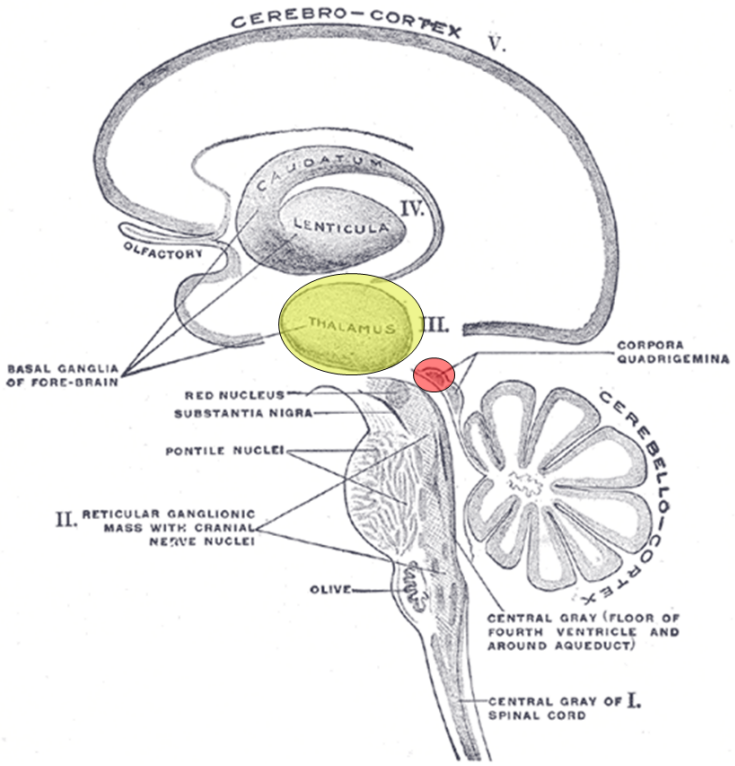

Figure 2.3.: *The position of the thalamus within the central nervous system (marked with the yellow region). The SC is also visible (superior part of the corpora quatrigemina, marked in red region). Image adapted from Gray (1918).*

2.1.2.2. Thalamus

The thalamus lies directly superior to the midbrain (see Figure 2.3) and has been highlighted as an important centre of multisensory integration (Briggs and Usrey, 2008; Cappe et al., 2009,1; Cudeiro and Sillito, 2006). Traditionally the thalamus was considered a relay of sensory neural signals, with almost all cortical areas receiving sensory input via the thalamus (Alitto and Usrey, 2003), however recent studies have discovered evidence of multisensory processing within the thalamic region (Cappe et al., 2009; Henschke et al., 2015). In a 2009 study, Cappe et al. (2009) demonstrated that connections originating from distinct cortical regions

converge onto thalamic neuronal populations. The study identified thalamic regions of the macaque monkey that comprised feed-forward and feedback thalomocortical and corticothalamic projections to somatosensory, auditory, and premotor areas. As a result of this landmark finding the thalamus is now considered an early multimodal integrator, with four theories as to how this sensory integration might be accomplished:

1. The thalamus relays sensory information to cortical areas, resulting in cross-modal temporal binding with the sensory information arriving to the cortex from other brain areas.
2. The thalamus locally processes the sensory information and relays the multimodal outcome to the cortex.
3. The thalamus locally processes sensory information for each modality, and then projects these information streams forwards to converge onto distinct sensory cortical regions, where they undergo multisensory integration.
4. The thalamus acts as an intra-cortical messenger; cortico-thalamo-cortical connections are an alternative medium to cortico-cortical connections for rapid and secure communication (Henschke et al., 2015).

2.1.3. Sensory integration in the cortex

The cerebral cortex is abundant with brain regions receiving and responding to multisensory input. The extent of multisensory processing areas in the neo-cortex is such that researchers in neuroscience have considered the hypothesis that the whole structure is inherently multisensory (Ghazanfar and Schroeder, 2006; Stein and Stanford, 2008). The multisensory processing areas in the cortex can be roughly divided into two categories: high order multisensory association areas and primary sensory areas.

2.1.3.1. High order association areas

Applying the above criteria for identifying multisensory brain regions (see Section 2.1.2), several cortical areas can be classified as multisensory. The superior temporal sulcus (STS), the intraparietal complex (IPC), and the prefrontal and premotor cortices (PFC and PMC, respectively) are regarded as critical centres for multisensory processing (see Figure 2.4, regions marked in red) (Clemo et al., 2012; Ghazanfar and Schroeder, 2006; Klemen and Chambers, 2012).

Superior temporal sulcus The STS area of the temporal lobe receives input from audio-visual modalities and is believed to play an essential role in the perception of speech by integrating audio-visual cues (Ghazanfar, 2009). The STS activates during the integration of visual, auditory, and somatosensory stimulation (Beauchamp et al., 2008), and also in cases in which the visual stimulation is only imagined (Berger and Ehrsson, 2014). The STS is known to amplify its response to temporally synchronous audio-visual cues, but exhibit a reduced activation in asynchronous conditions. However, in the macaque monkey, the STS comprises a much higher percentage of multimodal neurons rostrally (approx 36-38%) versus caudally (approx 12%) suggesting the STS is segmented into functionally distinct sub-areas, only some of which are multisensory (Ghazanfar and Schroeder, 2006; Klemen and Chambers, 2012). Due to its large size and structural inhomogeneity, the role and function of the STS in SI may vary depending on the sub-area activated, thus the functional parameters of that sub-area must be considered when analysing the experimental results generated from this region.

Intraparietal complex The intraparietal complex (IPC) located in the posterior parietal cortex (PPC), comprises multisensory areas including the ventral and lateral intraparietal areas (VIP and LIP, respectively) and the temporo-parietal

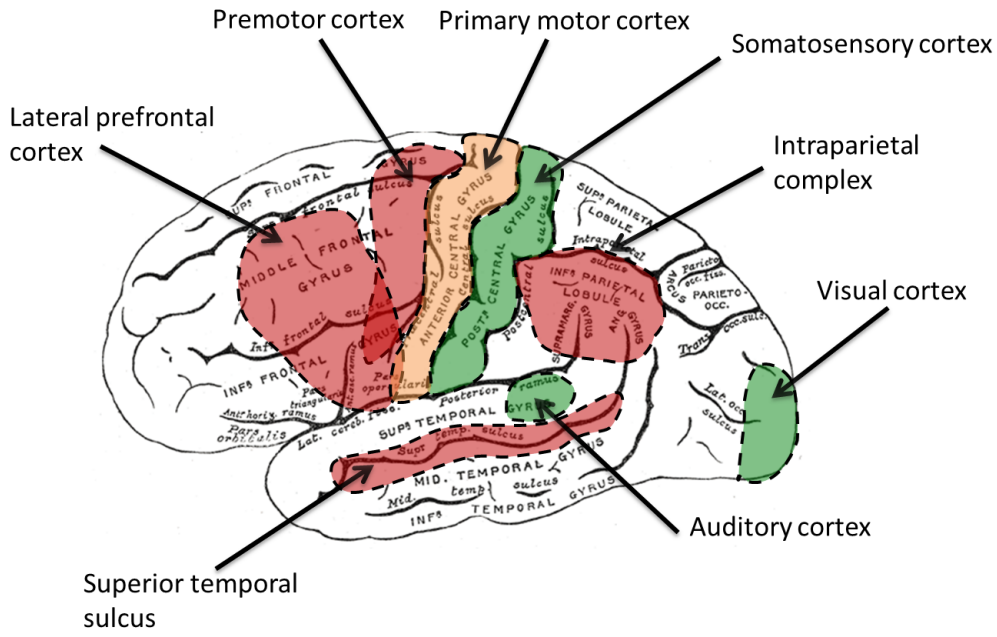

Figure 2.4.: *Cortical areas of multisensory integration. Green areas are low level sensory cortical areas, red areas are high-order multisensory centres, and the orange area is the primary motor cortex. Image adapted from Ghazanfar and Schroeder (2006); Gray (1918); Klemen and Chambers (2012).*

junction (TPJ). The IPC is proposed to integrate sensory information for the facilitation of multisensory-guided movements (Cappe et al., 2012; Ghazanfar and Schroeder, 2006). The VIP and LIP areas are responsible for hand and eye movement control, and exhibit task-specific response strengths (Cappe et al., 2012). Their role in multisensory integration is supported by anatomical and functional evidence: the VIP neurons respond to visual, auditory, tactile and vestibular stimulation, whereas the LIP area receives input encoding eye position, auditory and visual stimulation. The TPJ lies at the intersection between the temporal and parietal cortices, and is believed to play a role in head orientation (Ghazanfar and Schroeder, 2006). In addition to multisensory-guided motion, the intraparietal complex has been linked to cross-modal integration of speech in human functional connectivity studies (Miller, 2005), and more recently, to bodily self consciousness (Apps et al., 2015; Ionta et al., 2014) and motor intention (Desmurget and Sirigu, 2012).

Premotor cortex The motor cortex comprises three main areas: the primary motor cortex (M1), the supplementary motor area (SMA), and the premotor cortex (PMC). The motor cortex is involved in the precise planning and execution of motion, relying on a somatotropic representation of the body parts (Graziano and Aflalo, 2007; Meier et al., 2008) and complex network dynamics to drive the motor response (Graziano, 2011). Of these three areas, the PMC is highly multisensory; it receives auditory, visual, and somatosensory input from the cortex. Neurons in the PMC exhibit a rare trait in multisensory integration: PMC neurons produce a comparable output when stimulated by input from the same action, regardless of the reporting sensory modality. That is, any action irrespective of whether it is observed, performed, or heard, will produce an equivalent neuronal output within the PMC (Keysers et al., 2003). This supramodal multisensory feature of the PMC may explain the area's role in conscious behaviour (Romo and De Lafuente,

2013). Co-activation of the PMC and the parietal LIP area has been linked with a person's awareness of movement intention (Desmurget, 2013; Desmurget and Sirigu, 2009). It is important to note that the activation of the PMC by visual and auditory stimuli is elicited only when the source stimulus is located near the body (Brozzoli et al., 2011). Although the exact function of the PMC is not yet fully understood, the integrative qualities of this brain area provide a platform for studying SI from the perspective of the wider network dynamic interactions and state space trajectories (Graziano, 2011).

Prefrontal cortex The prefrontal cortex (PFC) is the brain area directly anterior to the PMC, in the anterior frontal lobe. The PFC is associated with many high-order behavioural functions, and the lateral PFC (see Figure 2.4) is of particular interest for SI research (Cappe et al., 2012). The lateral PFC is divided into the ventrolateral and the dorsolateral PFC (VLPFC and DLPFC, respectively) (Fuster, 2001). The VLPFC and the DLPFC receive input from a range of sensory modalities (auditory, visual, and somatosensory), in addition to receiving input from other multisensory areas, including the STS (Fuster et al., 2000; Romanski et al., 1999). In the VLPFC, auditory related functions are dominant (Sugihara et al., 2006). Tasks integrating auditory-visual information such as communication, natural language recognition, and working memory perceptual processing are the responsibility of the VLPFC (Romanski, 2007). The DLPFC is predominantly a coordinator of multiple sensory modalities (Klemen and Chambers, 2012), and activity in this area is associated with task performance during the division/switching of attention in response to multimodal stimulation (Johnson and Zatorre, 2005,0).

2.1.3.2. Primary sensory areas

The primary sensory areas, such as the primary visual cortex, the primary auditory cortex, and the primary somatosensory cortex (V1, A1, and S1, respectively, see Figure 2.4, regions in green) were traditionally considered exclusively unisensory (Mesulam, 1998). However, over the last decade, neuroanatomical, electrophysiological, and behavioural studies have provided evidence that sensory integration from multiple modalities occurs within the primary sensory areas (Cappe et al., 2012; Ghazanfar and Schroeder, 2006; Klemen and Chambers, 2012; Stein and Stanford, 2008). For example, A1 is activated by visual, somatosensory, proprioceptive and motor modalities during specific tasks of vocal communication (Ghazanfar, 2009; Lakatos et al., 2007). Electrophysiological studies in humans have shown that A1 is involved in the very early convergence (<50 ms) of audio-visual multisensory interactions (Cappe et al., 2010; Giard and Peronnet, 1999). These studies provide important evidence for independent multisensory processing in the A1, before the stimulation can be transmitted to, and processed by, the high-order association areas. Evidence of neuroanatomical connections converging in S1 and V1, and originating from the other primary sensory areas strengthens the hypothesis that early sensory integration occurs in the primary cortices (Ghazanfar and Schroeder, 2006).

2.1.4. Models of sensory integration

Having identified many of the brain regions activated during integration of sensory modalities, the next step is to identify the model that defines how the brain systematically resolves SI. In other words, how do environmental unisensory stimuli converge to form an integrated information stream, encoding the perception of the environment and enabling seamless motion? In the traditional view, a hierarchical

model is constructed based on the anatomical connections between different cortical regions, and the view that the primary sensory areas are unimodal in nature (Mesulam, 1998). In this model (see Figure 2.5), the primary sensory areas are at the bottom of the hierarchy, processing information from the relevant sensory modality and feeding that information into the high-order association areas. From there, the integrated information is sent to the motor cortex for planning the movement in light of the integrated sensory stream.

Multiple studies have uncovered evidence that cannot be explained by this hierarchical model. For example, the hierarchical model does not explain the purpose of cortical connections between the primary sensory areas (Cappe et al., 2012), nor the early multisensory activity found in the primary sensory areas before the sensory information has reached the high-order association areas (Cappe et al., 2010; Giard and Peronnet, 1999; Stein and Stanford, 2008). Additionally, well documented sensory integration mechanisms outside of the neocortex, such as SI processes in the SC and the thalamus, are not included in the hierarchical model. In contrast to this hierarchical model where information converges at the top level, the current view of the mechanisms of SI is one of brain-wide interconnected networks. Integration processes occur across many brain regions, and modulation of SI processes can occur in a downstream (e.g. from high-order association areas to lower cortical areas), upstream (e.g. from sub-cortical to cortical areas), and lateral fashion (e.g. between the primary sensory areas) (Cappe et al., 2012; Ghazanfar and Schroeder, 2006; Klemen and Chambers, 2012; Stein and Stanford, 2008). Figure 2.6 outlines the complex interactions between the brain regions examined in this subsection, and indicates that much of the brain engages in SI processes. Cortical oscillations, which have been studied for their role in conscious processes (Cheyne and Ferrari, 2013; Siegel et al., 2012), are proposed as the communication

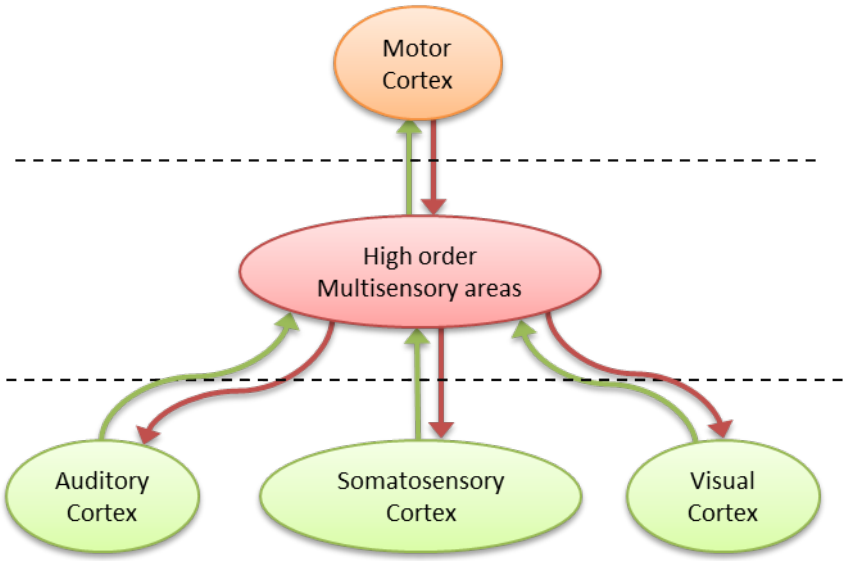

Figure 2.5.: *Hierarchical model of sensory integration. In this model, the low-level primary sensory areas process unisensory streams, that are then fed to high-order multisensory areas for integration. In the motor cortex, the integrated infromation is applied to the generation of movement output. Figure adapted from Cappe et al. (2012); Klemen and Chambers (2012).*

protocol within this complex network of brain regions (Kaiser and Naumer, 2010; Lakatos et al., 2007; Romo and De Lafuente, 2013; Senkowski et al., 2008).

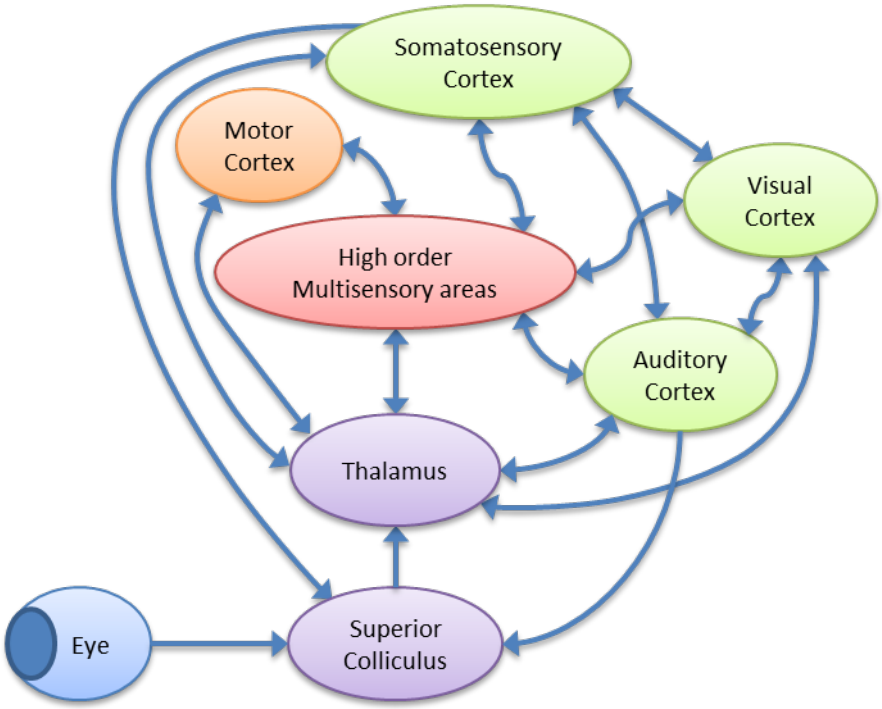

Figure 2.6.: *A system-wide model of sensory integration. This model includes the cortical connections between the primary motor cortices and some of the sub-cortical regions involved in SI processes. In contrast to the hierarchical model, integration is not a result of a converging system, instead it is derived by network-wide processes and lateral connections across multiple brain regions. This model is based on the current views of SI mechanisms Clemo et al. (2012); Ghazanfar and Schroeder (2006); Klemen and Chambers (2012), however, it does not contain all of the brain-regions, and their connections, that have been identified or hypothesised to play a role in SI. Nevertheless, network-wide models such as this one represent the paradigm shift to viewing SI as a synergetic process across brain regions, encoding mechanisms, and timescales.*

Despite these recent breakthroughs and the paradigm shift to regarding SI as a system-wide process, there are still many challenges to overcome before the exact mechanisms of SI are fully understood. First, the role of the primary sensory areas in sensory integration is poorly defined; contradictory to the evidence for SI in the primary sensory areas, lesions or electrical stimulations in these areas produce simple and exclusively unimodal sensory behaviours. This contrasts with

the more complex multimodal behaviours observed under similar conditions in the high-order multisensory areas (Stein and Stanford, 2008). Second, the brain mechanisms that encode the sensory information are still largely unknown, and the map of interconnected brain regions does not uncover the signal processing methods employed by the brain for unifying sensory streams. Furthermore, there is no standardised definition for multisensory areas, and there are no universal criteria that can be applied across brain region, for defining an area as multisensory (Ghazanfar and Schroeder, 2006). Any brain-wide model of SI is inherently incomplete without addressing the definition of multisensory areas, and it is unclear what brain regions and processes to include in the model without a precise definition. In addition, due to the temporal and spatial limitations of brain imaging devices, signals that indicate SI activity within a brain region could be originating from small-scale unisensory architectures within that brain region (see Figure 2.7) (Klemen and Chambers, 2012).

2.2. Measuring sensory integration I: Neural activity correlates

The brain regions involved in multisensory processing were identified in Section 2.1, however, simply identifying these neural architectures and the connections between them is insufficient for a complete model of SI. In order to fully understand the distinct mechanisms underlying SI, it is necessary to uncover the signalling protocols that encode sensory information (Ghazanfar and Schroeder, 2006). This subsection reviews the methods for determining neural correlates of multisensory processing by measuring brain activity.

2.2.1. Low level recordings: Single cell activity and local field potentials

Perhaps the most well-defined multisensory processes are those governing single-cell sensory integration. Single unit recordings using patch clamps have enabled the recording of the cell membrane electrical potential. This technique has allowed the study of SI at the single cell level (Meredith et al., 1987; Meredith and Stein, 1986). As outlined in Section 2.1.1, a single multimodal neuron fires when it receives stimulation from one modality from a given set of sensory modalities. Additionally, in the case of subthresholding, a neuron can have its output modulated by concurrent input from a non-dominant modality. This modality-dependent spiking activity is used as the low-level neural correlate for SI (Clemo et al., 2012).

Moving the focus from single neuron recordings to higher spatial resolutions, local field potentials (LFP) refer to activity measured from within a small neuronal population. An LFP is the aggregated voltage fluctuation resulting from the neuronal synaptic activity neighbouring the recording electrode (Sharott, 2013), and is used in conjunction with single-cell recordings to provide evidence for subthreshold neurons (Stevenson et al., 2014). LFPs are very sensitive to electrode positions, and can often record activity originating in distant brain areas (Kajikawa and Schroeder, 2011). To address this issue, multisensory studies employing LFP, such as those by Lakatos et al., on somatosensory processing in A1 (Lakatos et al., 2007), employ multi-site recording electrodes and the spatial derivative of the signal to estimate the current flow (Einevoll et al., 2013). Current-source estimation techniques minimise external influences from remote brain regions such that multisensory activity can be correctly separated from activity originating in disparate sensory regions.

2.2.2. Cortical and subcortical areas: fMRI and EEG

Single cell and LFP recordings fail to capture the system-wide processes of spatially distinct brain areas involved in SI. Owing to their invasive nature they are mostly used for *in-vivo* (animal) or *in-vitro* (cell) studies, both of which provide limited insight into human SI processes. To understand the brain-wide processes of SI in the human brain, non-invasive and large-scale recording techniques must be employed to complement the results of low level recordings. In the following paragraphs, brain-wide recording techniques and studies applying these methods are reviewed.

2.2.2.1. Functional magnetic resonance imaging

Functional magnetic resonance imaging (fMRI) is a technique that uses variations in strong magnetic fields to record the blood oxygenated level dependent (BOLD) signal in brain regions (Ogawa et al., 1990). fMRI features a high spatial resolution, but has limited temporal resolution. Typically a whole-brain snapshot every 1-2 seconds captures BOLD signal with a resolution of tens to hundreds of thousands of neurons (Stevenson et al., 2014). Commonly, fMRI data is analysed in an event based manner: a stimulation event defines the type of the trial, and pre- and post-stimulation activities are compared, along with comparison of activity between different types of events (Friston et al., 1998). A study by Miller (2005) of SI in speech perception is an example of applying fMRI for investigation of multisensory processes. In this study, the event was the onset of a visual stimulation of a person's mouth, alongside an auditory stimulus produced by that movement. The trials were divided into those which presented the two stimuli synchronously, and those that had a delay between the visual and auditory stimulus onsets (asynchronously). By comparing activity between synchronous and asynchronous trials, the researchers identified three areas (SC, anterior IPS, insula) that were sensitive

to the stimulation offset. Furthermore, by comparing activity from trials in which participants noticed the delay against those trials in which participants perceived the stimuli as synchronous (did not notice a delay), the brain regions responsible for the perceptual fusion of the senses were characterised (middle STS, middle IPS, Heschl's gyrus, inferior frontal gyrus).

fMRI has been used to provide neural activity evidence for defining areas as multisensory (Beauchamp et al., 2008; Klemen and Chambers, 2012; Stevenson et al., 2014). In this type of experiment, activity from a brain region is recorded during unisensory stimulation only, and during multisensory stimulation. For example, an fMRI experiment for audiovisual processing would be composed of three types of trials: auditory only, visual only, and audiovisual stimulation. The post-stimulus data can be analysed for multisensory processing using two criteria; the additive criterion and the maximum criterion (Stevenson et al., 2014). To fulfil the additive criterion, the sum of the activity from a multisensory trial must exceed the sum of activity from the unisensory trials. Applying the earlier example, the audiovisual activity should surpass the sum of the visual only and auditory only activity. However, this superadditive effect has only been shown in a handful of fMRI studies, due to the large, in-homogeneous neural populations recorded with fMRI (Stevenson et al., 2014). The maximum criterion can be fulfilled if the activity during the multisensory stimulation is greater than the maximum generated activity from any single modality trial. To illustrate this using the previous example, if neither the visual only nor the auditory only stimulation activities were larger than the audiovisual activity, then the maximum criterion would be fulfilled. The maximum criterion is less stringent than the additive criterion, producing weaker evidence of SI in a brain region (Angelaki et al., 2009; Beauchamp, 2005; Stevenson et al., 2014).

The additive criterion and maximum criterion are not the only tools for investigating SI using fMRI data. Another notable technique is fMR-adaptation (fMR-A) which uses neural adaptation to target specific neurons, rather than relying on a region's average activity (Grill-Spector and Malach, 2001). When neurons are constantly stimulated by an event the subsequent BOLD activity decreases; if a repeated stimulation generates stimulation specific activity within a neuronal population, the BOLD signal would decrease over time. Conversely, if no adaptation is reported, this is evidence that this area is not responding to the stimulus (Grill-Spector, 2006). Brozzoli et al., used fMR-A to show the role of the premotor cortex in near body space coding. They demonstrated that premotor neurons would adapt upon visual stimulation by a moving object located near the subject's hand, where the subject could see their hand. However, no adaptation was observed when the object providing visual stimulation was either at a distance from the body, or where the subject could not see their hand. This study provides evidence that the PMC is involved in peri-personal space coding (Brozzoli et al., 2011).

Although fMRI studies are becoming widespread for unravelling SI mechanisms, the limitations of the technique such as its low temporal resolution and the assumptions of the analysis models must be considered when discussing any evidence brought forward by fMRI data (Stevenson et al., 2014). As mentioned in Section 2.1.4, fMRI data cannot provide definitive answers on a brain region's composition of supramodal or multimodal neurons; the same results can be produced by a population of supramodal neurons, an inhomogeneous population of unimodal neurons, or by homogeneous unisensory sub-populations within the recorded region (see Figure 2.7) (Klemen and Chambers, 2012).

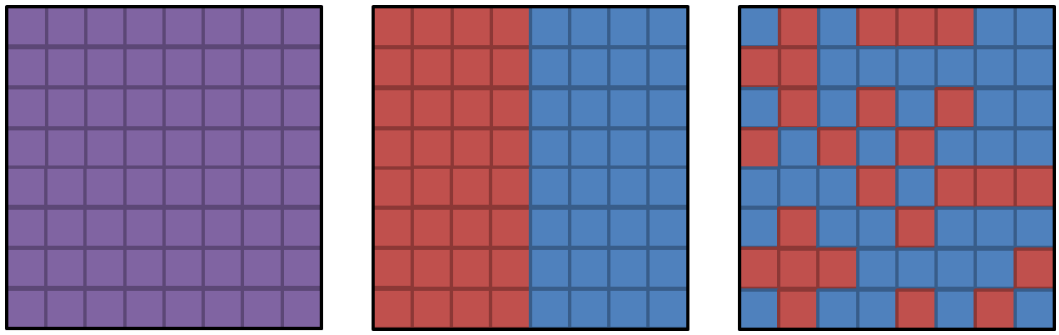

Figure 2.7.: *Possible scenarios for fMRI data indicating that an area has multisensory activity: (left) The area is uniformly composed of multisensory neurons; (centre) The area is at the junction of two distinct unisensory processing areas (red and blue), which are outside of the spatial resolution of the fMRI; (right) The area inhomogeneously comprises unisensory neuronal populations (red and blue) (Klemen and Chambers, 2012).*

2.2.2.2. EEG

The electroencephalogram (EEG) is a non-invasive recording technique that detects the oscillations of electrical activity generated by millions of neurons as electrical potentials travel outwards towards the scalp (Buzsaki et al., 2012; Nunez, 1974). The recorded EEG signal has a high temporal resolution with EEG devices having a sampling rate ranging from 500Hz to 5kHz, however, the scalp electrodes afford a low spatial resolution with typical recordings using 32 to 128 electrodes to cover the entire scalp. Additionally, EEG has a limited ability to report activity originating from deep brain regions.

The event-related potential (ERP) is one of the predominant analysis techniques of EEG data for SI investigation (Stevenson et al., 2014). ERP refers to a time-locked change in the recorded scalp potential due to a specific event/stimulus. By averaging multiple trials, positive or negative peaks are observed at a specific temporal delay post-stimulation (Luck, 2014; Sutton et al., 1965). Within the context of SI, evidence for early engagement of low-level cortical regions in multisensory processing is provided by ERP studies (Ghazanfar and Schroeder, 2006). Using ERP, Giard and Peronnet (1999) reported that activity from the auditory cortex

was sensitive to audiovisual processing. In this object detection experiment, two audiovisual objects were presented to the participants. Each object had a defining visual shape and auditory note, and the participants were instructed to identify the type of object for each presentation. In each trial the object could be presented visually, aurally, or both visually and aurally simultaneously. Applying the additive criterion for SI to the amplitude of the ERP, the study found that ERP activities located above the auditory cortex at approximately 90ms post-stimulus were significantly different between unisensory and multisensory presentation of the objects. These results suggested that this early activity marks the integrative role of low-level sensory cortical areas, and shifted SI theory towards a system-wide process perspective (Ghazanfar and Schroeder, 2006; Klemen and Chambers, 2012; Stevenson et al., 2014).

Audio-visual sensory convergence is the subject of a number of ERP-based studies: Stekelenburg and Vroomen (2007) showed the speeding up of neural activity due to ecologically valid audio-visual processing, while Cappe et al. (2010) used an audio-visual paradigm to establish ERP as a research tool for multisensory processing. In a recent study,González-Franco et al. (2014), showed how changes in ERP consistent with pain perception (Fan and Han, 2008) could objectively measure body ownership, a cognitive process linked with multisensory integration. ERP has widespread applications for investigating sensory processing, including evaluating the visual processing speed of natural scenes (Fabre-Thorpe et al., 2001), uncovering visuo-tactile effects in somatosensory processing (Press et al., 2008), and studying the mechanisms of the intention and awareness of body motions (Gentsch et al., 2012; Rigoni et al., 2013).

Despite its usefulness as an experimental tool, ERP analysis has a number of limitations. When using ERP there is a strong assumption that the neuronal response is time-fixed to the stimulating event (Pfurtscheller and Lopes da Silva, 1999),

however, ERP activity is not stable across trials and neural activity unrelated to the sensory integration task (e.g. motor activity, background cognitive tasks) is present within the signal (Stevenson et al., 2014). In addition, this background activity may be affected by the stimulation event itself (Makeig, 1993). This is especially problematic when using the additive criterion with ERP analysis: activity that is unrelated to sensory processing is added twice, once for each of the unisensory trials, but once in total for the multisensory trials (Stevenson et al., 2014). Hence, although ERP is an important method for evaluating SI activity, it has limited ability to characterise the extent of the integrative processes captured (Makeig, 1993).

Due to its high sampling frequency, EEG data are often divided into frequency bands (see Table 2.1). A different method for analysing the EEG signal takes into account the spectral development of the signal over time. Initially proposed by Pfurtscheller (1977), this method measures the change in the amplitude of spectral power for a specific range of EEG frequencies surrounding a stimulation event. The changes in the power spectrum amplitude in relation to the synchronisation (increase in amplitude) or desynchronisation (decline in amplitude) of the underlying neuronal population activity, are termed event-related synchronisation (ERS), and event-related desynchronisation (ERD), respectively (Pfurtscheller and Lopes da Silva, 1999). The ERS/ERD techniques require the specification of a narrow band of frequencies of interest. In the original article describing ERD, Pfürtscheller showed ERD in alpha power during an eyes-closed task. ERS/ERD of specific frequency bands underlie different cognitive processes, with recent studies showing that activity at the upper end of the gamma band is correlated with distinct brain mechanisms (Cheyne and Ferrari, 2013; Darvas et al., 2010). To address this process specific activity, an expansion of the ERS/ERD method is used: the event-related spectral perturbation (ERSP) method covers the entire range of EEG fre-

quency band powers from mu to high gamma, thus offering a higher dimensionality view of the spectral landscape during multisensory processing (Makeig, 1993).

Band name	**Frequency (Hz)**
Delta	< 4
Theta	4 - 7
Mu	8 - 12
Alpha	8 - 15
Beta	16 - 31
Low gamma	32 - 69
High gamma	70 - 100

Table 2.1.: *EEG frequency bands. These figures are a general guideline for the range of frequencies referred by the authors when a band name is stated within a publication, the exact frequencies used may vary between research groups.*

Spectral methods are used to link alpha activity in the PMC with the process of body location (Lenggenhager et al., 2011), and to link the mechanism of body ownership and imagery of motion with the mu and beta frequency bands (Evans and Blanke, 2013). In an ERSP study, Kanayama et al. (2012) showed that EEG activity across different frequencies and temporal distances from the stimulation onset can correspond to separate SI tasks. The experimental protocol consisted of blocks of visuo-tactile hand stimulations, where the blocks consisted of congruent and in-congruent trials, at a ratio of either 80:20 or 20:80. This research demonstrated that gamma band activity and gamma-theta coupling were modulated by the percentage of congruent events within a block of trials, whereas late theta activity was correlated to congruency of stimulation, regardless of whether that block of trials was mostly congruent or in-congruent. The effect of 'stimulation expectancy' on each activity pattern (i.e. a greater percentage of congruent trials predicts that future stimulation will be congruent) clearly differentiates the roles of gamma and late-theta activity as markers for SI mechanisms. Spectral methods reinforce evidence of multisensory integration from ERP findings, by combining

spectral analysis to the EEG data, without changing the experimental protocol (González-Franco et al., 2014). Due to the richer data afforded by this higher dimensionality, studies in SI over the past decade have focused on the spectral activity to better understand multisensory processing in the cortex (Kaiser and Naumer, 2010).

2.2.2.3. Brain network approaches

The above sections on fMRI and EEG discussed SI processes for individual brain regions, however, as noted in Section 2.1.4, to capture a complete picture of the mechanisms of multisensory convergence, activity must be observed from a brain-wide perspective. Both fMRI and EEG data can be analysed using a brain-wide approach. fMRI data can be analysed using the effective connectivity method, to enrich the correlation of activity between brain regions by classifying the activity as direct or indirect connectivity (Klemen and Chambers, 2012; Valdes-Sosa et al., 2011). EEG data can be explored within a large-scale framework by creating networks of features extracted from the data (Siegel et al., 2012). One such feature is phase-locking, a condition during which the oscillatory activities between two distinct neuronal populations have a constant phase difference (Senkowski et al., 2008). Phase-based dynamics have been observed in the motor cortex as a marker of motor function modulation (Miller et al., 2012), and visuo-tactile integration is also suspected to be modulated by gamma based phase-locking networks (Kanayama et al., 2009).

A hybrid experimental paradigm implements concurrent recording of EEG and fMRI data (Arumana, 2012). This technique merges the high temporal resolution of EEG with the high spatial resolution of fMRI. Employing this technique could greatly impact our current understanding of SI by providing rich evidence of the spatio-temporal networks of activity in the brain (Kaiser and Naumer, 2010). An

enhanced picture of brain activity that provides the precise location of activity using fMRI, alongside simultaneous recording of activity via EEG can uncover new mechanisms of SI.

2.3. Measuring sensory integration II: Behavioural and perceptional correlates

Multisensory processing can be studied by examining the behaviours and perceptions of participants during experiments on sensory convergence. Perception is measured by asking the participant to identify the nature of the stimulation during unisensory and multisensory trials (Stevenson et al., 2014). Multisensory processes are then identified via the different behavioural outcomes.

2.3.1. Investigation for behavioural metrics through transcranial magnetic stimulation

An example of a behavioural metric used to measure the effect of SI is the subject's reaction time between stimulation onset and reporting of the event. (Pasalar et al., 2010) showed that the subjects' reaction time, when asked to identify which of their fingers was touched, was shorter when they were given congruent visual information of that same finger being touched. More importantly, using transcranial magnetic stimulation (TMS) to temporarily inhibit the function of the PPC, this multisensory advantage was eliminated. The value of this study was not only to show that congruent visual stimulation aids response times, but also to uncover an integral, causal relationship between activity of the PPC and visuo-tactile convergence. TMS has been widely used to affect the behaviour of participants in order to investigate processes of SI (Newport and Jackson, 2006; Stevenson et al.,

2014). TMS experiments can be further enhanced by using imaging techniques to pinpoint the exact centres of activity that can be inhibited for specific actions; for example, Tamè et al. (2012) used fMRI guided TMS to investigate the early somatosensory processing of vibro-tactile stimulation in the S1 region.

2.3.2. Sensory simultaneity and temporal order judgement

One of the universal experiences shared by humans is a fluid perception of environmental stimuli, regardless of the perceived sensory modality. Both external physical parameters, such as the speed at which the stimulation travels through space, and our internal sensory-specific processing times, guarantee a temporal difference in the arrival of information from two sensory modalities reporting the same event (Keetels and Vroomen, 2012). For example, due to the speed of light being faster than the speed of sound, and due to the different internal processing times for visual and auditory stimuli, any audiovisual cue farther than 15m away will have a considerable time lag, with the auditory input arriving after the visual input. This distance outside of which all audio-visual events should be perceived as time-lagged is called the 'horizon of simultaneity' (Vroomen et al., 2004). In reality, humans perceive simultaneity for audiovisual events at distances much farther than 15m. To explore the limits of sensory delays that are perceived as simultaneous, an experimental paradigm has been generated to artificially introduce a temporal lag between stimulation of different senses. This delay between stimulation is termed the stimulation onset asynchrony (SOA) (Keetels and Vroomen, 2012). Subjects are asked to judge either i) the order in which each modality was presented (i.e. the temporal order judgement, TOJ) or ii) if the two stimulations were presented synchronously (i.e. the simultaneity judgement, SJ).

Both TOJ and SJ tasks are used to report accuracy and reaction time as behavioural measures of SI. Other metrics from these judgement tasks include the

point of subjective simultaneity (PSS), referring to the SOA that produced the highest perception of simultaneity, and the just noticeable difference (JND) which is the smallest possible SOA for which the subject can accurately report synchrony/asynchrony. Interestingly, it has been shown that the PSS depends on the order that the stimuli are presented (Fink et al., 2006; RUTSCHMANN and LINK, 1964), and can be modulated by the ecological validity of the stimulus (Levitin, 2000). Caution must be taken when interpreting the TOJ and SJ results, as the results can be inconsistent between studies (Keetels and Vroomen, 2012; Vatakis and Spence, 2008), due to the various biases that are introduced from one experimental protocol to another (Linares and Holcombe, 2014; van Eijk et al., 2008). To illustrate how sensitive TOJ tasks can be, Pérez (2011) reported that the learned direction of reading text (left to right, right to left) can affect the subject's measures of TOJ. Petrini et al. (2009) reported that SJ tasks can be modulated by expert knowledge, with expert drummers outperforming novices at noticing audio-visual asynchronies presented in a simulated drumming interface.

2.3.3. Recalibration of senses

The ability of the brain to adapt to consistent sensory mismatches is called sensory recalibration (Keetels and Vroomen, 2012), and it was recently shown that sensory recalibration is not only possible in the spatial domain, but also in the temporal domain (Vroomen et al., 2004). In the temporal recalibration paradigm, participants received an initial exposure to multisensory stimulation with a fixed SOA, followed by a TOJ task. Using both audio-visual and audio-tactile stimulations, it was demonstrated that an initial exposure with SOA shifts the participant's PSS, such that the participant reported the greatest simultaneity at an SOA closer to the initially presented delay (Keetels and Vroomen, 2008; Vroomen et al., 2004). For example, participants who experienced pre-exposure to audiovisual stimuli with a

fixed SOA of 150ms reported a PSS of 26ms, whereas without the pre-exposure, the same participants reported a PSS of 20ms. In addition, temporal calibration between one set of modalities affects the perception of further multimodal processes. Di Luca et al., showed that audio-visual temporal recalibration can affect the reaction time in visuo-tactile perception, suggesting an interplay between the temporal perception of different sensory modalities (Di Luca et al., 2009). The effect of sensory recalibration could explain in part the absence of the horizon of simultaneity: the brain compensates for constant delays between stimuli by shifting the sensory perception to achieve a perceived effect of synchrony (Keetels and Vroomen, 2012).

2.3.4. Prior entry effect

During a multisensory TOJ task the modality that is attended to has a profound effect on the reported PSS (Spence et al., 2001b). This 'prior-entry effect' is linked with acceleration in processing time for the attended sensory modality (Spence and Parise, 2010). In contrast, attending to a modality can also lead to a diminished reaction time, if stimulation is delivered in the non-attended modality (Spence et al., 2001a). In an extension to the subjective nature of TOJ, Seibold et al. (2011) coupled the prior entry effect with ERP analysis of the post-stimulus auditory activity. This result provided neural evidence to support behavioural studies for SI processing facilitation of the prior-entry effect. Both the prior entry effect and the temporal recalibration are biases that can affect TOJ tasks (Linares and Holcombe, 2014) as discussed in Section 2.3.2.

2.3.5. Illusions that affect perception

A powerful tool in the study of multisensory integration is the use of illusions; the perceptive shift from non-illusory to illusory conditions allows the discovery of SI mechanisms underlying conscious experience (Blanke, 2012; Jones, 1988; Keetels and Vroomen, 2012). For example, the Müller-Lyer optical illusion in which two lines perceived to be of unequal length are in fact equal (Morgan et al., 1990), has been used to investigate how egocentric cues have similar effects in both visual and tactile versions of the illusion (Millar and Al-Attar, 2002). Audio-visual integration has been investigated using the McGurk effect, a compelling illusion during which the perceived sound of syllable is altered by visual information from the mouth (Keetels and Vroomen, 2012; Macdonald and McGurk, 1978; Stevenson et al., 2014). For example, 82% of participants that were shown a video of a person pronouncing the 'ba' syllable, with a synchronous audio recording of the 'ta' syllable, perceived the sound as 'da' (Macdonald and McGurk, 1978). In addition, audio-visual convergence has been investigated with ecologically valid scenarios, such as sound-length modulation from visual cues (Schutz and Kubovy, 2007; Schutz and Lipscomb, 2007). Schutz and Kubovy (2007) used two types of audio-visual stimuli, i) musical notes produced with the intention to be long and ii) musical notes that were intended to be short. Along with the auditory musical stimuli, an accompanying visual information of the performer's stroke that produced that note was presented. However, despite the intentions of the expert music performer to produce long and short notes, the actual length of the notes the performer created were of equal length due to the physical limitations of the instrument. Importantly, the notes that were intended to be longer were perceived by subjects to be longer when presented with congruent visual information. Conversely, this causal relationship between vision and audition is not observed during tasks that use ecologically irrelevant, non-causal stimuli. This poses the question

of whether different mechanisms of sensory convergence are modulated based on the method that the stimulation is presented.

2.3.5.1. Motion illusions

Audio-visual illusions are not the only tool available for SI experimentation. Illusions of motion are widely used to study the neuroanatomy of tactile senses and provide theories on sensory feedback processes (Jones, 1988; Lederman and Jones, 2011; Seizova-Cajic et al., 2007). The illusion of motion induced by the subcateneous vibration of tendons was first described by Goodwin et al. (1972). In their experiment, a blindfolded participant is seated with their elbows resting on a table and their lower arm slightly raised above the table's surface. One arm is assigned at random as the stimulated arm and the other is assigned as the tracking arm. The subject is instructed not to resist any reflex motions and to mirror the position of the stimulated arm with the tracking arm, such that both arms are at the same angle. By vibrating the bicep tendon of the subject's stimulated arm at 100Hz, Goodwin et al., showed that an illusion of motion is created for the blindfolded subject; the vibrated muscle is experienced to be stretching by the participant and thus they move the tracking arm to match the perceived trajectory. Goodwin et al., attributed this effect to the activation of muscles spindles; the results provided insight to how body movement is perceived in space (i.e. the sense of proprioception). It is important to note that visual feedback extinguishes this illusion: when participants can see their stimulated arm, no motion illusion is perceived.

Taking advantage of this ability to induce illusory motions, (Roll et al., 2009; Thyrion and Roll, 2009,1) produced illusory, multi-joint complex motions in a set of experiments. In their first experiment, they explored the additive effect of motion imagery and tendon vibrations to the illusory motion of the wrist (Thyrion

and Roll, 2009); they demonstrated that congruent motion imagery with tendon vibration could create a stronger illusory effect. Later studies by Shibata and Kaneko (2013) supported this finding by demonstrating that faster illusory motions were perceived by participants when motor imagery was congruent to the applied vibrations. In a subsequent experiment, Roll et al. (2009) sequentially vibrated multiple tendons to reproduce modelled and recorded activity of the muscle spindles during a target 2D single-joint movement (wrist or ankle). The effect observed was that motionless subjects were able to recognise and faithfully reproduce the illusory 2D motion. In a third experiment, Thyrion and Roll (2010) reported that by inducing tendon vibration on muscles of multiple joints (biceps, triceps, pectoralis, deltoid, and the shoulder abductors), it was possible to reproduce 3D movement illusions. These studies demonstrate the opportunities for extending the motion illusion and its potential as a tool for studying SI mechanisms.

An increasing number of experiments are employing this tendon vibration illusion either alone or in combination with other stimuli, for a variety of sensory motor and body representation studies. Ehrsson et al. (2005b) applied tendon vibrations to the wrists of a participant in two conditions: i) the participant was resting their hands on their waist, and ii) the participant's hands were not in contact with their body. Vibrations in the condition without body contact induced the motion illusion of the arms moving. Conversely, tendon vibration of the wrist while the hands were resting on the participant's waist induced the illusion of a shrinking waist. This study led to the identification of activity within the intraparietal sulcus as a neural correlate for the brain mechanism of body size representation.

Another set of experiments studied the effect of combined stimuli on the perception of motion. Combined tactile and proprioceptive stimuli were used to induce a motion illusion through tendon vibration alongside tactile feedback by a rotating disk (Blanchard et al., 2011; Kavounoudias et al., 2008). These experiments

showed that synergistic activation of tactile and proprioceptive stimuli produce a stronger illusion of motion, compared to tactile or proprioceptive stimulation alone Blanchard et al. (2011). Blanchard et al. (2013) studied the perception of illusory motion with trimodal stimulation via visual, tactile, and proprioceptive feedback. They observed that trimodal congruent stimulation of the wrist flexion evoked an illusory motion, demonstrating that the effect of each modality on the resulting illusion was not equal, with proprioception being the most important for coding velocity. Using trimodal stimulation it was shown that proprioceptive stimuli generated by tendon vibration affected visuo-tactile coupling (Palluel et al., 2011). The effect of congruent visuo-tactile stimulation on accurate self-localisation reports by participants was extinguished with vibration of the participants' ankles. This was theorised to be due to the proprioceptive stimulation interfering with the visuo-tactile integration. The combined effect of the senses was also observed with fMRI, and showed that the brain network activated during the illusory motion was similar between unisensory only stimulation, regardless of the modality used to produce the illusion. However, activation patterns were significantly different in trials in which the illusion was produced by multimodal stimulation (Kavounoudias et al., 2008). During trials with multimodal stimulation, activation was observed in the inferior parietal lobule, the STS, the insula-claustrum region and the cerebellum, providing further support for a SI model of diverse interconnected brain regions.

Illusions have the abilities to translate from one modality to the other (e.g. Millar and Al-Attar (2002)), to adapt to the nature of the stimulation (e.g. Schutz and Kubovy (2007)), and to transfer across body location with varying effects (e.g. Ehrsson et al. (2005b); Palluel et al. (2011)). The studies reviewed in this subsection illustrate that by using illusions as tools in experimental paradigms, diverse opportunities arise for investigating cognitive processes and SI mechanisms.

2.4. Chapter conclusion

This chapter examined the anatomical areas involved in SI ranging from the activity of single neurons to large cortical areas. It presented evidence supporting a large, interconnected brain network as a model of SI: a model which involves a multitude of brain processes occurring across most of the brain. The chapter reviewed the methods for measuring SI in the brain, both through the collection of biophysical evidence, and through behavioural and perceptive reports from participants. It discussed how specific methods can only provide a evidence for distinct multisensory convergence processes, offering a narrow outlook of the immense set of SI processes that take place concurrently within the brain. Finally, this chapter outlined the importance of behavioural and perceptual subjective accounts for the study of SI. This subjective evidence, along with the objective biophysical measurements, can greatly impact the field of SI and explain the many unexpected results that sensory illusions bring forward. The next chapter will review research into a specific cognitive process and its perceptual illusion that has been extensively used to uncover SI processes: the sense of self and the illusion of body ownership.

3. The sense of self: owning and moving the body

Chapter 2 reviewed the anatomical structures and underlying mechanisms of SI and introduced the experimental methods to measure SI cognitive processes. This chapter focuses on a cognitive process that is widely studied within the context of SI: the sense of identifying with one's own body. The chapter first frames body ownership from a philosophical perceptive and explores the relation between the sense of body ownership and the process of recognising oneself as being the agent of a self-generated action. This chapter then explores the neural correlates that are involved in body ownership, and presents the subjective and objective measures for quantifying body ownership. It also expands the earlier discussions on using illusions as tools for studying SI (see Section 2.3.5) from the perspective of illusory body ownership. Finally, this chapter reviews the experimental paradigms that are used to uncover the mechanisms of body ownership, and by extension SI, and aims to identify a research avenue that can address the objectives of the project, as identified in Chapter 1.

3.1. The sense of self

The sense of self, or self-identification, is one's ability to perceive one's personal identity. The sense of self can be divided into two distinct senses: a) the sense of self-ownership, and b) the sense of self-agency, ergo self-identification is elicited both by having a body and by being the cause of said body's actions. This section formally introduces body ownership and agency of motion and discusses their connection to SI.

3.1.1. The sense of body ownership

Under normal physiological conditions, people experience a sense of ownership over their body and body parts; this sense is termed 'body ownership' (de Vignemont, 2011; Gallagher, 2000; Tsakiris, 2011). Body ownership is an unconscious process, i.e. one does not need to think about the status of one's body or body part in order to elicit the sense of ownership. It is a multi-modal process, requiring the participation of a number of sensory stimuli to elicit a strong sense of body ownership (Blanke, 2012; de Vignemont, 2013,1; Ehrsson, 2012; Ehrsson et al., 2005a; Tsakiris, 2011). For example, the sense of owning one's arm is due to knowing where the arm is (proprioception), feeling any objects that the arm might be touching (tactile feedback) and visually identifying the arm as being an arm and occupying the correct position relative to one's body (vision). It is important to note that the congruent sensory information about one's arm, originating from two or more different sensory streams, is what grants the sense of body ownership, and conflicting sensory stimulation can lead to dis-ownership of body parts (discussed in more detail below) (de Vignemont, 2011). The dependence of body ownership on multisensory integration is supported by neurological data. The sense of body ownership is accompanied by activation of visual, somatosensory, and motor areas

in the brain (Blanke, 2012; Ehrsson et al., 2005a; Graziano, 2011). These neural correlates and anatomical structures identified as playing a role in body ownership are discussed in Section 3.2. The link between body ownership and sensory convergence is the motivating factor for exploiting this specific perceptual process for studying SI.

3.1.1.1. Embodiment and tools

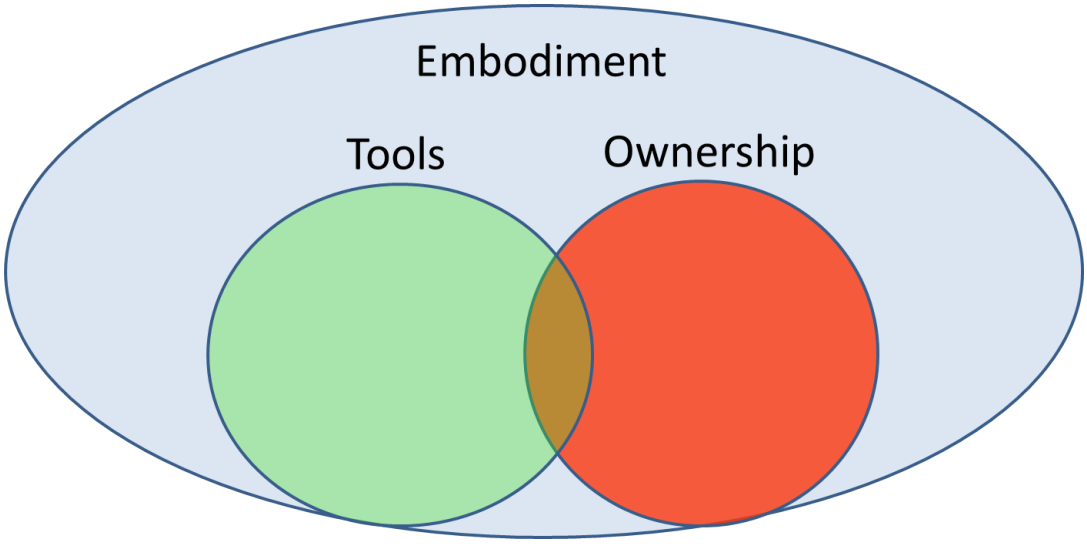

Figure 3.1.: *Venn diagram illustrating the relationship between embodiment of tools and body ownership as proposed by de Vignemont de Vignemont (2011). Tools and ownership share some embodiment criteria, but are distinct experiences of embodiment.*

The term 'embodiment' is often used in the literature on body ownership, however, the distinction between ownership and embodiment is unclear and often contradictory. In some reports, embodiment is used interchangeably with ownership, whereas in others, ownership is exclusively linked with governing self-attribution, and embodiment is linked with self-localisation. In either case, embodiment is not clearly defined. To address this, de Vignemont (2011) proposed the definition of embodiment as 'the ability to process properties of an object in the same way as body properties are processed'. In effect, embodiment and ownership are neither

synonymous, nor are they completely opposing terms. Embodiment is considered a superset of processes, with body ownership representing a subset of objects that can be embodied (see Figure 3.1). This philosophical distinction is important as it accounts for the embodiment of tools (de Vignemont and Farnè, 2010). It has been experimentally demonstrated that tools can affect the body representation in the same way as body ownership, by altering the perceived size of peri-personal space (Cardinali et al., 2009). However, when embodying tools no threat over the embodied object is observed. This differers distinctly from ownership where an object that is perceived as part of the body elicits a neural and behavioural response to threat (Ehrsson et al., 2007; González-Franco et al., 2014). For example, there is a clear distinction between being confident in using a wooden spoon to stir food at high temperature, versus using one's hand for the same job. This distinction can be explained under this definition of embodiment; embodying a tool and owning a body are both specialised and distinct processes of embodiment. It also explains why restrictions on objects that can be sensed as 'owned' (e.g. objects that look and feel like body parts) do not impede the embodiment of tools (de Vignemont, 2011; de Vignemont and Farnè, 2010). The power of this philosophical definition of embodiment demonstrates the importance of considering philosophical reports of cognitive processes when discussing results of ownership experiments.

3.1.1.2. Illusory ownership

From the definitions of ownership and embodiment given in the above section, it follows that an object can be sensed as 'owned' if it fulfils certain criteria. Specifically, if an object has certain properties that are processed in the same way as corresponding properties of a body part, and matches the sensory output expected of a body part (e.g. the object looks and feels like a body part) then it can be owned and sensed as being part of one's body (de Vignemont, 2013). In healthy

individuals, these criteria are naturally fulfilled by their body, however, they can also be fulfilled by foreign objects, resulting in a person sensing an artificial, out-of-body object as part of their body: this effect is termed the 'illusion of body ownership'. Illusory body ownership in healthy individuals was first demonstrated by Botvinick and Cohen (1998) in their experiment on the 'rubber hand illusion' (RHI). In the RHI paradigm proposed by Botvinick and Cohen, a test subject is seated with their left arm lying on a table and hidden from the subject's view behind a screen. A realistic rubber model of an arm with a hand is placed in front of the subject. The experimenter then uses two paint brushes to simultaneously stimulate the subject's real hand (hidden from view) and the observed rubber hand, while the gaze of the subject is concentrated on the rubber hand. After ten minutes of stimulation the subjects reported that they experienced the stimulation from the brush on the rubber hand, rather than on their real hand. After the experiment, the subjects are blindfolded and asked to estimate the position of their left hand, by pointing at it with their right hand. This induces proprioceptive drift, where the subjects' estimation of left hand location drifts towards the location of the fake arm. Botvinick's and Cohen's original RHI experiment was key to establishing the role of sensory integration in body ownership and has since been one of the most widely used tools for studying ownership (de Vignemont, 2011). Over the last twenty years, RHI has been extended to include several body parts and a variety of experimental paradigm configurations, leading to the umbrella term 'Body Ownership Illusion' (BOI) to describe the diverse examples of illusory body ownership. Section 3.3 provides a detailed review of experiments employing BOI.

3.1.2. Agency of motion

Agency of motion refers to the perception of causal responsibility for movement of one's body part, and to the ability to differentiate between movements produced actively (by oneself) and passively (by an external source) (David, 2012; Gallagher, 2000). Correct agency of motion is identifying oneself as being the cause of moving one's arm when waving good-bye, or recognising the external source of motion when one's arm is moved by a third party. Agency of motion and body ownership are intrinsically linked; moving a body and having a body are both necessary for self identification. However, agency of motion is a separate process to body ownership and has distinct behavioural signatures, supporting anatomical structures, and electrophysiological correlates (Kalckert and Ehrsson, 2012; Tsakiris et al., 2010). For example, in terms of perceptual differences between the two, a moving rubber hand can be perceived as owned without feeling agency over its motion, and conversely, agency over a moving object does not require the object to be 'owned' (Kalckert and Ehrsson, 2012). In terms of the neuro-anatomical differences, agency is dependent on the efferent signals of motion in conjunction with the prediction and monitoring of its effects, whereas ownership is linked to the integration of afferent signals and possibly to an internal representation of body parts (see Section 3.2) (Blakemore et al., 2002; Botvinick and Cohen, 1998; David, 2012; Kalckert and Ehrsson, 2012; Tsakiris et al., 2010).

3.1.2.1. Intending and imagining to move

Agency of motion is closely linked with the conscious emergence of the intention to move, the moment at which the planning of a movement is consciously perceived in the brain. Research on the neural activity underlying motion intention has identified the role of the SMA and the PPC in the early stages of motion planning (Desmurget and Sirigu, 2009,1; Vesia and Davare, 2011). Libet et al. (1983), found

that neural activity observed before voluntary movement not only predicts the movement itself, but also precedes the point in time at which conscious motion intention emerges, by more than a second. This result has been reproduced in several studies (Bai et al., 2007,1; Rigoni et al., 2013) and has raised questions about volition, free will, and self-identification: does this early activity correspond to the preparation of motion, or does the escalating neural activity background give rise to conscious intention (Desmurget, 2013; Haggard, 2008)?

Related to motion intention is 'motor imagery', the mental execution and rehearsal of a specific motion, without generating any actual body movements. Motor imagery is used as a tool to study agency (Jeannerod, 2001,0) and it was demonstrated that the neural architectures involved in motor imagery and their resulting neural activity correspond to those of motion intention (Jeannerod, 1994,9, 2001). Generation of similar output with real or imagined stimulation was discussed for STS in Section 2.1.3.1; similarity of output whether from real or imagined stimulation is common to both motor imagery and SI, and suggests a link between the two cognitive processes (Gallese and Lakoff, 2005). Furthermore, similar to activity induced by the intention to move, activity generated by motor imagery can be used to predict movement (Aflalo et al., 2015; Chin et al., 2010; Niazi et al., 2011; Pfurtscheller and Neuper, 2001; Williams et al., 2013).

3.2. Neural correlates and measures of ownership

To investigate SI mechanisms, the multisensory nature of body ownership must first be identified. This can be achieved by identifying the neural signature of ownership (the neural activity and cortical areas involved) and matching those results with evidence from SI research (see Section 2.1). Alternatively, the presence and perceived strength of ownership can be measured during BOI experiments,

and conditions that modulate the strength of ownership can be discussed relative to SI. This section reviews experimental methods for measuring the strength, the anatomical architecture, and the neural signature of ownership alongside models that explain how ownership is achieved in relation with SI.

3.2.1. Subjective and behavioural measures

To assess the strength of the RHI, Botvinick and Cohen (1998) asked participants to rate their experience of the rubber hand on a seven point Likert scale ranging from 'agree strongly' to 'disagree strongly' . Participants were instructed to respond to questions on their perceived location of the brush stimulation (i.e. on their real hand versus on the rubber hand), and on their feeling of ownership over the rubber hand. The results showed that affirmative responses from the participants correlated with a sense of ownership towards the rubber hand. In another experiment participants were asked to report their experience on ownership of the rubber hand during two contrasting conditions. On the congruent trials, both the rubber hand and the real hand were stimulated in exactly the same way, whereas on incongruent trials, stimulation of the rubber hand and the real hand was inconsistent (a) a delay in stimulation was introduced, b) the brush was moved in different patterns, c) the rubber hand was positioned and oriented differently to the real hand)[1] (Bekrater-Bodmann et al., 2014; Ferri et al., 2013; Kanayama et al., 2009; Longo et al., 2008; Perez-Marcos et al., 2012; Sanchez-Vives et al., 2010; Tsakiris et al., 2010). When participants were asked to rate their sense of ownership, affirmative ownership responses were reported in the congruent condition, whilst disagreement about owning the rubber hand was re-

[1]Herein, for all BOI studies, the terms 'congruent' and 'incongruent' will be used to differentiate consistent and inconsistent stimulation conditions with a single exception: when the stimulation inconsistencies are exclusively temporal (e.g. delays between stimulation of the real and fake body) the terms 'synchronous' and 'asynchronous' may be used instead.

ported in the incongruent condition. Participants' responses to threatening the fake hand has also been used to measure the strength of the illusory ownership (Armel and Ramachandran, 2003; Ehrsson et al., 2007; González-Franco et al., 2014; Guterstam et al., 2011; Petkova, 2011). Participants were asked to rate perceived threat towards their body when being presented with threatening visual cues towards the rubber hand once RHI was induced (e.g. a knife, a needle, or a hammer approaching or hitting the rubber hand). Perceiving a real bodily threat when a harmful cue is presented is evidence of ownership of the rubber hand; an embodied but not 'owned' object would elicit no perception of bodily threat, as discussed in Section 3.1.1.1 (de Vignemont, 2011).

The extent to which questionnaires are useful measures of perceptual experiences has been questioned in the literature (de Vignemont, 2011,1; Slater and Garau, 2007). For example, in some studies of BOI, the illusory response from participants was found to be weak during congruent conditions (e.g. Longo et al. (2008), see Table 3.1). Furthermore, during incongruent stimulation the expected result of responses of strong disagreement is often not reported, with some experiments reporting positive ownership or very weak disagreement (e.g. Perez-Marcos et al. (2012); Rohde et al. (2011), see Table 3.1). These results pose the question of whether the introspective account of ownership, as recorded by questionnaires, reflects the sense of ownership or the judgement of ownership (de Vignemont, 2011). Although some studies have elicited stronger illusion followed by an agreement of disembodiment (Kalckert and Ehrsson, 2014; Slater et al., 2008), a repeatable, accurate, and objective measure of ownership is necessary to compare the results across studies, and to better assess how specific conditions affect the strength of the illusion.

A perceptual measure for illusory ownership takes advantage of body representation and proprioceptive changes in terms of peri-personal space. During BOIs

Reference	n	BOI strength	
		Congruent	*Incongruent*
Longo et al. (2008)	131	+0.4*	-1.2*
Perez-Marcos et al. (2012)	32	+1.5*	-0.25*
Kalckert and Ehrsson (2014)	40	+1.7*	-2*
Costantini et al. (2016)	37	+1.5*†	+0.8*†
Ehrsson et al. (2005a)	32	+1.2*	-1.9*
Bekrater-Bodmann et al. (2014)	25	+3.23**	+2.10**
Rohde et al. (2011)	20	+3*†	+1*†
Slater et al. (2008)	21	+2*†	-2*†

Table 3.1.: *Studies measuring the strength of BOI using questionnaires. The reported strength refers to the average (mean or median†) response on questions of ownership (e.g. "I felt the rubber hand as my own"). n: number of participants. *: Answer was given on a 7-point likert scale, ranging from 'completely disagree' to 'completely agree' (-3 to +3). **: Answer was given on a scale of 0-10 ranging from 'none at all' to 'most intense'.*

the perceived space occupied by the body shifts towards the location of the fake body. As mentioned above, when asked to indicate the location of their real hand after RHI, participants tend to indicate a position closer to that of the rubber hand (Botvinick and Cohen, 1998; Longo et al., 2008). This proprioceptive drift correlates with the size of the fake hand, even if unnaturally long (Kilteni et al., 2012), however, this drift has not been correlated with reports of ownership (Holmes et al., 2006; Kilteni et al., 2012), and studies have found conditions for which proprioceptive drift can exist without illusory ownership (Maselli and Slater, 2014; Perez-Marcos et al., 2012; Rohde et al., 2011), suggesting a sensory recalibration effect on proprioception, separate and independent to the process of ownership.

3.2.2. Neural correlates and biophysical measures

The sense of body ownership has been investigated by examining the biophysical signals that are correlated with BOI. Biophysical measures have the advantage of providing an objective framework to assess illusory ownership strengths and compare the results between BOI studies, and also provide evidence for the brain mechanisms that underpin body ownership.

3.2.2.1. Skin conductance response

Skin conductance response (SCR)[2] is a measure of the skin electrical conductance changes due to stimulation that invokes activity in the sympathetic nervous system (Boucsein et al., 2012). SCR can be categorised into a) tonic SCR, the 'normal' steady-state SCR amplitude before stimulation, and b) the phasic SCR, which refers to the post-stimulus change. SCR is used as a measure of arousal and emotive states, and has been shown to correlate with illusory hand ownership (Armel and Ramachandran, 2003; Tsuji et al., 2013). Many BOI studies have used SCR as an objective measure of ownership and bodily threat perception (Armel and Ramachandran, 2003; Ehrsson et al., 2008; Farrow et al., 2012; Ferri et al., 2013; Hägni et al., 2008; Newport and Gilpin, 2011; Petkova, 2011; Romano et al., 2014; Senna et al., 2014; Tsuji et al., 2013), however the use of SCR is restricted, as it is not currently possible to classify the cause of the phasic SCR; any stimulation that induces sympathetic nervous system activity can generate a phasic SCR (Boucsein et al., 2012). Furthermore, phasic SCR can be observed in the absence of an external stimulation, or after the presentation of a novel cue/stimulus. These limitations, along with the large subject-to-subject tonic

[2]SCR is also known as galvanic skin response (GSR), and electrodermal activity (EDA). In line with the cited literature, SCR will be used herein.

level and phasic response variabilities, must be accounted for in the experimental design and the interpretation of results.

3.2.2.2. Brain imaging

To identify the brain areas responsible for body ownership, studies implement BOI paradigms whilst recording brain activity using imaging techniques (see Section 2.2.2.1). By comparing activity between congruent and incongruent trials, the regions of brain activity that correlate with the strength of the illusory ownership can be identified. Areas where activity was observed to correlate with the strength of the illusory ownership include the PMC, the intraparietal regions and TPJ, and the cerebellum (Bekrater-Bodmann et al., 2014; Blanke et al., 2015; Ehrsson et al., 2005a; Gentile et al., 2015; Grivaz et al., 2017; Guterstam, 2016; Guterstam et al., 2015; Ionta et al., 2014; Petkova, 2011; Tsakiris et al., 2010). Studies using near-infrared spectroscopy (NIRS) (Arizono et al., 2016; Shimada et al., 2005) and positron emission tomography (PET) (Tsakiris et al., 2007) have reported similar results, specifically highlighting the interaction between the premotor cortex and parietal regions in body ownership and SI processes. Furthermore, it is theorised that sub-processes are carried out within this network: a) the frontal lobe identifies multisensory incogruencies and inhibits activity propagation, thereby blocking multisensory convergence and false ownership, b) interactivity between the premotor - intraparietal cortices underpin congruent/incongruent perception of stimulation, and is involved in the modulation of the feeling of ownership (Gentile et al., 2013; Tsakiris et al., 2007). The consensus from these imaging studies is that a bilateral, right-dominant brain network, involving frontal, parietal, and cerebellar regions, underpins the process of self-identification and body ownership (Gentile et al., 2015,1; Ionta et al., 2014; Tsakiris et al., 2007).

3.2.2.3. EEG

The methods for studying ownership using EEG are similar to these previously identified for the study of SI (see Section 2.2.2.2). Evoked potentials and ERPs recorded over the S1 (primary somatosensory) region have been recorded in illusory ownership. Press et al. (2008) recorded ERP from central EEG electrodes over the S1 and PMC areas (C3, Cz, C4) and observed a stronger negative response (N140) during congruent trials of RHI versus incongruent trials. S1 activity was also observed by Aspell et al. (2012), who reported differences in early (30 - 50ms, P40) and late (110 - 200ms) activation of S1 between congruent and incongruent conditions of a RHI experiment. This suggested that S1 plays a sensory convergence role for: a) early visuo-tactile integration, and b) for late stimulus conflict detection and processing. This theory was supported by results from Dieguez et al. (2009) who reported ERP evidence of early involvement of S1 in multisensory convergence. Although studies have focused on different ERP components originating from S1, ERP activity originating from other brain areas also plays a role in body ownership: using analysis of ERPs Zeller et al. (2016,1) proposed a network comprising activity between the PMC, occipital regions, and S1 to be responsible for multisensory convergence and body ownership. Their study provides electrophysiological evidence that supports the theory from imaging data (see Section 3.2.2.2) that fronto-parietal interactions are involved in eliciting the sense of ownership.

In addition to ERP studies, frequency methods have been employed to uncover the neural correlates of body ownership. Changes in mu band activity (over S1 and the motor cortex) (Evans and Blanke, 2013; González-Franco et al., 2014), alpha band activity (over the PFC) (Lenggenhager et al., 2011), and gamma band activity (over parietal regions) (Kanayama et al., 2009,1) are reported to correlate with the illusory ownership of fake bodies. Kanayama et al. (2016) applied a

causal model of dynamic oscillation, which can determine causality and direction of activity between brain regions, to propose two networks of oscillatory activity in the alpha-beta band as sub-mechanisms of RHI: 1) a fronto-parietal network that is negatively correlated with the strength of the illusory ownership and 2) a late (550 - 750ms) parieto-somatosensory network that correlates with proprioceptive drift. The fronto-parietal information flow is theorised to inform processes in the parietal region of perceived incongruencies in stimulation, thus reducing the strength of the illusion and maintaining a true perception of the body schema. Conversely, late information from the parietal cortex to S1 is considered responsible for sensory adaptation and proprioceptive drift.

EEG recordings can be used as an objective measure of threat, complementary to SCR; the brain's response to bodily harm can be measured using ERPs (Fan and Han, 2008; Li and Han, 2010; Meng et al., 2012,1). Capitalising on this research, González-Franco et al. (2014) demonstrated a correlation between bodily threat and i) ERP (P450), ii) mu ERD, and iii) subjective reports of ownership. This approach introduces a multimodal framework for measuring illusory body ownership and demonstrates that aggregating the results from multiple independent measures could produce a robust and widely relevant body ownership measure.

3.2.3. Anatomical evidence from health conditions

Healthy individuals experience the sense of body ownership effortlessly, however, certain disorders can render a person incapable of experiencing it. These conditions have varying degrees of severity and identifying their underlying cause can provide valuable insight into the brain areas necessary for functional body ownership. Asomatognosia is an umbrella term for any stroke-induced condition in which a patient fails to recognise, and/or misattributes, the ownership of a limb (the limb affected is contralateral to the stroke-afflicted brain region) (Feinberg

et al., 2010). In mild cases of asomatognosia, the patient feels confused about, or unaware of the ownership of the afflicted limb, but can realise their error when their ownership over that limb is pointed out to them. For example, a patient with asomatognosia of their left arm can (temporarily) regain ownership of the arm by tracing the continuity of their body from their shoulder down to the affected arm. Somatoparaphrenia is an aggravated case of asomatognosia, which inflicts a delusion of dis-ownership so strong that the patient is unable to dispel the dis-ownership of the affected limb, despite indisputable proof to the contrary (de Vignemont, 2011; Feinberg et al., 2010). Finally at the severe end of the spectrum lies body-integrity identity disorder, wherein the patient experiences a delusion of dis-ownership so intense that the patient feels the compulsion to amputate the otherwise healthy limb (Brang et al., 2008; de Vignemont, 2011; First, 2005). These conditions of body dis-ownership result from damage in the motor cortex (Blanke, 2012; Jenkinson et al., 2013), frontal lobe (Jenkinson et al., 2013), and parietal lobe (Feinberg et al., 2010), consistent with the neural activity evidence discussed in Section 3.2, for the involvement of these regions in body ownership.

Despite the contribution to knowledge on body ownership processes, there are limitations to the conclusions drawn from investigating health disorders. On the one hand, lesions in the brain areas involved do not always result in dis-ownership, leading to the hypothesis that other conditions must co-exist in order to abolish ownership (Feinberg et al., 2010). On the other hand, cognitive processes cannot be fully understood by looking only at the damaged areas of the brain (David, 2012). Furthermore, these conditions do not cause an absolute loss of body ownership; patients still experience ownership over unaffected limbs/body parts, thus indicating that the lesions affect a limb-specific ownership process, rather than a break down of a system-wide, body ownership mechanism (Blanke, 2012).

Disabilities and ownership Studies of individuals with disabilities provide crucial insights into the mechanism of ownership. Ehrsson et al. (2008) observed that the RHI could be induced on the missing limb of amputated patients. In this study, experimenters brushed the fake arm observed by the participant, simultaneously with the participant's stump. Although the finger that was brushed in the fake arm does not exist on their body, the subjects reported ownership over the hand, and were susceptible to proprioceptive drift in the reaching task. Additionally, ownership was confirmed on a psychophysical level using SCR. It is important to note that although some subjects reported the experience of strong illusions of ownership, on average, the results of this experiment produced weaker illusions than the original RHI experiment. This may be due to the fact that it is impossible to induce spatially congruent stimulation at the amputees' stump. Alternative information from disabilities is gathered from patients with phantom limb pain, the experience of pain in a missing or amputated limb (Hebb et al., 1998; Weeks et al., 2010). Phantom limb pain provides case studies on body representation with a potential application in understanding body ownership; although immaterial, the phantom limb is perceived to occupy a position in space and to be of a certain shape. By measuring the perceived shape of the phantom arm of a congenital amputee, Longo et al. (2012) concluded that although sensory integration plays a role in embodiment, the brain maintains a body representation that is sufficient to invoke the experience of embodiment, as is observed in the case of the phantom arm perceived by congenital amputees.

In perhaps the strongest support for the importance and necessity of body representation in body ownership, Petkova et al. (2012) discovered that the RHI is not induced in blind individuals. To reproduce the same stimulation to both sighted and blind participants, the somatic variation of the RHI (Ehrsson et al., 2005a) was used, where a participant's hand is moved to touch the rubber hand whilst

their resting hand is touched by the experimenter. Petkova et al., discovered that congenitally blind or severely visually impaired individuals are not affected by the somatic rubber hand illusion and concluded that blind individuals do not have a plastic representation of their body in space, thus are not susceptible to the illusion.

3.2.4. Models of ownership

Given the variety of brain regions involved and activity patterns identified in body ownership experiments, researchers have proposed several different models for the sense of ownership; ranging from parsimonious models explaining specific experimental results, to hybrid models combining neural correlates and mathematical approaches. Armel and Ramachandran (2003) suggested a simple bottom-up approach, extrapolating from perceptual fluidity of illusory ownership to include non-body shaped objects. They theorised that ownership is governed by a single necessary and sufficient condition: visuo-tactile congruence of stimulation. However, other studies were unable to replicate their result, observing more rigid constraints (e.g. body specific shape, congruent proprioceptive orientation) in the objects that can be perceived as owned (Makin et al., 2008; Tsakiris et al., 2010). Makin et al. (2008) proposed a simple model for ownership that focuses on the peri-personal location of the stimulus. In this model, the PMC is suggested to integrate visuo-proprioceptive input from the fake and real hand into a unique body representation state, i.e. the location of the perceived hand in a combination of the two postures. Then, the visuo-tactile sensory streams are assessed for congruence in the PPC and if confirmed, the ownership illusion is elicited. Tsakiris et al. (2010) proposed a more comprehensive model that included validating the object to be owned for being of the correct shape and in a congruent spatial position to be part of the body. In this model the sensory input is com-

pared against a valid body schema (at the right TPJ) and a valid posture (at the primary (S1), and secondary (S2) sensorimotor cortices). The PPC and the PMC integrate the information and monitor the congruency of the sensory information. Finally, the resulting conscious experience of ownership, correlated with activity in the right insular lobe, adapts the body representation models used by TPJ, and the somatosensory cortices. Conversely, based on their EEG results, Kanayama et al. (2016,0,1) propose that a fronto-parietal network maintains the representation of the body schema, whereas Maselli and Slater (2013) propose that regions of multimodal and visuo-proprioceptive bimodal neurons (see Section 2.1.1) are responsible for assessing sensory input for validity against the body schema.

Models of brain connectivity have been enhanced by adopting a computational approach to ownership. For example, the error minimisation theory states that illusory ownership results from the process of minimising sensory incongruencies, similar to the SI theory for explaining sensory recalibration (see Section 2.3.3) (Kilteni et al., 2015; Seth, 2013). Alternatively, models applying Bayesian causal inference predict the cause of a given stimuli based on prior knowledge about that cause and the conditional probability of the observed stimulation (Kilteni et al., 2015; Seth, 2013). For example, using Bayesian causal inference a model can estimate if a visual (flash) and auditory (loud noise) stimuli are a result of a common source or have two distinct causes, based on the probability of one, or multiple, causes existing given the audio-visual input. Seth proposed a hybrid model of ownership using Bayesian inference within the concept of error minimisation. The prior knowledge was considered to be the subject's high-level body representation, and the conditional probability refers to the likelihood of each sensory modality to correctly report ownership (Seth, 2013). For example, during the RHI, congruent stimulation from the participant's visual and tactile streams results in a weighted probability that the fake body is embodied, and that the

disagreement between visuo-tactile stimuli and the subject's proprioceptive feedback is an error of proprioception. This model accounts for the illusory ownership and the generation of proprioceptive drift during the RHI. Although this model does not have support from neuroanatomical and neural correlate studies, EEG studies by Kanayama et al. (2016,1); Zeller et al. (2016) have used Bayesian causality to support their cognitive findings (see Section 3.2.2.3). Kilteni et al. (2015) have proposed using artificial neural networks that simulate the anatomical structures and the theorised ownership mechanisms as a framework for investigating theoretical models of body ownership.

Despite efforts to create a unifying model for the process of self-identification and the mechanisms of SI these models are diverse due to the insufficient amount of cognitive data to decisively support or discard any one theory. New paradigms, replication and standardisation of BOI experiments, and a combination of neuroanatomical and mathematical models, will lead to breakthroughs on how ownership and SI are accomplished in the human brain (Blanke, 2012).

3.3. Manipulating body perception and SI: beyond reality

This chapter has outlined the multisensory nature of body ownership, the range of experimental methods, and the theories proposed to explain how the experience of ownership is elicited in the brain. This section reviews experiments that use BOI experiments as a tool for studying ownership. It introduces technological advances in virtual reality (VR) that have enabled researchers to use high quality VR equipment in experimental studies. This has allowed research to progress beyond the physical constraints of reality and to expand the set of hypotheses that can be tested in a lab environment. By designing a paradigm with stimulation that cannot be experienced in the real world, theories on conscious mechanisms can be tested for validity. BOI studies that use one such paradigm (temporal asynchrony) will be reviewed and their potential to further investigate brain processes of body ownership will be discussed.

3.3.1. Virtual reality as a platform for studying illusory ownership

Slater et al. (2008,0) first demonstrated that the physical manifestation of an object is not necessary for body ownership. They used a VR-based experiment to replace the rubber hand with a VR projection of an arm and hand. By applying visual cues (at the virtual hand) and congruent tactile stimulation (at the participants' real hand), the participants reported ownership over the virtual hand. This virtual hand illusion has also been demonstrated to induce a strong illusion in the absence of tactile stimulation: Sanchez-Vives et al. (2010) showed that by introducing movements of the real hand, which controlled the synchronous and

matching movement of the virtual hand, test subjects experienced a strong illusion of ownership over the virtual hand. In a related study using a brain-computer interface (BCI), it was demonstrated that identifying motion imagery in EEG activity and using this to present congruent motion of the virtual hand, illusory ownership was induced in the absence of tactile or motor feedback (Perez-Marcos et al., 2009). Furthermore, Maselli and Slater (2013) demonstrated that a high visual fidelity and realistic virtual body, viewed from a first person perspective is sufficient to induce illusory ownership in the absence of any other congruent stimulation. Using VR, body ownership studies can be expanded from illusory ownership of a single limb to illusory ownership of an entire virtual body (i.e from RHI to BOI) (Ehrsson, 2007; Lenggenhager et al., 2007; Petkova and Ehrsson, 2008; Slater et al., 2009).

Implementing VR in studies of body ownership has allowed experimental paradigms to transcend the physical constraints of the real world. For example, by showing a virtual body from a third person perspective, out-of-body and body-swapping experiences were demonstrated (Ehrsson, 2007; Lenggenhager et al., 2007; Petkova, 2011; Petkova and Ehrsson, 2008; Slater et al., 2009,1). Other illusions of unrealistic body schemas that were first demonstrated using rubber hands, such as owning supranumerary limbs, (Ehrsson, 2009; Guterstam et al., 2011) were also reproduced and further investigated within a VR paradigm (Newport et al., 2010). Newport et al., found that although ownership was felt for two extra virtual hands, only one of the virtual representations was used to plan movements, thereby indicating a diversion between body representation and planning of motion. Other paradigms that studied unrealistic body conditions showed ownership of virtual hands of four times the length (Kilteni et al., 2012) and up to four times faster than the real hand (Kokkinara et al., 2015). These results reinforce the idea that body representation is malleable and can be influenced by congruent sensory stim-

ulation. Furthermore, plasticity of ownership has been correlated with changes in perception; illusory ownership of a radically different body has been demonstrated to induce perceptual changes. Studies that induced a BOI in white participants, with bodies of black avatar showed a reduction in the participants racial bias (Banakou et al., 2016; Farmer et al., 2012), whereas a BOI using the virtual body of a child affected the perception of body size in the adult participants (Banakou et al., 2013).

The prevalence of virtual reality experiments for studying ownership illusions is understandable due to the efficiency and wide possibilities of the virtual world; subjects experience identical proprioceptive matching between the real and virtual hand location, the experimenter has greater control over the parameters of the experiment (e.g. appearance of the fake body), and experimental design can be simplified by replacing the physical objects with virtual ones. Importantly, using VR as a research tool opened the doors to experimentation of body ownership with experimental designs that range from difficult, to near-impossible to recreate in the physical world. The ability to manipulate the experimental parameters to what is not physically possible allows researchers to test what theories predict about body ownership and SI under unrealistic conditions; results that confirm or disprove these theories can shape the understanding of SI.

3.3.2. Experiments on temporal stimulation incongruence

Using the virtual body illusion paradigm, it was possible to study the contribution of different factors to the strength of the illusion: synchrony of visuo-tactile stimulation, continuity of the virtual arm with the body, alignment difference and distance between the artificial/real hand (Perez-Marcos et al., 2012). BOIs have shown that body continuity and synchrony of the visuo-tactile feedback are important factors in the strength of the illusion, whereas alignment and distance

differences between the virtual and real hands could be tolerated to an extent, without breaking the illusion. Despite the importance of temporal synchrony in BOI, few studies have investigated the systematic modulation of stimulus onset asynchrony (SOA) and its effects on body ownership; most experiments use an inter-stimulus temporal discrepancy > 500ms for the asynchronous trials. Shimada et al. (2009) first showed the diminishing illusory strength when visual delay of stimulation is > 300ms. In an fMRI study, Bekrater-Bodmann et al. (2014) reported further evidence for the temporal window for illusory ownership falling within the range of +/- 300ms; no statistically significant differences in the subjective reports, nor in the imaging data were observed in the 300ms SOAs against the synchronous conditions. These results are in contrast with SI experiments reporting that visuo-tactile asynchronies can be detected for SOA of 100ms or less (Fink et al., 2006; Kanabus et al., 2002; Keetels and Vroomen, 2012; Levitin, 2000). The difference in the SOA perceived as asynchronous in temporal order judgement (TOJ) tasks, and the time window that affects the strength of illusory ownership, poses important questions for SI and body ownership mechanisms. For example, is the temporal window of synchrony perception different during a BOI than during non-illusory conditions? Are the delays perceived as asynchronous, and then the stimulus incongruence is suppressed by other SI processes to maintain the illusion?

Few studies have systematically investigated delays smaller than the 300ms temporal window to uncover the brain processes that are active during small asynchronies. Recently Maselli et al. (2016), demonstrated that the temporal window for integrating senses is modulated by ownership; the JND (just noticeable differences) for asynchronous stimulation of a virtual hand was 117ms and significantly dropped to 105ms when the hand was replaced by a virtual stick. Other recent studies (one as a result of this PhD project) have shown that significant drop in

ownership strength can be observed in conditions under 300ms (Costantini et al., 2016; Ismail and Shimada, 2016; Zoulias et al., 2016b). These recent studies attempt to bridge the temporal gap between the sense of ownership and the convergence of the senses. By identifying why that difference in temporal windows is observed and the responsible brain processes, a temporal framework is introduced for understanding the relation of body ownership and SI mechanisms.

3.4. Chapter conclusion

This chapter examined the conscious process of body ownership from a variety of perspectives: the philosophical framework, the anatomical and brain activity evidence, and the experimental methodologies to induce illusory body ownership. It reviewed the body of work that has already been conducted in the field, and identified potential avenues for future research with the aim of understanding the underlying mechanisms of body ownership and SI. The chapter reports that VR platforms greatly enhance the illusory ownership experience and can induce BOI with visual feedback alone. Furthermore VR paradigms can generate conditions beyond what is physically possible, thus can be used to create complex paradigms to validate theories and models of body ownership. This chapter reviewed experiments that use delayed cues to an illusory owned body and discussed the temporal framework that they introduce and identified research questions that can further the understanding of mechanisms of body ownership. The next chapter will outline the design and development of experimental methods, conducted as part of this PhD project to address the temporal framework and objective measurement of body ownership, based on the existing experimental protocols that were reviewed here.

4. Experimental platform and analysis tools

Chapter 3 reviewed the experimental platforms used to investigate body ownership, and specifically identified virtual reality (VR) as a powerful tool for studying cognitive processes. As VR allows researchers to extensively manipulate experimental parameters, experiments that implement VR to create stimuli beyond what is physically possible are a useful tool to validate theories of body ownership. Chapter 3 also discussed the necessity for a standardised, objective method for measuring the strength of body ownership illusion (BOI), in order to allow cross comparison of results across studies. Furthermore, Chapter 3 identified the systematic manipulation of small delays in BOI as a novel research avenue for investigating body ownership and sensory integration (SI). This chapter outlines the process of creating a VR-BOI platform for conducting experiments to investigate SI by manipulating the timing and presentation of visual and tactile cues. The revisions in scope, functionality, and aims of the produced platform will be discussed: this changes were brought forward during incremental development and testing throughout the platform design and construction cycle. This chapter will present the validation experiments and the pilot study conducted to test the platform. Finally, the chapter will outline the operational and technical specifications

of the ultimately produced platform which was further used in the experiments discussed in Chapters 5 and 6.

4.1. Exploration stage of platform design

In the initial platform design and specification stage a variety of stimulation modalities and biophysical sensing methods were investigated. The goal of this broad approach was to produce a platform that could allow testing of a variety of SI properties related to body ownership, whilst also establishing a novel testing platform; novel both in terms of other platforms described in the existing literature, as well as in terms of available facilities and infrastructures within the University of Reading where this PhD project was conducted. This section describes the initial exploration stage, discussing the original specifications, the feasibility of each proposed feature, and finally the outcomes for the next design stage of the platform.

4.1.1. Scope and aims

Based on the literature of existing platforms and experiments (see Section 3.3), the available technology and the feasibility of developing new tools, and project aims (see Section 1.2.2) the specifications and scope of the platform were initially described as following. The aim of the platform is to elicit a VR-BOI using a high fidelity human model that matches the anatomical properties of each test subject. Furthermore, the platform aims to create an illusion of body motion using tactile and proprioceptive feedback along with congruent visual stimulation (see Section 2.3.5.1). This set-up aims to produce a faithful virtual representation of a real body and evoke a very strong illusion of ownership and agency. To provide the spatio-temporal neural correlates of SI processes, the platform must

allow joint recordings of EEG and fMRI whilst eliciting the illusion. Experiments using this platform could then vary the congruency of the visual, tactile, and proprioceptive stimulation to create variation in the perceived body ownership and motion agency. Analysing the neural signature of this variation is expected to address the research questions identified in Section 1.2.

4.1.2. Designing the virtual avatar

As outlined in the literature review (see Section 3.3.1), the realism of the human avatar plays a critical role for the induction of BOI. Two methods of producing a virtual representation of a human body were investigated: (i) 3D scanning a physical body and importing it into the virtual environment presented by the platform, or (ii) producing a parametric based human model.

4.1.2.1. Scanning with the Kinect

At the beginning of the project the possibility of using a Kinect® sensor (Microsoft) for obtaining a topological and colour-textured model of each individual was explored. The Kinect sensor is a device with an RGB and a depth camera able to produce images that record the distance and the colour of any object in the device's field of view, within a limited distance from the sensor. The set-up consisted of two devices that were oriented to the same frame of reference - this was achieved by presenting within the view of both cameras a physical planar object of known dimensions. An optimisation algorithm using least squares of errors for the received position and dimension of the planes was then used to create a transformation matrix to re-orient the two cameras. Additionally, a green screen was used as a background in order to extract the colour of the arm. Using this set-up a software solution was developed that was able to scan the shape and the

colour of an individual's arm. However, this methods produced 3D models with visual artefacts due to small alignment errors and mismatch between the colour images. As a result commercially available solutions for producing 3D scans were explored as an alternative.

4.1.2.2. Commercially available solutions

Instead of creating a tool for scanning, a number of commercially available solutions were researched for 3D scanning using a Kinect sensor. Two of the reviewed programs, KScan3D® (LMI technologies Inc.) and Artec studio® (Artec Group) delivered acceptable results and provided an easy-to-use user interface. A number of models from the two software solutions were produced and compared, with KScan3D being the favourable of the two due to the easier scanning process and the better results with colour mapping on the model. However, even using this commercial solution presented visual problems such as lower fidelity on parts of the model and holes in the finalised model (see Figure 4.1 and Figure 4.2 for scans obtained by Artec Studio and KScan3D, respectively). Holes in the model must be filled if they are in a visible to the subject area and additionally, they presented a challenge during the preparation stage of the model where the motion is produced, as will later be discussed in Section 4.1.2.4.

4.1.2.3. 3D parametric human model

As an alternative to 3D scanning the physical body of a human subject, the possibility of using a parametric model was investigated in parallel and compared with the results from the 3D scanning methods. One promising solution for dynamic creation of parametric 3D human models is MakeHuman® (MakeHuman team), an open source parametric modelling software. MakeHuman provides a user interface that can be used to design human models of any size, skin colour, or gender.

Avatars can be dressed with features (such as hair, skin, and clothes textures) from an accompanying texture library and the final model can be exported with a matching skeleton which can be further used for animation (see Section 4.1.2.4). An example of a model created with the MakeHuman software can be seen in Figure 4.3. Models created with MakeHuman were compared with the models from KScan3D (see Figure 4.4). Although the parametric model looked less like the individual than the scanned model, the very realistic skin texture and the smooth, human skin looking surface (in contrast to the bumped scanned model) made it a more appropriate choice for realistic modelling to use the parametric model as the virtual avatar of the participant, especially when considering that a first person view would only include parts of the model where 3D scanning produced consistently poorer results (for example, top of the arm as seen from first person perceptive, see Figure 4.4).

4.1.2.4. Preparation of the model: Skeleton and insertion in a 3D environment

In order to animate a 3D model a skeleton must be produced. A skeleton, in the 3D modelling sense, is a collection of universal joints that control the deformation of the meshes of a given model. Models created through 3D scanning a human body are not produced with a matching skeleton: instead, a skeleton must be designed from scratch. To animate the 3D scanned models, a skeleton was designed using Blender® (Blender foundation), a free and open source professional modelling software. On the contrary, models designed using the MakeHuman software can be animated immediately as they have pre-built skeletons, as discussed previously. After a model with a skeleton is obtained the next step is animation. To animate a model its skeleton can be controlled directly in a game engine environment by modifying the rotation of any given bone within the skeleton. Alternative

an animation can be created in a modelling software such as Blender, which can be then played back in the virtual world on demand. For comparison purposes, the models created through the different methods were imported to Unity® (Unity Technologies) game engine. The models created by Artec studio, KScan3D and MakeHuman that were compared in the environment can be seen in figures Figure 4.1, Figure 4.2, Figure 4.3 respectively.

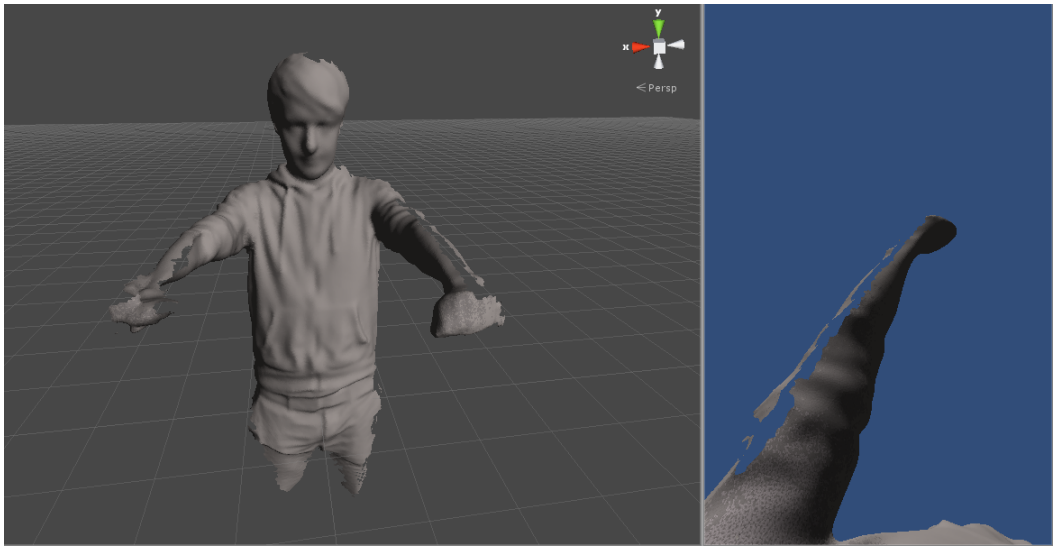

Figure 4.1.: *3D model of scanned subject, scanned using Artec studio® software, imported in the virtual environment and see from a first person perspective (right).*

Figure 4.2.: *Example of a 3D model by KScan3D®. Visual artefacts on the arm and torso can be seen (right).*

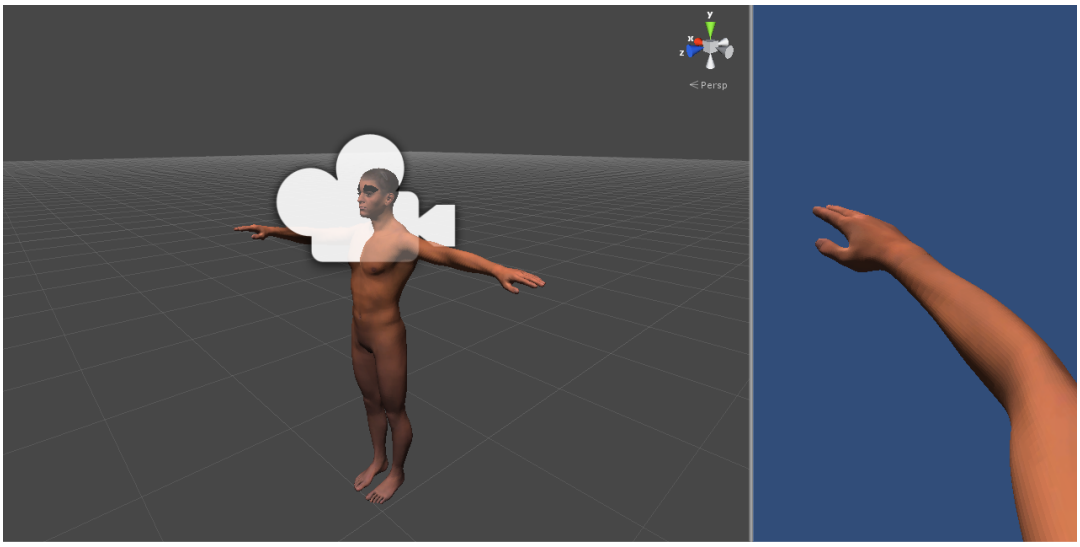

Figure 4.3.: *Parametric 3D human model, obtained by MakeHuman® software, rendered in the virtual environment.*

4.1.3. Presentation of avatar

To provide an immersive experience in the virtual world, a head-mounted display (HMD) is the most appropriate solution as it provides visual occlusion of the participant's real body, and can project the virtual avatar into the same proprioceptive location as the subject's body. Commercial HMD are costly and low resolution, however, in 2013 the Oculus Rift® DK1 (Oculus VR, Inc.) was developed as an entry-level, consumer VR device. This model of HMD offers a 110 degree diagonal field-of-view, 60Hz display refresh rate, and high resolution display at low cost (approximately £250 in 2014). Given its low cost and high specifications, an Oculus Rift DK1 HMD (henceforth referred to as Rift) was purchased for use in experiments to be conducted outside of the fMRI scanner. The Nordic Neurolab VisualSystem, an fMRI compatible HMD capable of providing 3D stereo images was available for use for presenting the virtual environment and avatar inside the fMRI scanner.

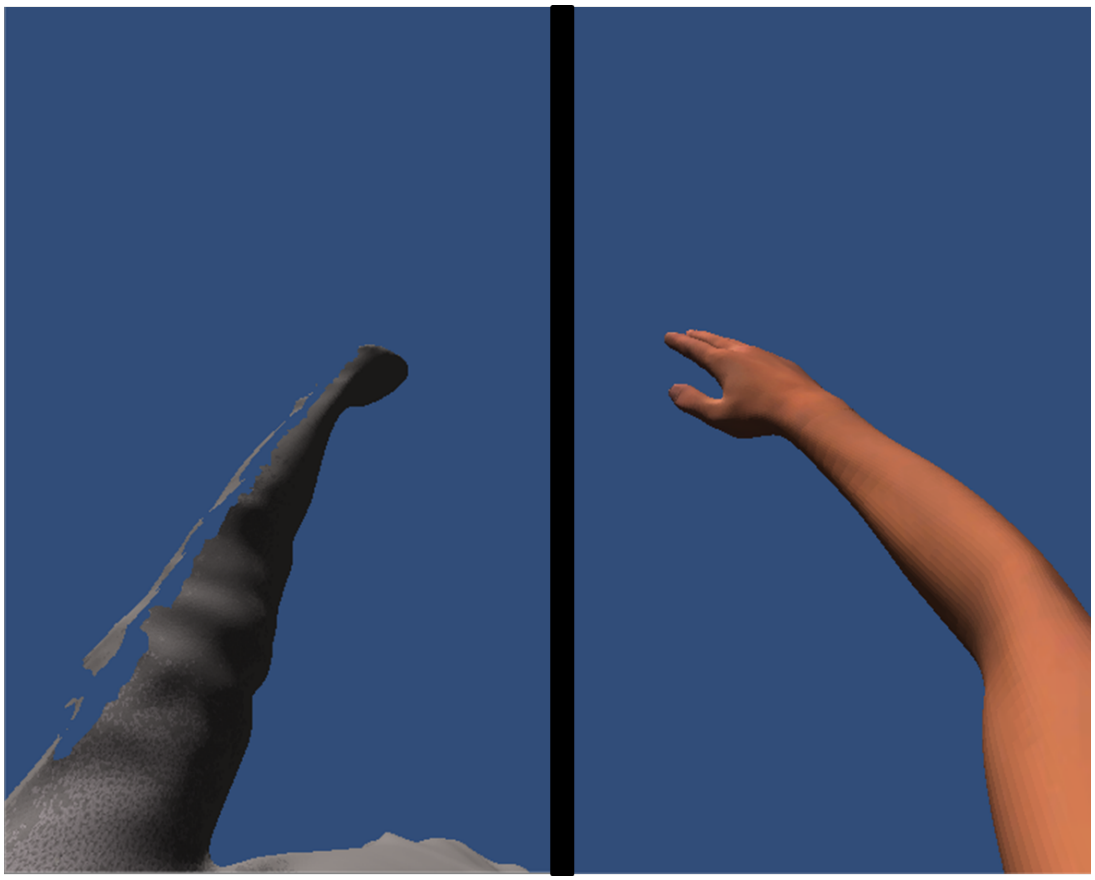

Figure 4.4.: *Comparison of generated 3D body avatars from first person perspective. Avatar quality of 3D scanned and reconstructed arm (left) versus parametric generated arm model (right), as viewed from a first person perspective. The scanned arm model has portions missing and the arm is not clearly defined.*

4.1.3.1. Using Oculus Rift with EEG

To assess the ease of use of the Rift while recording EEG activity a short test was run while a participant was wearing both the EEG cap and the Rift. The aims of the test was to assess the feasibility of presenting visual stimulation with synchronous EEG recording and to provide evidence of any potential discomfort from the user's point of view. The test confirmed that the Rift could fit alongside with the EEG cap without trouble and that no discomfort after wearing the device for 30 minutes was detected. Figure Figure 4.5 shows the two devices worn simultaneously. As there were no previous studies using this device, a pilot experiment

was conducted to assess the Rift's operation during co-registration of biophysical data (see Section 4.2).

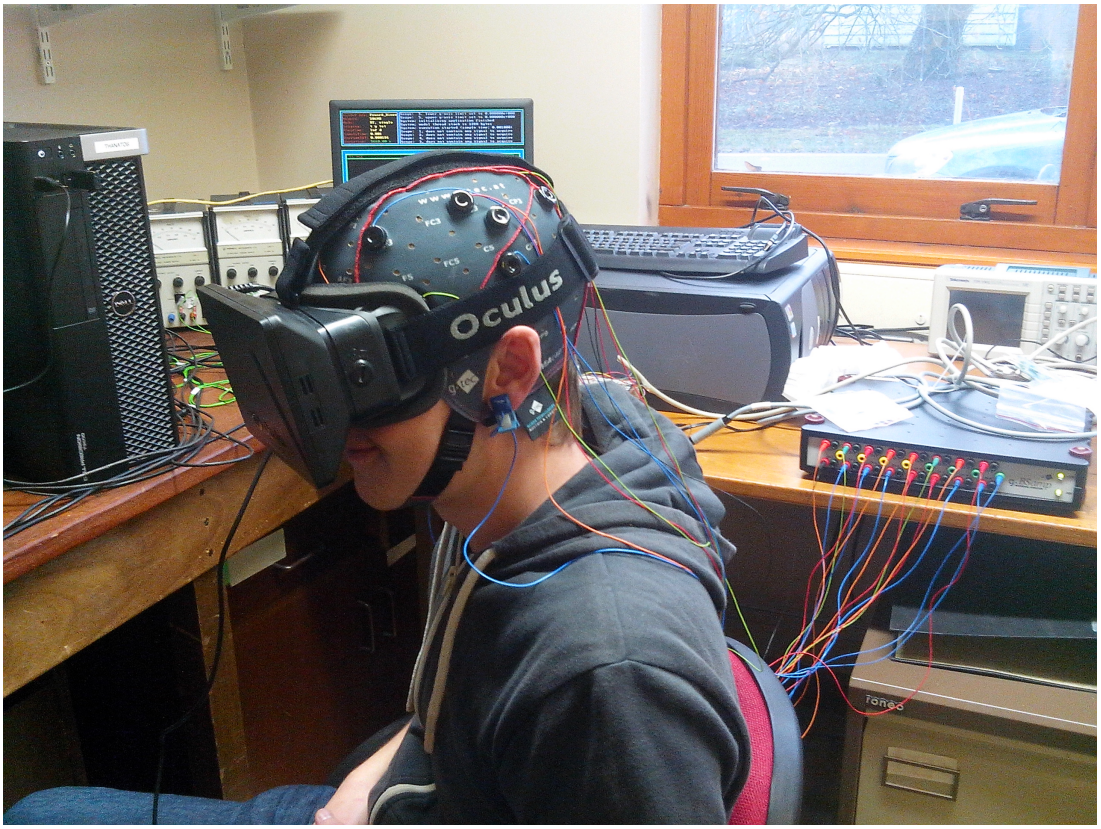

Figure 4.5.: *Test subject using the Oculus HMD while simultaneously recording 16 channel EEG.*

4.1.4. Tendon vibration

As identified previously (see Section 2.3.5.1) the tendon vibration illusion can be used as a feedback mechanism to study SI processes. At the exploratory stage of the platform, tendon vibration was investigated as a potential feedback mechanism through purpose-built engineering solutions, discussed below. To provide suitable vibratory stimulation to the muscle in order to produce a proprioceptive illusion of motion, the developed solution was designed to conform to the following objectives:

- Must be able to reliably deliver vibration in the range of 60 Hz to 80 Hz at an amplitude of up to 2 mm (Goodwin et al., 1972; Jones, 1988).

- When coupled with a load (human skin) the device must retain the frequency of the vibration and produce an amplitude of at least 0.5 mm (Goodwin et al., 1972).
- The frequency and amplitude of the device must be controllable during real-time experimentation to allow for the presentation and extinction of the target tendon vibration illusion (Jones, 1988).
- The device must be scalable so multiple tendons can be vibrated during the experiments.

4.1.4.1. Limitation posed by fMRI compatibility

As stated earlier (see Section 4.1.1), the scope of the experimental platform included fMRI scanning. As a result, the tactile stimulation mechanism should be designed to be safe to use inside the room of the fMRI. This extra requirement is because the fMRI surrounding environment poses limitations in the design of devices that are to be used inside it. Materials must be non ferromagnetic as the high magnetic field of the coil of the scanner can attract magnetic object with lethal speeds when in range. Additionally the changing magnetic fields can induce currents to materials that are electric conductors and this can lead to both equipment damage but also to severe burn risks if the electric conductor gets heated due to the induced currents. For a device to be deemed fMRI compatible the three following conditions must be met (Montant et al., 2009):

- The device must be made of fMRI safe materials (non ferrous, non conductive).
- The device must not introduce noise in the scanning processes.
- The device must work as intended inside the fMRI room (i.e. no change of operation between inside and outside the fMRI room).

4.1.4.2. Tactile stimulation systems for use inside the fMRI

Hydraulic solution A simple solution for pneumatic or hydraulic vibration was designed. This mechanism was inspired by previous work in pneumatic actuation inside the fMRI environment (Montant et al., 2009; Yu et al., 2009,0). The proposed solution uses a motor as an actuator of a pneumatic of hydraulic cylinder. The cylinder forms a closed system with a pipe and an end effector that is situated inside the fMRI room. By vibrating the piston at a given frequency, the end effector will produce vibration due to the pressure wave that is transmitted through the pipe. Before implementing the hardware solution, a theoretical model of the behaviour of the system is required to address implementation issues such as the required rating of the motors needed to actuate the end effector and choice of model parameters that produce efficient operation (e.g. pipe diameter). The mathematical derivation of the model and the theoretical results are presented in Appendix A.

Using the model as a guide, a prototype of the system described was created in order to assess the feasibility of developing such a system for the final experiments. The prototype, shown in figure Figure 4.6, was tested with different pipe length and confirmed the feasibility of creating a vibration over a distance. Measurements from the fMRI room were taken in order to set the minimum required length of the pipe that is required to reach the subject's arms inside the scanner. The mechanism shown in Figure 4.6 (rotor and link, pipe adaptors, and the end effector) was designed using the Solidworks® (SolidWorks Corp.) cad drawing software and was 3D printed in ABS plastic.

Piezoelectric solution In parallel with the design of the formerly described system, the design of a piezoelectric vibrator was also attempted, based on similarly designed systems (Nagel et al., 2005; Uffmann et al., 2002). Using a 555 timer

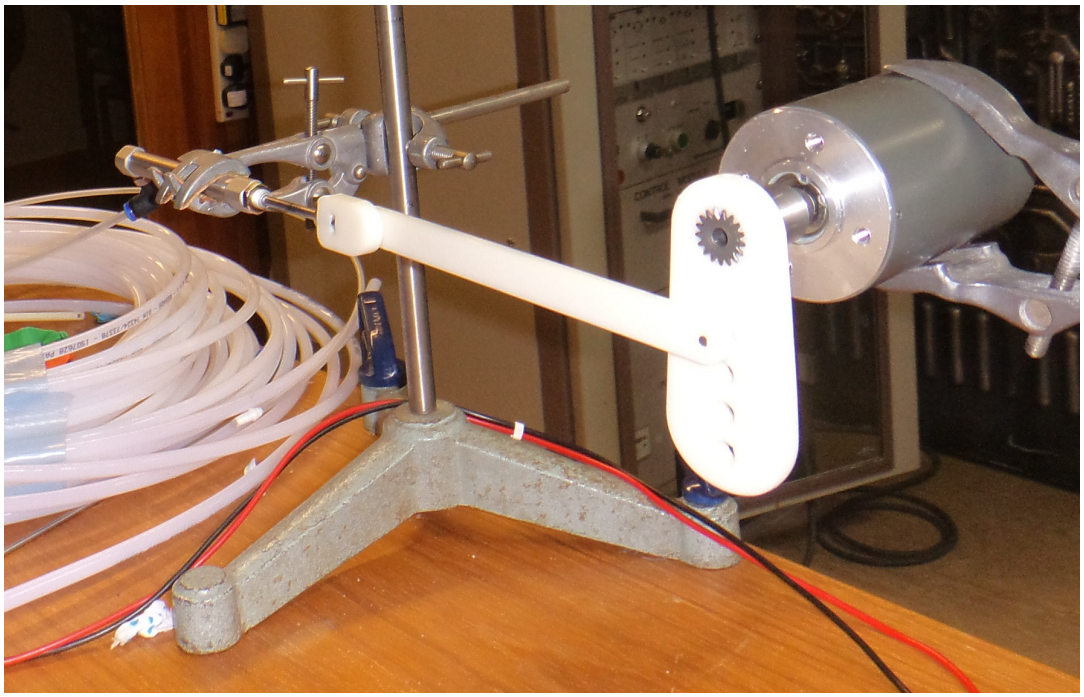

Figure 4.6.: *Pneumatic prototype for delivering vibratory stimuli in the fMRI environment. A motor actuates a pneumatic cylinder that forms a sealed system with an end effector that is connected a long nylon pipe. The pipe and the end effector are fMRI safe (made out of materials that can safely be inside the machine's magnetic field.*

circuit design, a power supply and a 12 mm Murata piezoelectric sounder, it was possible to produce vibrations of the required frequency. However, due to limitations in the vibration amplitude the design was abandoned in favour of the hydraulic system with the view to resume it if needed by creating a lever mechanism to amplify the amplitude. One of the main concerns with the use of the piezoelectric design is the long cables needed to actuate it from outside the fMRI room the temperature of which must be monitored to avoid fire accidents and burn hazards.

4.1.5. Conclusions of initial platform design stage

In the initial design stage described in this section the specifications of the platform were investigated in terms of avatar design, VR presentation, and tactile feedback to the user. Considerations were taken for the compatibility and suit-

ability of the platform components with respect to the proposed brain activity imaging and measuring technologies. In terms of the avatar design, the considerable improvement in visual quality afforded by the parametric models resulted in their adoption within the platform design. In terms of tactile stimulation a prototype was produced that was capable of delivering vibro-tactile stimulation within the fMRI room. However, the use of fMRI technology was abandoned based on the development time taken to reach this stage of the project. The time requirements for developing an fMRI compatible platform were prohibitive within the scope of this project due to further efforts both in terms of using the fMRI (training, data acquisition and analysis) and in terms of further platform development (e.g. producing a stable tactile stimulation platform and testing for fMRI compatibility). Instead, the platform specification was updated for compatibility with EEG only recording, whereas fMRI use could be revisited at a later stage after the platform had been validated. Based on the preliminary findings on using the Rift simultaneously with EEG recordings (see Section 4.1.3.1) a pilot study was designed to assess the compatibility of the platform for EEG recordings - this pilot study is discussed in the next section.

4.2. Validation stage and pilot experimentation

The development of a novel VR-BOI platform required the assessment of its suitability as an experimental platform, in terms of: a) quality of the recorded data, b) ease of use in an experimental setting, and c) virtual experience generated, before conducting further experiments aiming to study BOI. This section outlines the pilot study conducted for assessing the VR-BOI platform. The results from this experiment were presented at the EMBS IEEE International Neural Engineering Conference (Zoulias et al., 2015).

4.2.1. Scope and aims

The pilot experiment aimed to assess the suitability of the using the Rift HMD whilst recording biophysical data, and to evaluate the platform for its use in future experiments. Previous experiments had shown that it was possible to record EEG during a BOI experiment that used a high-cost HMD validated for research, however, the Rift used in this project is a consumer product, not-tested for its capacity for research. To validate the Rift for use in EEG research, participant comfort whilst wearing the EEG cap and Rift, and confounding electrical noise impact on the EEG signal by the Rift was measured in this experiment. Based on these aims, two hypotheses were tested: 1) the Rift would produce no significant noise artefacts in the EEG data and thus would be a suitable platform for BOI experiments, and 2) visual feedback from the virtual avatar would produce stronger motor imagery - induced ERD.

4.2.2. Procedure

Nine healthy participants (3 female, age range: 22 - 28yr, mean age: 24yr) from the University of Reading volunteered for this experiment. The experiment was reviewed and approved by the University of Reading, School of System Engineering, Ethics Committee. The experiment consisted of two parts during which EEG was recorded: a) a 2D component in which the participants received visual stimulation from a computer screen, and b) an immersive VR component in which the participants received visual stimulation while wearing the Rift. In both components, the same virtual environment (a human avatar in a sitting position) and pre-recorded prompts were used. The VR and 2D components had two tasks in common: (task1) an eyes open/closed task to record alpha band EEG, and (task 2) an arm movement task in which the participant had physically move their arm

as instructed. The arm movement instruction was “Keeping the elbow on the table, raise the arm, and lower it to the table again”. In task 1, a pre-recorded oral prompt (open/close) was used to instruct participants to open and close their eyes. In task 2, a visual cue (a black cross) signalled which hand to move, and an aural cue (a short ’beep’) was used to instruct the onset of motion. Tasks 1 and 2 aimed to assess any EEG signal differences when wearing the Rift versus not wearing the Rift. The VR component had one extra task aimed to investigate the effect of visual stimuli on motor-imagery ERD. In this task (task 3) participants were asked to imagine performing the same motion as in task 2 but without producing any actual/physical movement under two conditions: a) in the ’imagine-only’ condition the virtual avatar remained stationary, and b) in the ’imagine + visual presentation’ condition, the avatar performed the movement that the participant was asked to imagine.

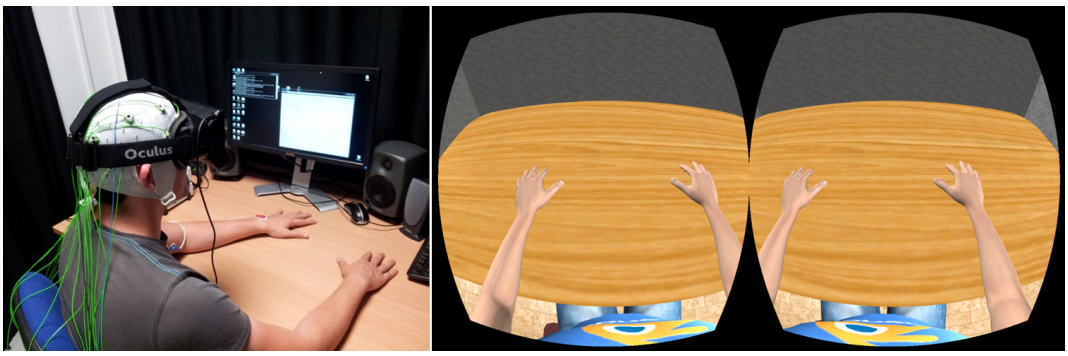

Figure 4.7.: *Experimental setup of pilot study. Left: participant simultaneously wearing the Rift over the EEG cap. Right: first-person view of the participant when wearing the Rift.*

Table 4.1.: *Experimental design of pilot study. Two factor (wearing/not wearing the Rift) compared against two tasks. The effect of virtual reality feedback is also assessed in Task 3 for the 'wearing the Rift' factor only.*

	Wearing the Rift		Not wearing the Rift HMD (control)
Task 1	Eyes open/ closed		Eyes open/ closed
Task 2	Raise arm (left/right) while keeping elbow on the table		Raise arm (left/right) while keeping elbow on the table
Task 3	Imagine raising the arm		N/A
	w/ visual feedback	w/out visual feedback	

4.2.3. Pilot study results

4.2.3.1. EEG noise due to the Rift HMD

To test the suitability of the Rift whilst recording EEG signal from the participant the results from Task 1 and Task 2 were compared between the two conditions (i..e. the participant: (i) wearing, or (ii) not wearing (control), the Rift). Initially, a visual inspection of the raw data showed no observable difference in the data recorded. A statistical comparison was then performed between the two conditions, focusing on the effect of the HMD on recorded band power. The average power for bands of EEG (see Table 2.1) were compared statistically using a lineal mixed model with condition (wearing or not the HMD) as a fixed effect and participants and electrodes as a random effect. The statistical tests were performed in R using the nlme package (Pinheiro et al., 2017).

In task 1 the average signal power for each EEG band was calculated as the mean power derived by the fast Fourier transform during the period of interest

(eyes open, and eyes close periods individually) for all frequencies within the given frequency band. No statistical difference was observed between wearing and not wearing the Rift (*Alpha band: F(1, 3932) = 1.49, P = 0.222,* see Figure 4.8; *Beta band: F(1, 3932) =1.53, P = 0.2168*, see Figure 4.9). The alpha power was significantly higher during the eyes closed period versus the eyes open period, whereas beta band power was affected to a much lesser extend, both as expected.

In task 2 a similar procedure was followed, but concentrating on the period just before and during the participant's arm motion onset in order to compare ERD/S differences. To calculate the ERD power, the spectrogram of the 2 second period surrounding the movement onset was subtracted from a spectrogram of the same length from 5 second and onwards before the movement onset. Alpha band ERD values between the motion and rest period were compared when participants wore or were without the Rift (see Figure 4.10, Figure 4.11). No statistical significance was observed between the ERD values when wearing or not wearing the HMD (*F(1,269) = 3.18, P = 0.0758 ,* see Figure 4.12).

Taken together, the results from task 1 and 2, along with the visual inspection of the raw data for artefacts and general EEG discontinuities, showed that no significant interference in the EEG signal was generated due to the use of the Rift HMD.

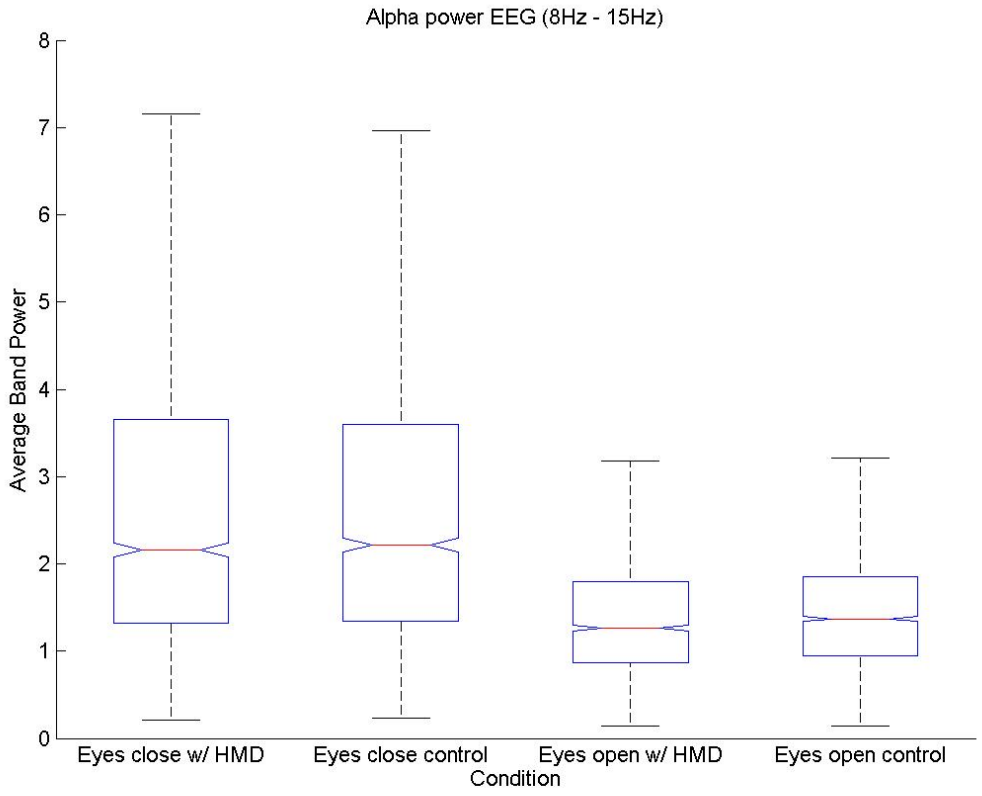

Figure 4.8.: *Alpha band power during eyes open and eyes closed periods. No statistical difference was observed when wearing the Rift versus not wearing the device ($P = 0.222$). A clear difference between the eyes close vs the eyes open condition is observed as expected.*

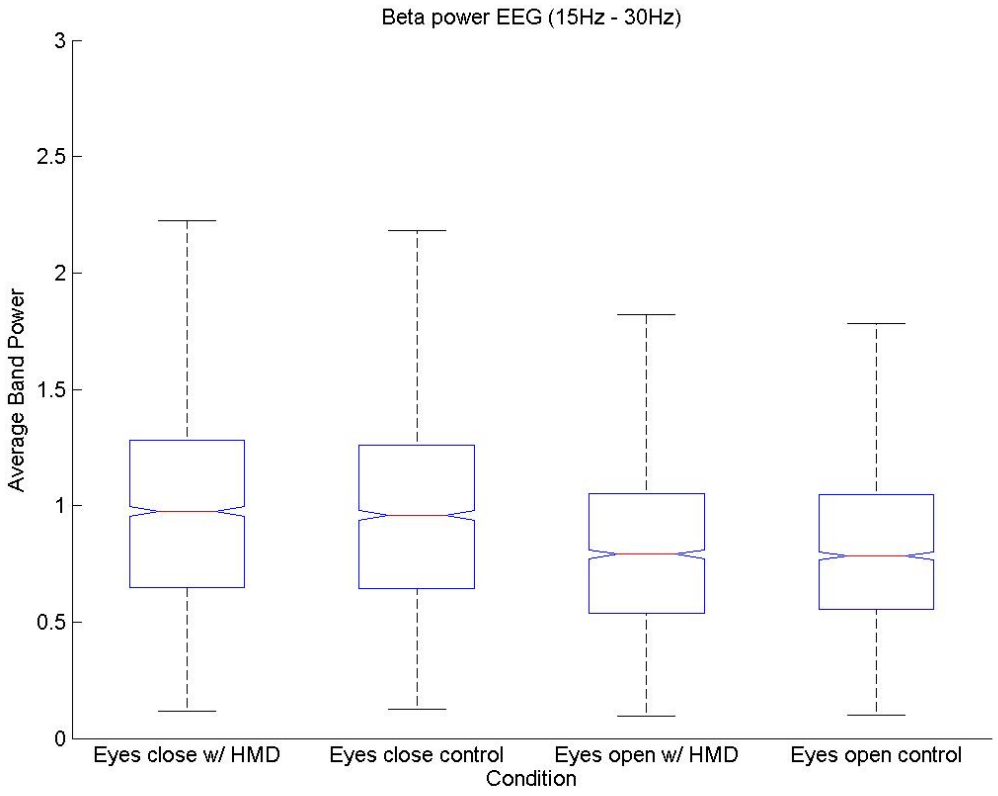

Figure 4.9.: *Beta band power during eyes open and eyes closed periods. No statistical difference was observed when wearing the Rift versus not wearing the device ($P = 0.2168$). The eyes closed period have a much smaller effect to beta band power than to alpha.*

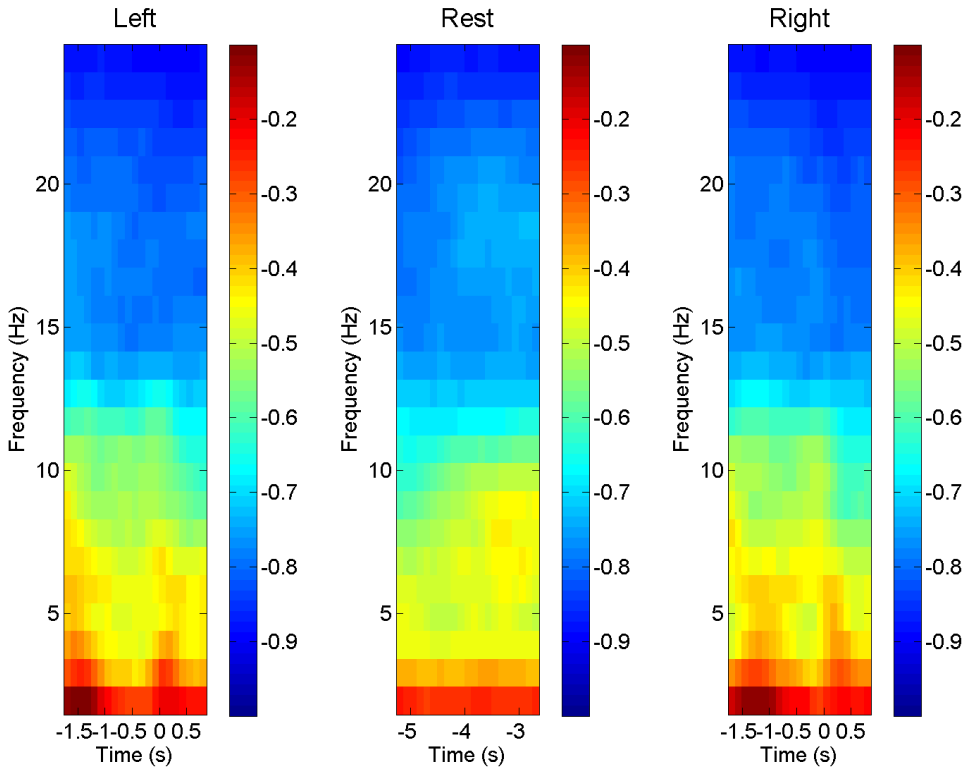

Figure 4.10.: *Spectrograms during rest, and left and right arm movements for the control condition (w/out the Rift). Spectrograms of EEG activity from the Cz electrode averaged across all participants and trials. The values of power have been normalised in the range of -1 to 1, with the limits being the minimum and maximum recorded power.*

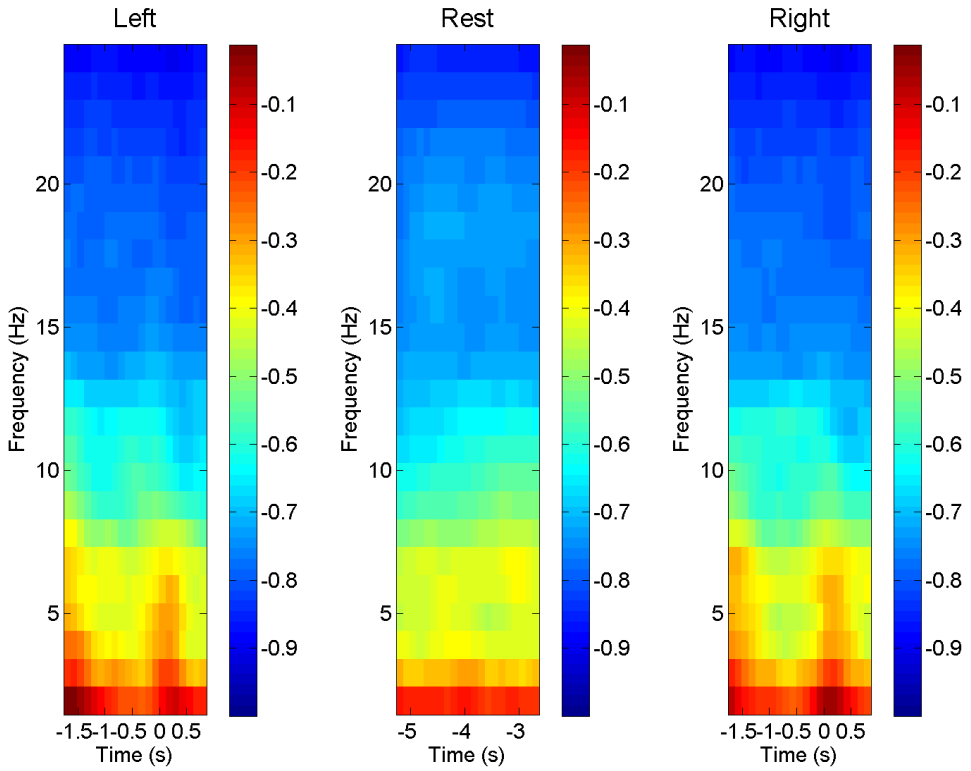

Figure 4.11.: *Spectrograms during rest, and left and right arm movements when wearing the Rift. Spectrograms of EEG activity from the Cz electrode averaged across all participants and trials. The values of power have been normalised in the range of -1 to 1, with the limits being the minimum and maximum recorded power.*

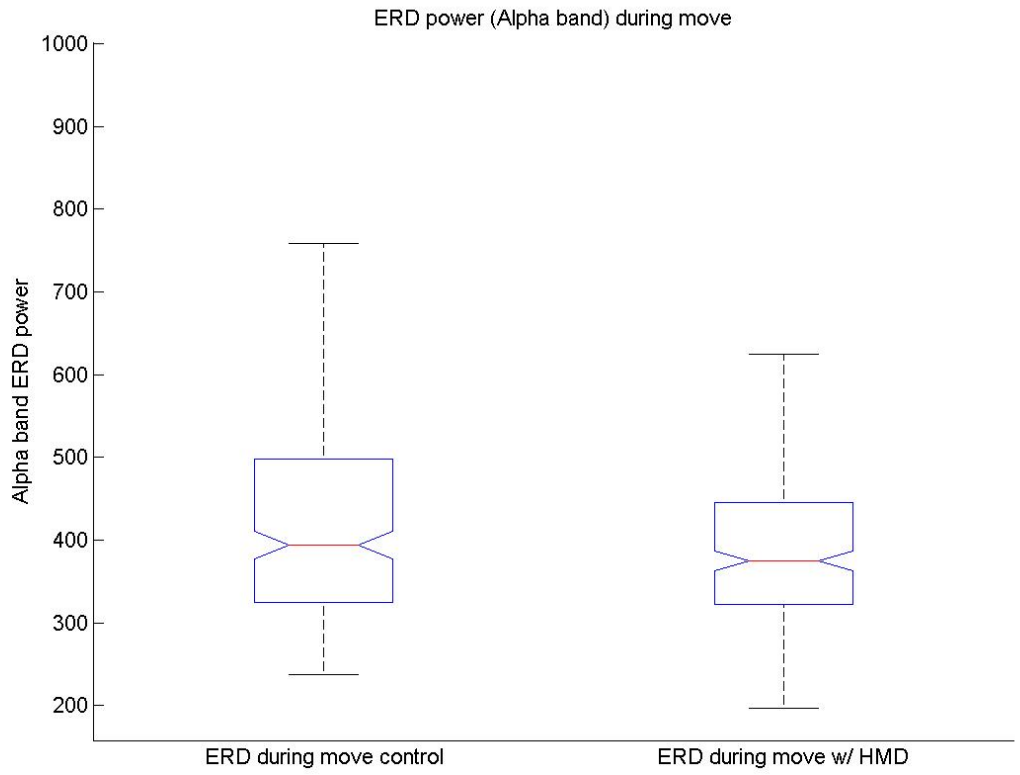

Figure 4.12.: *Comparison of alpha band ERD during arm movement between wearing and not wearing the Rift. No significant difference in ERD was observed ($P = 0.0758$).*

4.2.3.2. Visual feedback aiding motion imagery ERD

To investigate the effect of visual feedback on motion imagery related ERD, the results from task 3 were analysed in terms of ERD strength between the condition with congruent visual feedback (i.e. the arm moving as imagined) and control condition (i.e. no movement of the virtual avatar). It was observed that mu and beta band ERD induced by motion imagery was significantly larger when congruent visual stimuli were presented versus ERD during the only imagining condition (*mu band: F(1,3227) = 4.49, P= 0.0341, beta band: F(1,3227) = 4, P = 0.0456*). This result can be interpreted as a reinforcement of the mental imagery through visual feedback, which in turn produces a stronger ERD signal, a known marker for motion imagery (McFarland et al., 2000; Nam et al., 2011; Pfurtscheller and Neuper, 2001), that can be captured through the EEG. A subsequent study by Kondo et al. (2015) investigating the effect of visual feedback on ERD based BCI performance provided supportive evidence for the strengthening of ERD response due to visual feedback. More importantly, in terms of the platform design, task 3 provided evidence of the viability of the platform to conduct EEG based experiments and marked a significant milestone in the design of the experimental platform.

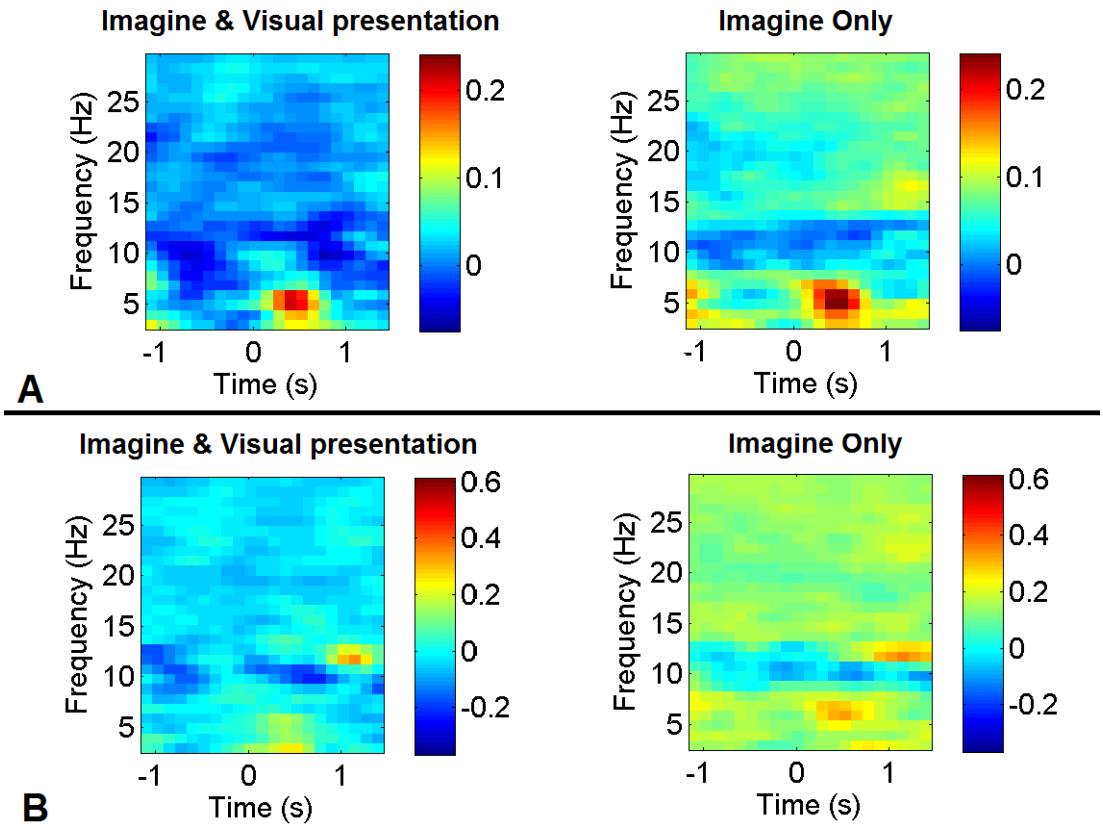

Figure 4.13.: *Spectrograms demonstrating ERD elicited by motion imagery. A) Average ERD spectrogram across all subjects, electrode C3, B) Example subject average spectrogram. Left) Condition of congruent visual input with motion imagery. Right) 'Imagine Only' condition. Mu and beta band ERD was significantly stronger in the condition where visual feedback reinforced the mental motion imagery (P= 0.0341 and P = 0.0456, respectively). The values of power have been normalised in the range of -1 to 1, with the limits being the minimum and maximum recorded power.*

4.2.4. Conclusions and next stage

The pilot study proved the suitability of the Rift HMD for EEG recordings (task 1 and task 2) and demonstrated that the experimental platform can be successfully used for conducting experiments aimed to address questions of SI brain processes (task 3). This fulfilled some of the specifications of the platform outlined earlier (see Section 4.1.1), however, certain goals were still unmet - most notably the requirement for multimodal sensory input. Furthermore, the pilot study brought forward a consideration about the synchronisation of the timing between stimulation of the participant and biophysical recordings: in the above setup signal

simultaneity is assumed by the internal processor clock timing of the PC that is presenting the virtual world and simultaneously records EEG activity (see Section 4.3.4.1). Thus it was necessary to identify any delays of the recording and visual presentation streams individually and to synchronise them for the subsequent data analysis - this is necessary due to the timing of the brain processes regarding SI being in the range of tens of ms, as discussed in Section 2.3.2. The following section described the final stage of the platform design based on these considerations, which was subsequently used for the experimentation of SI processes.

4.3. Final experimental platform

This section describes the final experimental platform constructed for the VR-BOI experiments of this PhD, based on the findings and insights derived from the process described in the previous two sections. Based on the initial requirements, the aim of this platform is to create an immersive virtual environment that induces a BOI. The platform must be capable of delivering tactile feedback to mimic the visual stimulation observed through the VR device, and must facilitate adjustable temporal congruency between visual and tactile stimulation. The SOA should be accurate and replicable so that conditions of small and large sensory delays can be compared. Additionally, the platform must allow subjective data from questionnaires to be recorded, and to co-register biophysical recordings including EEG and SCR. These recordings aim to provide an objective measure of the strength of ownership, and enable the neural correlates of body ownership to be investigated.

The final design of the experimental platform is discussed in this section in terms of visual and tactile stimulation, self report and biophysical measuring capabilities,

and synchronisation algorithms and techniques used to comply with the comments discussed in the previous section.

4.3.1. Virtual reality: avatar, environment, and questionnaires

Having identified its potential for EEG experimentation the Oculus Rift HMD was used for presentation of the virtual environment and avatar. As outlined in the literature review (see Section 3.3.1), the realism of the human avatar plays a critical role for the induction of BOI. The MakeHuman® (MakeHuman team) open source program was used to design two high fidelity, full body avatars, one of each gender. Using the Unity® 3D (Unity Technologies) game engine, a virtual room was created to mimic the physical room in which the experiments were conducted (see Figure 4.14). The 3D avatars were animated using the Blender® (Blender Foundation) modelling software to match the stationary seated posture that the participants were instructed to take during the experiment, such that the avatar was positioned in the virtual room in the same anatomical posture and relative location as the subject.

In the virtual room, a screen was included on the desk for the presentation of self-report questionnaires, and through which participants recorded their responses by scrolling left/right with an Xbox® controller. The participant was instructed to hold the controller on the left hand and could view through the possible responses in a 7-point likert scale from “Strongly disagree” to “Strongly agree” by moving the analogue stick of the controller left or right. By pressing the trigger at the back of the controller the a response was taken based on the currently displayed response under the question in the virtual screen (see Figure 4.14)

Figure 4.14.: *Virtual reality environment and avatar created. The avatar is seated on a desk within a room modelled after the room the experiments take place. A virtual screen on the desk is used for the subjective reports: answers in the scale of "Strongly disagree" to "Strongly agree" are displayed under the question and the participant can respond by selecting the most appropriate answer.*

4.3.2. Tactile stimulation

Tactile stimulation was investigated using two approaches: a) stimulation to induce illusion (see Section 2.3.5.1), and b) stimulation for visuo-tactile matching cues. Initially, development of vibro-tactile stimulators for illusory motion did not result in a strong reproducible illusory effect, and the development effort moved to creating a tactile stimulator that could deliver tactile stimulation matching the visually presented cue. To deliver the stimulation, a digital servo motor (MX-64A Dynamixel®) was chosen as it provides force feedback through a current sensor. A custom-made, 3D-printed arm accessory was designed to allow the attachment of two end-effector tools. Based on the experimental design discussed in the following

chapters (see), these custom end-effector tools were used for cue stimulation: i) a knife end-effector, and ii) a spherical end effector to match the visual cues (see Figure 4.15). The rationale behind selecting tapping stimulation versus brushing stimulation is the separation of temporal and spatial effects. For example, if an observed brush strokes the rubber hand, and after a small delay the real hand is stroked in the same pattern, participants might report the stimulation as synchronous but spatially incongruent. However, the tapping stimulus can only be perceived as temporally mismatched.

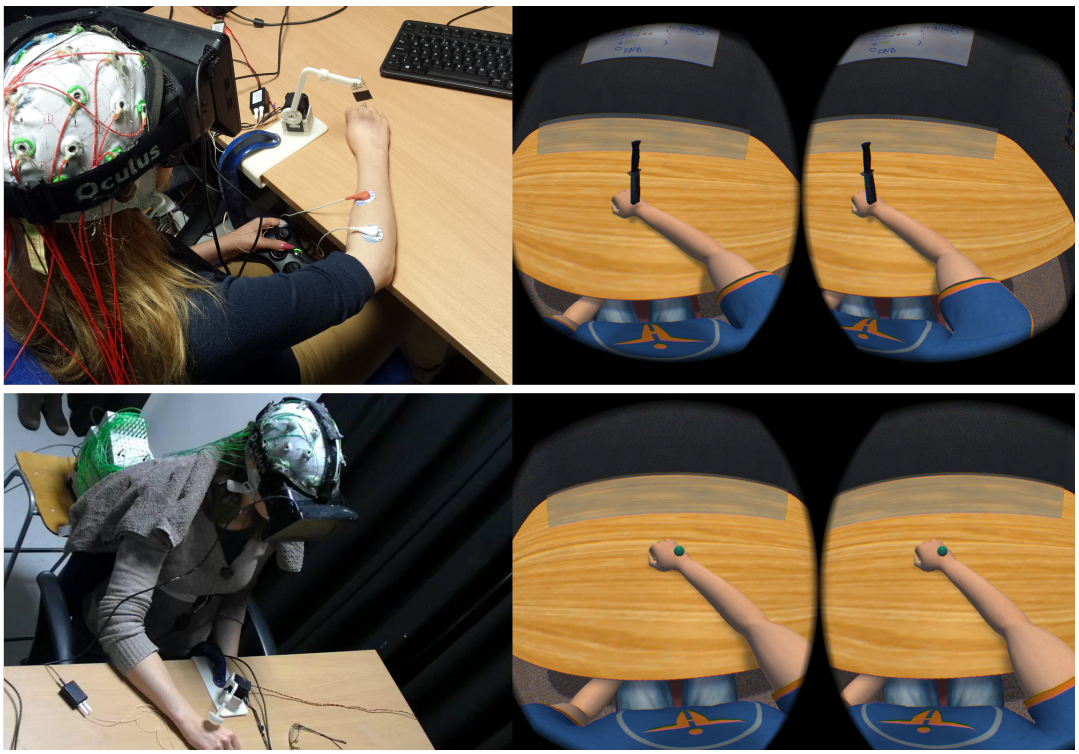

Figure 4.15.: *Visual and tactile sensory presentation mechanisms. Top: Knife, threatening stimuli. Bottom: Sphere stimulation. Left: Tactile stimulator adapted with the required tool to deliver the congruent cue. Right: Participant's view in the VR*

4.3.3. Biophysical measures

To measure the participant's biophysical responses during the experiment, a BrainAmp® (Brainproducts) EEG amplifier was used with 32 EEG channel capacity.

The BrainAmp EXG® add-on amplifier was used to record EMG, ECG, SCR, and breathing rate. Ag/AgCl electrodes were used for recording all electrophysiological signals. EEG electrodes were placed using the 10/20 system, EMG was recorded from the right bicep, ECG was recorded by electrodes on the ankles and left wrist, and SCR was recorded from the index and middle fingers of the right hand. The right hand was used for the SCR electrodes to minimise movement artefacts from the left hand, due to holding the Xbox controller and scrolling to answer the questionnaires. All data was analysed using Matlab® 2014b (Mathworks Inc.) and the EEGLAB v13.5.4.b software was used (Delorme and Makeig, 2004; Makeig et al., 2004) for data visualisation, filtering, artefact removal, and analysis. Specifically, artefact removal for EEG was performed by first applying a band pass filter (1-45Hz) and then performing the runica method implemented in EEGLAB and visually removing components in which eye-movement and general discontinuity artefacts were observed. For statistical analysis and presentation of the ERP results the Mass Univariate ERP Toolbox was used (Groppe et al., 2011).

4.3.4. Minimisation of delays and device synchronisation

As the experimental platform was purpose built within this PhD, it was necessary to assess the timing constraints introduced by the individual components. Identifying these delays fulfils two requirements: a) to define the limit of the smallest possible SOAs, and the interval between SOAs of different conditions, and b) to synchronise the signal streams from the different input (i.e. biophysical acquisition) and output (i.e. visual and tactile stimulation) devices. This section describes the experiments carried out to identify the sources of delay, and the minimisation, prediction, and synchronisation solutions developed to address these delays.

4.3.4.1. Stream synchronisation

The complex nature of this experimental platform requires the co-registration of data streams from different equipment. Two open-source software libraries for data stream synchronisation were used for multi-device synchronisation: the 'signal server' software (Breitwieser et al., 2012; Muller-Putz et al., 2011), and the 'lab-streaming layer' (LSL) (Kothe et al., 2016). The first experiment using the VR-BOI platform assessed the suitability of using the Rift in combination with EEG recording (see Section 4.2). For this experiment, the signal server was used to co-register the biophysical data from the BrainAmp, with the events from the VR application that signalled the visual presentation of cues in the HMD. Using the signal server to synchronise multiple devices requires each device to be added into signal server's software source in order for communication to occur. This limitation is overcome with the use of the LSL library: LSL only requires the inclusion of the LSL library within the VR-BOI platform to establish communication with a new device, thus the LSL library was used for subsequent experiments (see Chapter 5 and Chapter 6). An LSL outlet (purpose built within this PhD) runs in the background of the VR application to record visual events or data from the digital servo motor. Simultaneously, a second LSL outlet (BrainAmpSeries, available from LSL) records the biophysical data from the participant. Both LSL outlets timestamp and transmit the data to an LSL inlet (LabRecorder, available from LSL). The LSL inlet synchronises the two outlets to allow multi-stream co-registration. When the data is imported to the EEGLAB, meta-data embedded in the outlet stream allows the identification of channel parameters.

4.3.4.2. Prediction of tactile cues

Using a servomotor to provide tactile feedback generates a timing problem for visuo-tactile simultaneity. If presentation of the visual cue is reactive, i.e. the

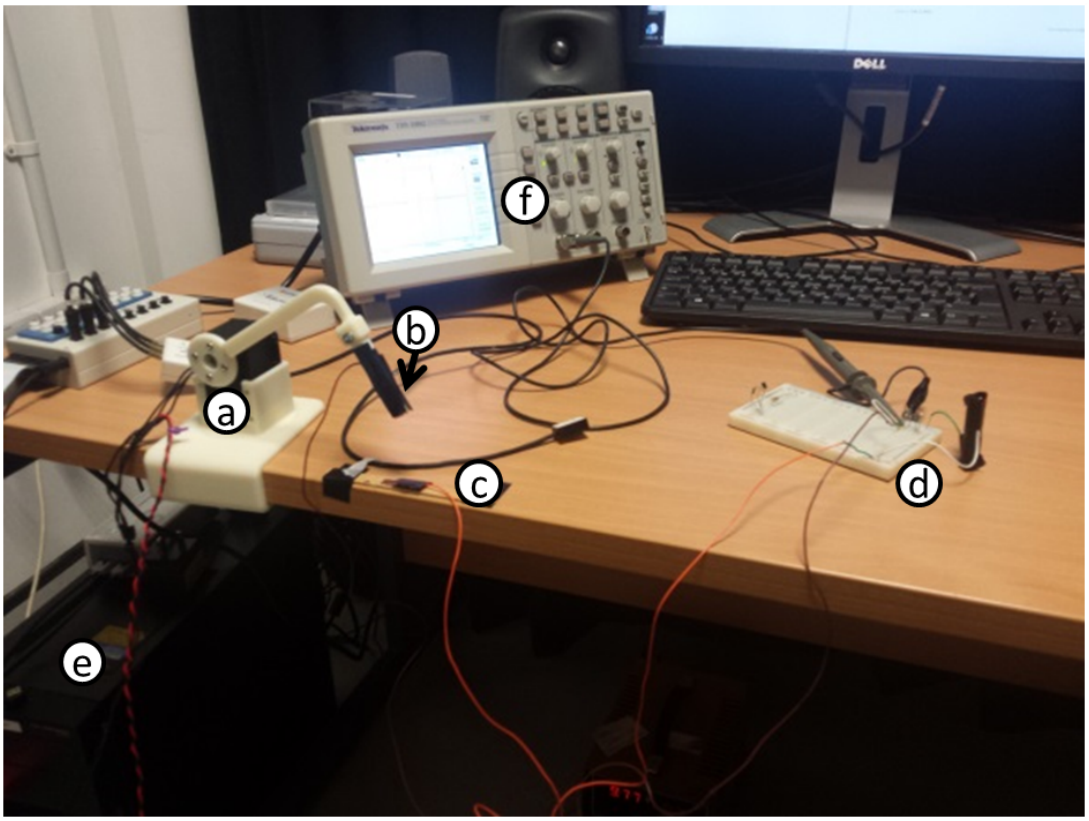

Figure 4.16.: *Test rig for measuring round-trip reaction time between servomotor impact and retraction. 1. The servomotor (a) end-effector (b) was covered in conductive copper tape that could close an open circuit upon impact with the open circuit (c and d); effectively creating a robotic switch. 2. By measuring the current drawn by the servomotor, which sharply increases upon impact with the open circuit, the time of impact can be reported back to the PC controlling the servomotor(e). 3. When a hit is detected by the application, the servomotor is immediately instructed to move in the opposite direction. 4. The voltage of the circuit is monitored by an oscilloscope (f), therefore the 'on' time period of the circuit is a measure of the time between sensing a hit (closing the circuit) and retracting the end-effector (opening the circuit).*

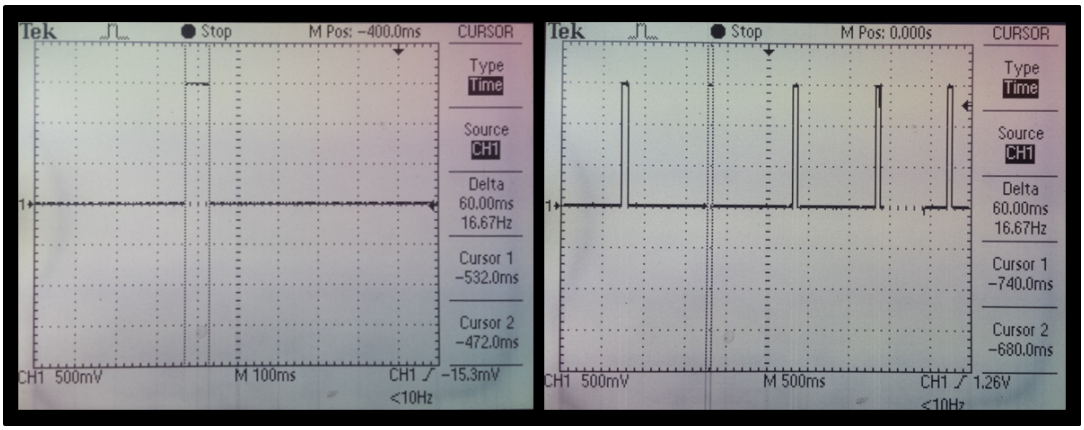

Figure 4.17.: *Oscilloscope recording of circuit voltage modulated by servo impact. Circuit 'on' time measured by the oscilloscope to be 60ms: this is the total time that the circuit remains closed. This is equal to the total time it takes the PC to register the impact of the servomotor with the circuit and to send a signal back to retract the servomotor. Left: single impact, as recorded on the oscilloscope. The voltage rises sharp from 0V to 1.5V when the servomotor closes the circuit. Right: Multiple hits recorded over a 5s period.*

visual cue is shown after the servomotor detects a 'hit' with the participant's body, then delays inherent with signal transmission and the HMD refresh rate could result in significant visuo-tactile asynchronies. To measure the delays of a reactive tactile cue presentation, the test rig presented in Figure 4.16 was developed. Using this test rig the total delay time was measured to be approximately 60ms (i.e. 30ms for the PC to register the impact, and 30ms for the servomotor to receive the instruction to reverse direction, see Figure 4.17). Irrespective of this delay, if a system can only present visual cues after registering a hit then it only produces tactile-leading conditions; whereas a system producing visual-leading conditions must estimate the onset of the tactile stimulation.

A prediction system was developed to minimise the delay in recording a tactile cue, and to allow for visual leading delay conditions. The time of impact can be derived given a known target (by assuming that the participant's hand does not move significantly after each trial) and a controlled speed of the servomotor. At the beginning of each experiment, the servomotor was calibrated and the time and

position of visual cue presentation was derived. This calibration takes into account the position of the participant's hand, a small degree of skin deformation (distance between servomotor first touching the skin and the servomotor's stop position), and a small tolerance. Prediction of the time to hit allowed the presentation of temporally incongruent stimulation, i.e. it was possible to predict when the servomotor would hit the hand thus visual stimulation could be presented ahead of the tactile stimulation. Inversely, for presenting tactile-leading cues, the time at which the servomotor first touched the hand was recorded, and then the visual cue was presented after a specified temporal delay. Using this technique, it was possible to limit the delays to within +/- 16.6ms, which is the period of the Rift's refresh rate (see figure Figure 4.18).

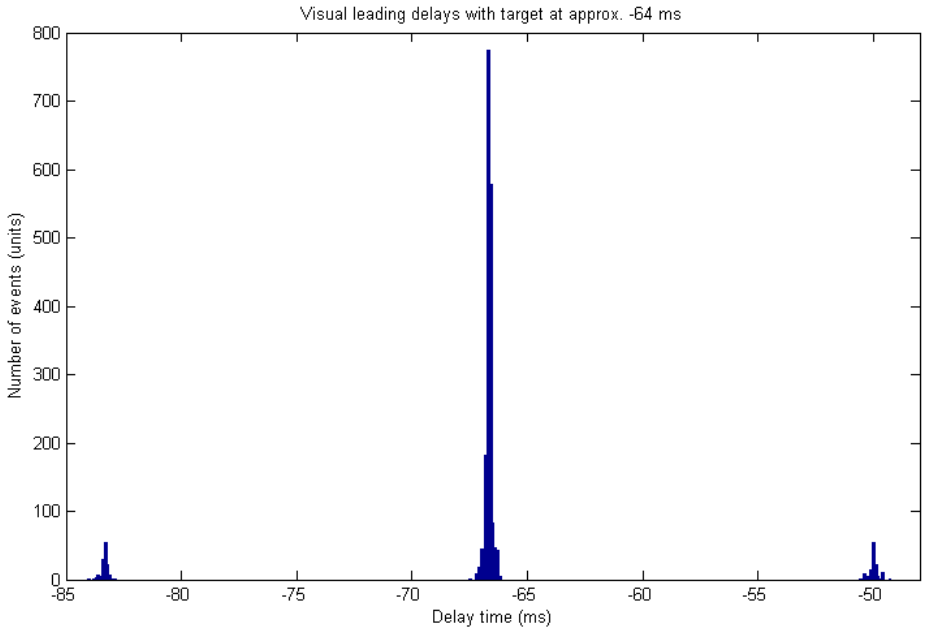

(a) Histogram of delays for visual leading cues with a target delay of approximately -64ms (actual target is -66.6ms, based on the 60Hz refresh rate). Prediction algorithm guarantees +/- 16.6 ms accuracy.

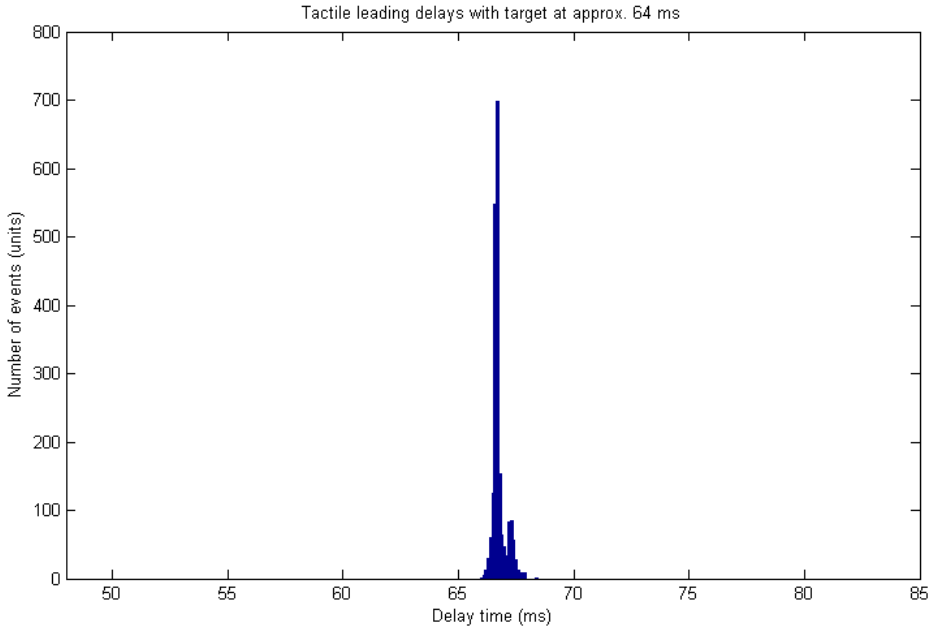

(b) Histogram for tactile leading cues with a target delay of approximately +64ms (actual target is +66.6ms, based on the 60Hz refresh rate). No prediction is necessary in tactile leading condition; time of impact is registered and a fixed delay is added to that time.

Figure 4.18.: *Verification of inter-stimulus delays: histograms showing visual leading and tactile leading delays recorded during Experiment 2. Positive delays correspond to tactile leading stimulation, whereas negative delays correspond to visual leading stimulation.*

4.3.4.3. EEG delays and synchronisation

An important factor for the analysis of the EEG signal is the relative timing between the presentation of cues and change in the EEG signal. Examining the neural activity correlated with a specific cue can provide evidence that supports or disproves hypothesis about the timing of brain mechanisms underlying body ownership and SI. More importantly, accurately reporting the timings allows cross comparison and/or replication of studies.

To measure the delays between EEG signal and the stimulating events in the current experiments the following test platform was used (see Figure 4.19): 1) a digital-to-analogue acquisition (DAQ) card (MF 624, Humisoft®) was used to output a square wave with 250ms pulse/50mV amplitude, and simultaneously record the same wave through its input port (see Figure 4.20, top). This signal was transmitted to a computer where it was registered using an LSL outle, which triggered an event at the positive edge of the square wave. The square wave from the DAQ was also physically connected to the BrainAmp amplifier which recorded the signal and transmitted the signal to the same PC where it was registered by a separate LSL outlet. By measuring the phase difference between the positive edge of the square wave and the positive edge of the BrainAmp signal, the lag of the EEG recording device can be estimated. Given that the DAQ card's input-output delay is in the order of microseconds, this estimated lag is accurate and equivalent to the total BrainAmp recording delay from the electrode to the PC. Using this method, the average delay was measured to be 46.7ms +/- 1ms (see Figure 4.20, bottom). This delay is taken into account when discussing the ERP results in Chapter 6.

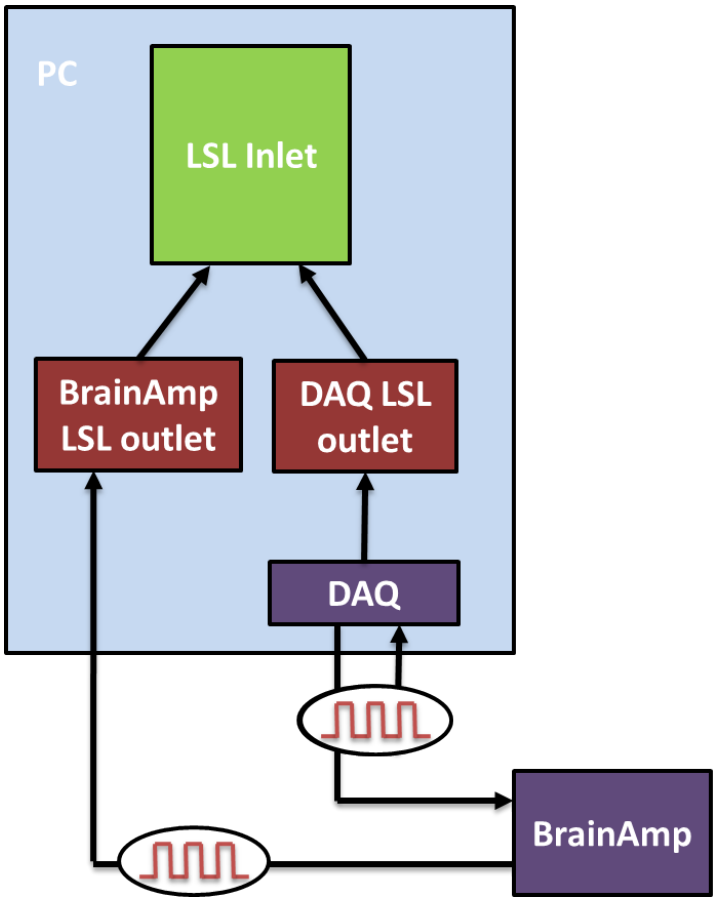

Figure 4.19.: *Test rig for measuring EEG equipment delay. A DAQ card generates a square wave which is simultaneously recorded by an LSL outlet. The same square wave is physically recorded by the BrainAmp and transmitted to an LSL outlet. By comparing the phase difference of the square waves, as recorded in the inlet the delay of the EEG equipment can be measured. Green box: LSL inlet. Red boxes: LSL outlets. Purple boxes: Physical devices. Cyan box: Host PC.*

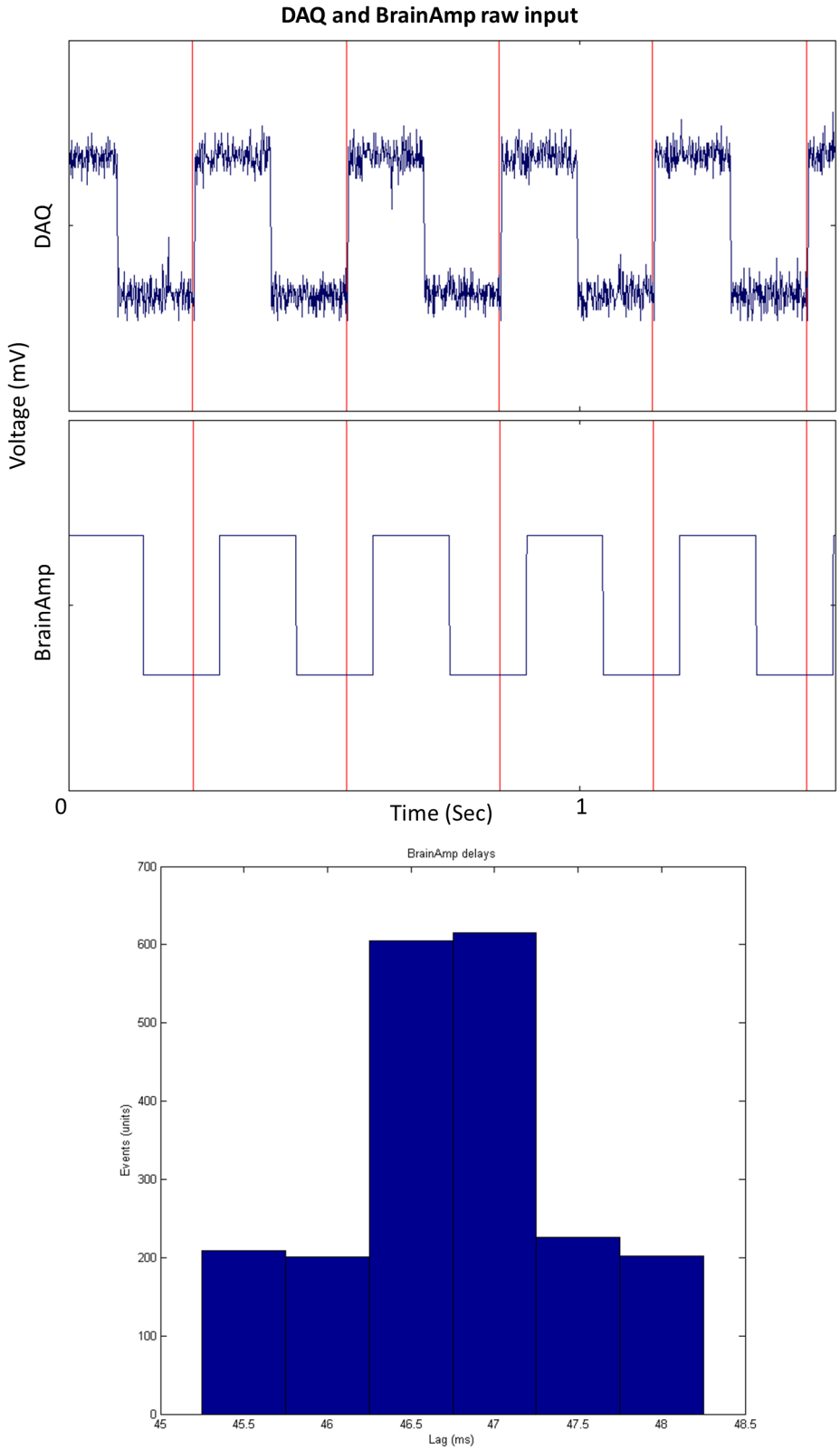

Figure 4.20.: *EEG equipment recording delays. Top: Square-wave signal, as recorded by the DAQ (top) and the BrainAmp amplifier (bottom). Red lines are the time of positive edge detection of the square wave recorded from the DAQ. Bottom: Histogram of BrainAmp recorded delay during a 10min period. Mean delay is 46.7ms with +/- 1ms accuracy.*

4.4. Chapter Summary

This chapter introduced the design of a VR-BOI experimental platform that was used to explore the mechanisms of SI. The chapter cover the entire process of the platform design, from the initial specification and requirements exploration, the validation stage, and finally, the end platform produced for conducting VR-BOI experiments. The chapter discussed the initial techniques that were investigated, the insights and outcomes of each design stage, and the platform elements that were rejected for the end design, along with the reasoning for those decision. The pilot study conducted for the validation stage was outlined and the results showing the suitability of the platform as a research tool for VR/EEG experiments were presented. The chapter also covered the process of producing tools for multisensory stimulation, delay minimisation and data stream synchronisation. In Chapter 5 and 6 two experiments conducted using this VR-BOI platform will be described: a threat-perception based experiment and a stimulus onset asynchrony (SOA) perception experiment. In each experiments, the experimental design and procedure will be overviewed and the analysis of the behavioural and biophysical results obtained will be presented and discussed.

5. Threat perception under visuo-tactile stimulation

This chapter will discuss the results from of an experiment investigating the threat perception under visuo-tactile stimulation, conducted using the VR-BOI platform that was described in Chapter 4. The chapter outlines the aims ans hypothesis of the experiment, presents the methods and the analysis of the self report and biophysical data, and finally discusses the significance of the results in terms of threat perception, body ownership, and sensory integration.

5.1. Aims and Hypotheses

The first experiment focused on earlier experiments on threat by González-Franco et al. (2014) and aimed to replicate their threat experiment in order to further investigate the effect of threat on body ownership using congruent visuo-tactile stimulation. The experiment aimed to investigate multiple markers of ownership, and by recording biophysical signals in combination with subjective reports of ownership, attempted to provide evidence towards an objective, universal method for measuring ownership. The first experimental hypothesis was that visuo-tactile congruence would produce stronger illusion of ownership, with a measurable effect on the brain activity as measured by EEG. The second hypothesis was that the

effect on the EEG from the cross-modal stimulation would be an accurate predictor of illusory ownership.

5.2. Methods

5.2.1. Participants

Twenty seven healthy participants (7 females, age range: 18 - 28yr, mean age: 20yr) were recruited from the University of Reading. The experimental design was reviewed and approved by the University of Reading, School of System Engineering, Ethics Committee. All subjects gave written consent to participate in the study and were compensated £10 for their time. Participants were right handed with normal or corrected to normal vision.

5.2.2. Procedure

At the beginning of each session, the participants were briefed on the experiment and were given a demonstration of the virtual environment, servomotor and end-effector, and the input system for answering the questionnaire presented in the VR environment (see Figure 4.14, Figure 4.15). The questions were answered on a 7 point Likert scale ("strongly disagree" to "strongly agree") and were recorded on a scale of -3 to +3 corresponding to "strongly disagree" and "strongly agree" respectively, where 0 represented "neutral" (see Table 5.4). After the briefing, the participants were prepared for EEG, ECG, EMG and SCR recordings. The participants took part in two experiments: Experiment 1 discussed in this section, and Experiment 2 discussed in the following Chapter. One participant was excluded from the analysis of Experiment 1 due to reporting no ownership. Each experiment lasted ~30min with a 5-10min break between the experiments. The

order of the experiments was randomly chosen *a priori* and was counterbalanced to avoid order bias. The participant wore the Rift throughout both experiments, but during the break between experiments the HMD was switched off to avoid fatigue.

5.2.3. Stimuli

This experiment aimed to investigate the behaviour of the subject as a function of multisensory stimulation. Each trial would start with the participant being instructed to look at their virtual right hand for approximately 10s. After that period, in the virtual environment a knife would appear in one of two places: i) in the middle of the table, approximately 20cm from the participant's hand, or ii) inside the participant's hand (see Figure 5.1). During the same trial the participant's real hand would be touched or not touched by the servomotor end-effector mock knife. Four conditions were thus obtained:

1. Knife seen in the hand only ('Hand' condition)
2. Knife seen in the table only ('Table' condition)
3. Knife seen in the hand and felt on the hand ('Hand & Feel' condition)
4. Knife seen in the table but felt on the hand ('Table & Feel' condition)

The stimulation lasted for 3s after which the knife disappeared, and the servomotor returned to its original location. It is important to note that the servomotor makes noise during movement, thus to avoid participants adjusting to the auditory cue, the servomotor would move in the opposite direction (away from the physical hand) during the 'seen only' conditions such that it would not prime the participant to which condition was about to be presented. After the stimulation, the subject was asked a question at random from a pool of three questions (questions 1-3, see Table 5.3). The reasons for including the per-trial questions were twofold: 1) a

more robust account of the experience was expected, and 2) the question acted as in-between task that separates trials. A block consisted of 40 trials, 10 of each condition, presented at a random order and lasted about 9 minutes. At the end of each block the participants were prompted to respond to seven questions, see Table 5.2. The entire experiment comprised three blocks for a total of 120 trials per subject. A summary of the experimental design is shown in Table 5.1.

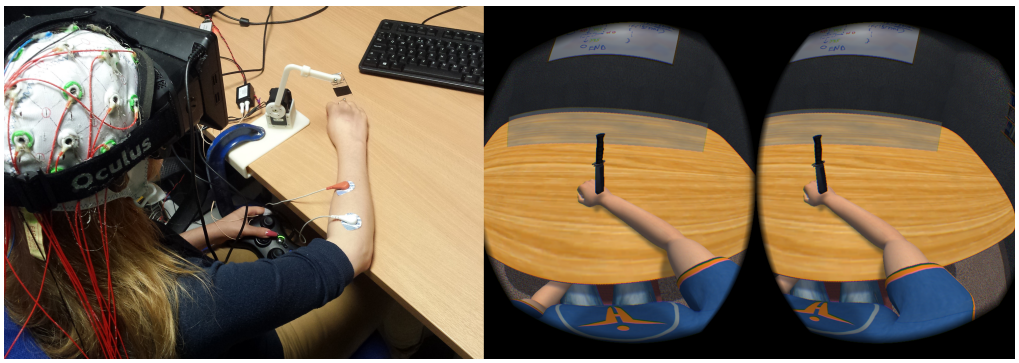

Figure 5.1.: *Experimental setup for threat perception experiment (Experiment 1). Left: Participant during the experiment. The servomotor is equipped with the mock knife end-effector. Right: The virtual environment from the point of view of the participant and threatening visual cue presentation*

Table 5.1.: *Experimental design for experiment 1. 2x2 factorial design with 1 factor the location of the visual threat (hand/table) and another the presentation of the tactile cue.*

		Visual stimulation of knife	
		Knife at Hand	Knife at Table
Tactile stimulation of hand	w/ stimulation	Hand and Feel	Table and Feel
	w/out simulation	Hand only	Table only

Table 5.2.: *Block questionnaire for experiment 1 (threat experiment). The entire questionnaire is asked at the end of each of the three, 40-trial long blocks.*

Knife experiment questions
1) I had the feeling that I might be harmed when I saw the knife inside the hand but didn't feel it
2) I had the feeling that I might be harmed when I saw the knife outside the hand and didn't feel it
3) I had the feeling that I might be harmed when I saw and felt the knife on the hand at the same time
4) I had the feeling that I might be harmed when I felt the knife on the hand but saw it on the table
5) I saw the knife as a threat to my body
6) I felt as if the hand I saw in the virtual world might be my hand
7) The hand I saw was the hand of another person
8) The hand I saw resembles my own hand in terms of shape, skin tone, freckles, etc.

Table 5.3.: *Per trial questions for experiment 1 (threat experiment). After each trial, one of these questions was presented to the participant at random.*

Knife experiment questions
1) I felt as if the hand I saw in the virtual world might be my hand
2) The hand I saw was the hand of another person
3) I saw the knife as a threat to my body

Table 5.4.: *Available answers for participants to choose from for answering each question. Participants saw the answers as the column on the left. Analysis of results herein is presented using the numerical equivalent on the right column.*

Answer	Numerical representation
Strongly disagree	-3
Disagree	-2
Somewhat disagree	-1
Neutral	0
Somewhat agree	+1
Agree	+2
Strongly agree	+3

5.2.4. Data analysis

The answers from the VR questionnaires were imported into R and were analyses using a linear mixed effect model. The four conditions were defined as a fixed effect for the model with each block and participant being treated as a random effect to account for the repeated measure design of the experiment. Multiple comparison correction for P-values was performed post-hoc in using the Bonferroni method and the multcomp and lsmeans R packages (Hothorn et al., 2008; Lenth, 2016). SCR response was measured as the difference between the maximum and minimum peak post stimulus and was analysed using the same method in R. EEG data was first pre-process for analysis (see Section 4.3.3). Artefact-free EEG processing for ERP presentation and analysis was performed using the Mass Univariate ERP Toolbox, and statistical significance per time point was tested using the t-test false discovery rate method by Benjamini and Hochberg (1995).

5.3. Results

5.3.1. BOI under visuo-tactile threat

Experiment 1 explored the visuo-tactile stimulation effect on ownership and bodily threat. In this experiment, participants were asked to respond to: a) the full experimental questionnaire after each block of 40 trials (see Table 5.2), and b) a single question randomly selected from a set of three questions after each trial (Q.1 - Q.3, Table 5.3). In the block questionnaires, the report of ownership (Q.6) averaged across all participants was positive (median = +1), and significantly different to the dis-ownership report (Q.7, median = -1, $F(1,77) = 262$, $P < 0.001$, see Figure 5.2). Answers between ownership and dis-ownership were negative correlated (Pearson's $\rho = -0.55$, $P < 0.001$). Taken together, these results suggest

that the experiment succeeded in eliciting BOI. The virtual arm was shown to be similar to the actual arm of the participants (22 participants reported positive in Q.8, median across all participants = +1). Answers to questions Q.6 and Q.8 were positively correlated (Pearson's $\rho = 0.48$, $P < 0.001$).

Block questions on the feeling of threat per conditions (Q.1 - Q.4. see Figure 5.3, top) were analysed for the effect of each condition on perceived threat. ANOVA showed that there was a significant difference on the reported level of threat per condition ($F(3,231) = 85.36$, $P < 0.001$) . Post-hoc analysis showed that participants reported the highest perception of threat upon congruent visual and tactile stimulation condition ('Hand & Feel' median = +2, $P < 0.001$ when compared against all other conditions). In the block questionnaires, no significant difference was observed between the 'Hand' and the 'Table & Feel' condition (for both, median = 0). Finally, the 'Table' condition resulted in the lowest perception of threat (median = -2).

Similar results on threat perception were obtained with the per trial questions (ANOVA: $F(3,985) = 206$, $P < 0.001$, see Figure 5.3, bottom): the 'Hand & Feel' condition resulted in the highest reports of threat (median = +1), and the 'Table' condition resulting in the lowest reports of threat (median = -2). In contrast to the block questionnaires, a significant difference in the report of threat was observed between the 'Hand' and 'Table & Feel' responses ('Hand' median = 0, 'Table & Feel' median = -1, $P < 0.01$).

The per trial questions showed that the highest reports of ownership in the 'Hand & Feel' condition (median = +2) followed by the 'Table' condition (median = +1) (ANOVA: $F(3,1063) = 214.4$, $P < 0.001$ see Figure 5.4, top). The 'Hand' condition responses were neutral (median = 0), and the 'Table & Feel' responses showed the lowest strength in ownership (median = -1). The per trial responses for the dis-ownership were symmetrical to the responses for the ownership question,

further indicating that BOI was elicited during the experiment (ANOVA: F(3,985) = 154.6, P < 0.001Figure 5.4, bottom).

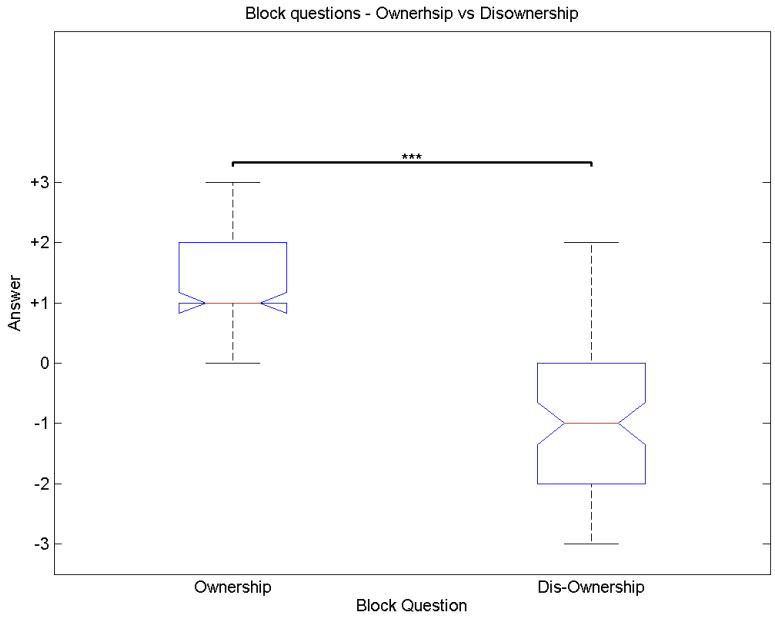

Figure 5.2.: *Ownership and dis-ownership, as reported in the end of block trials questions. *** : corresponds to p-values at 0.001 significant level. Red line is the median, top and bottom of boxes are the 75th and 25th percentile, respectively, whiskers correspond to approximately 99%.*

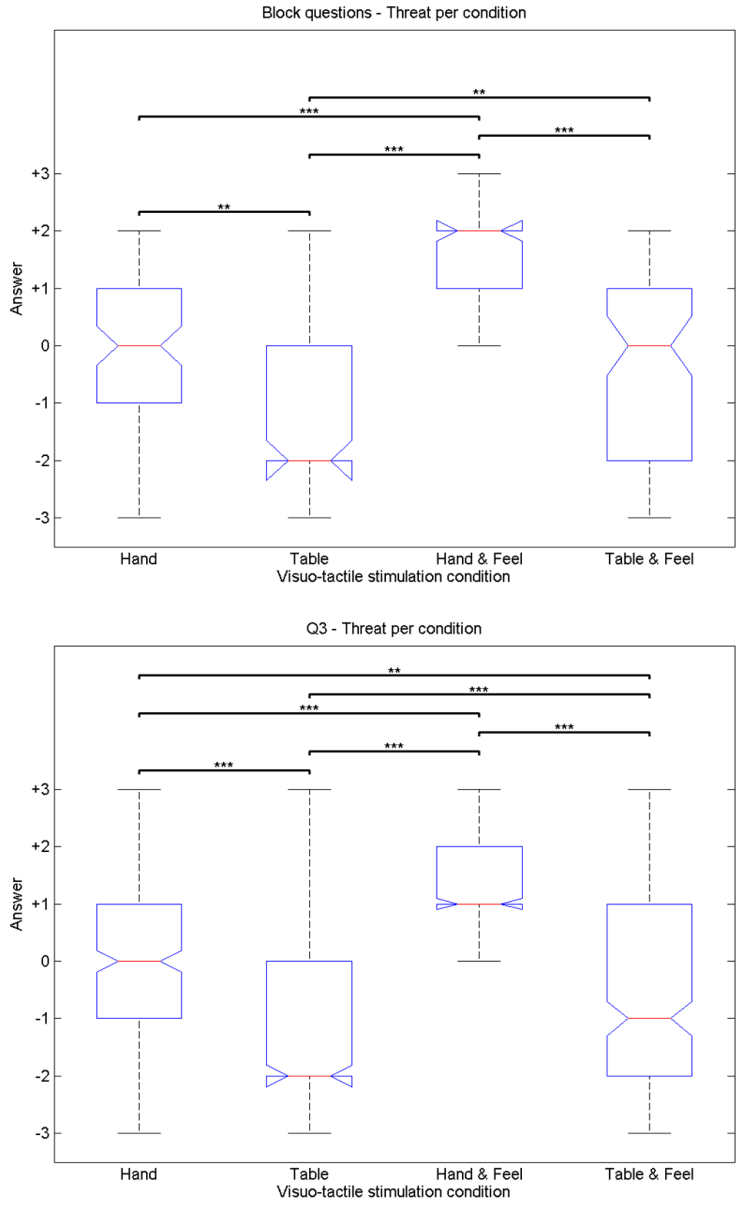

Figure 5.3.: *Reports of threat for each condition reported per trial and per block. Top: responses for felt bodily threat per condition, asked at the end of the block. Bottom: responses for felt bodily threat per condition when asked after each trial. * , **, *** : correspond to p-values at 0.05, 0.01 and 0.001 significant level, respectively. Red line is the median, top and bottom of boxes are the 75th and 25th percentile, respectively, whiskers correspond to approximately 99%.*

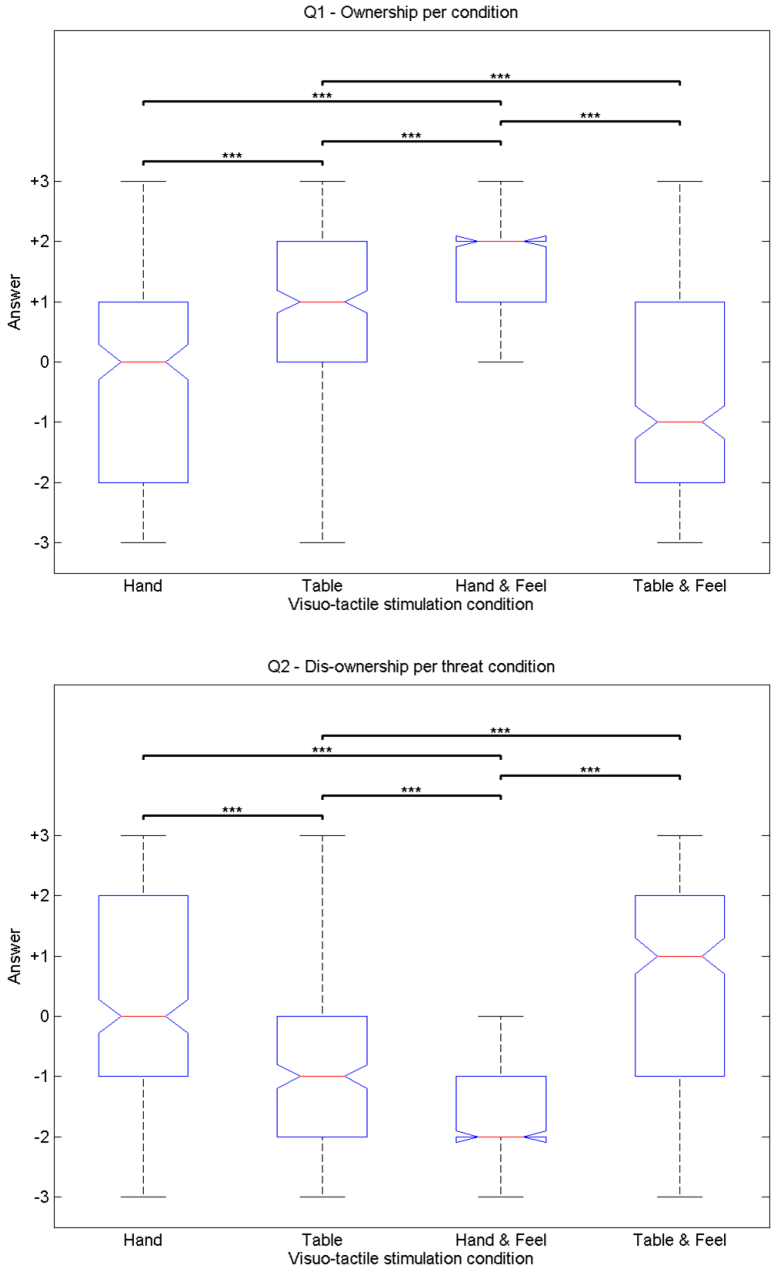

Figure 5.4.: *Ownership (top) and dis-ownership (bottom) reports per in per trial question. * , **, *** : correspond to p-values at 0.05, 0.01 and 0.001 significant level, respectively. Red line is the median, top and bottom of boxes are the 75th and 25th percentile, respectively, whiskers correspond to approximately 99%.*

5.3.2. Skin conductance response - measure of threat

SCR was recorded in Experiment 1 as a biophysical measure of the emotional response to threat (see Section 3.2.2). The SCR response for each trial was measured as the difference in micro Siemens (μS) between the maximum and minimum values of the SCR signal recorded in the 4s post-stimulus period. Trials were grouped by condition and participant, statistical analysis showed a significant effect on SCR between conditions ($F(3,1582) = 8.5$, $P < 0.001$). A post-hoc multiple comparison test (Bonferroni) showed a significant difference between the tactile conditions ('Hand & Feel', 'Table & Feel') and the 'Table' conditions ($P < 0.001$ and $P < 0.01$, respectively, see Figure 5.5). Additionally, the 'Hand' and 'Hand & Feel' conditions had significantly different SCR responses ($P = 0.036$, see Figure 5.5). Overall, the results showed that the tactile conditions had the largest SCR response, followed by the 'Hand' condition, with the 'Table' condition showing the smallest SCR response.

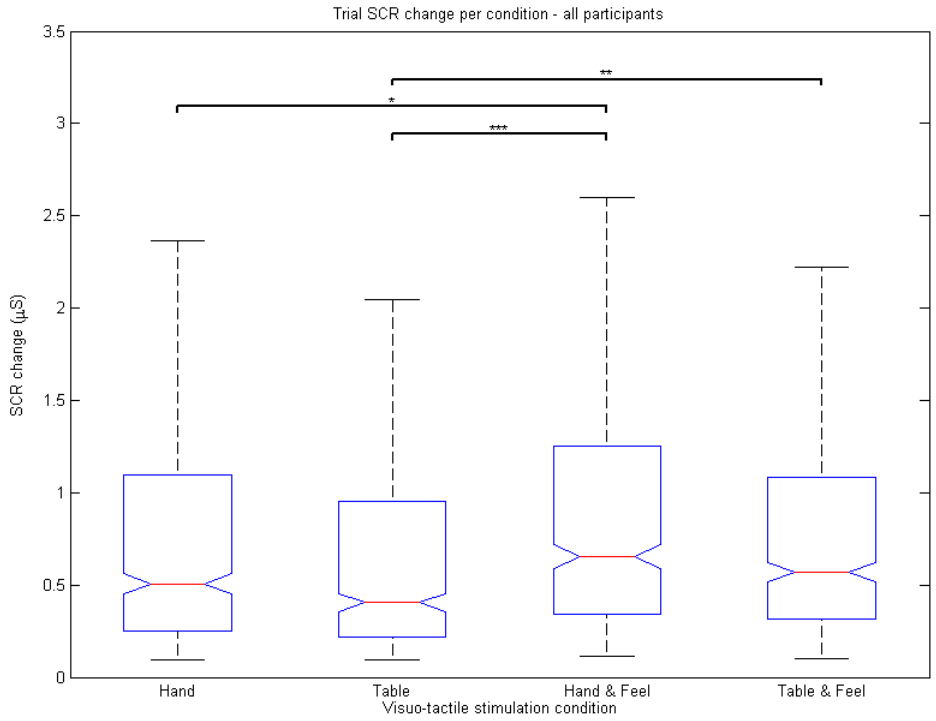

Figure 5.5.: *Comparison of post-stimulus SCR response per condition. The 'Table' condition has the lowest SCR response. * , **, *** : correspond to p-values at 0.05, 0.01 and 0.001. Red line is the median, top and bottom of boxes are the 75th and 25th percentile, respectively, whiskers correspond to approximately 99%.*

5.3.3. Event related potentials - measure of threat

Artefact-free EEG (see Chapter 5) recordings from each trial were baseline corrected using the 200ms pre-stimulus period to analyse the ERP components (see Figure 5.6 and Figure 5.7 for grand average ERP per electrode, and Figure 5.8 for grand average ERP per condition type). ERP components identified (ERP component time corrected for EEG equipment recording delays, see Section 4.3.4) were: a tactile P100 (60ms post-tactile stimulus), a visual P200 (150ms post-visual stimulus), and a threat based P400 (300-400ms post-stimulus). An N200 was also observed in all conditions (peak ranging with 200-250ms post-stimulus). Finally, a P500 was observed in the 'Table' condition only.

To investigate differences in the ERP components between conditions, the ERP taken from pairs of conditions were subtracted, with the resulting activity in the range of 0-500 ms post-stimulus tested against the null hypothesis of having a mean of 0μV. Significant deviations of the subtracted activity from the 0μV mean correspond to a significant difference between the conditions. In the 'Hand' / 'Table' pair, the P200 and P400 were shown to be significantly larger in the 'Hand' condition, whereas a P200b (200ms post stimulus) was observed in the 'Table' condition that was not observed in the 'Hand' condition (see Figure 5.9). Differences in the P400 condition were observed mostly in the posterior and anterior electrodes of the right hemisphere. In the 'Hand & Feel' / 'Table & Feel' pair, the 'Hand & Feel' condition significant difference was observed in the N200 component (see Figure 5.10).

The 'Hand & Feel' / 'Table' pair showed significant difference in the P100, N200/P200b, and P400. The differences in P400 between the 'Hand & Feel' / 'Table' pair were observed mostly in the right hemisphere, over the central electrodes (see Figure 5.11). These differences in ERP activity were also observed in the 'Table & Feel' / 'Table' pair (see Figure 5.12).

The 'Hand & Feel' / 'Hand' pair showed similar ERP activity differences to the 'Hand & Feel'/ 'Table' pair with one main difference: the two conditions had very little difference in the P400 component with the 'Hand' condition showing a slightly stronger P400 peak in the occipital electrodes and the 'Hand & Feel' condition showing stronger P400 in the central electrodes (see Figure 5.13). Furthermore, no difference in the P200b was shown, in contrast with the 'Hand & Feel'/ 'Table' pair, due to the absence of the P200b component in both the 'Hand' and the 'Hand & Feel' conditions. Stronger P400 in the posterior electrodes was observed more clearly (larger amplitude of difference across more electrodes and longer duration) in the 'Table & Feel' / 'Hand' pair, with the rest of the differences being similar to differences observed in the 'Hand & Feel' / 'Hand' pair (see Figure 5.14).

To summarise the results, a P400 modulated by threat was observed. The P400 component was more pronounced in the right hemisphere, with the visual harm condition ('Hand') resulting in stronger P400 in the posterior electrodes, whereas the tactile harm conditions resulted in P400 recorded more strongly over the central electrodes.

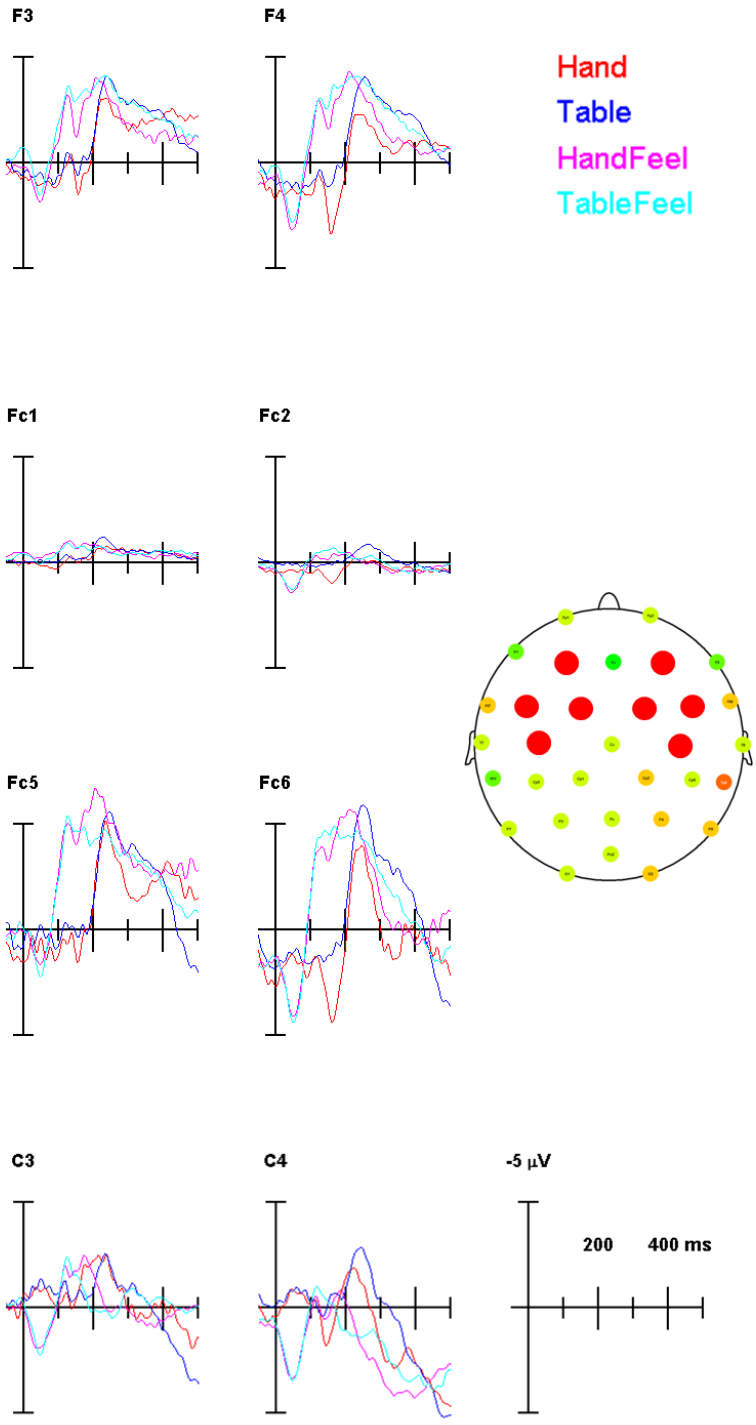

Figure 5.6.: *Grand average ERP per electrode: anterior electrodes. Time at 0ms corresponds to the presentation of stimulation. Each coloured trace shows the ERP for a given condition type (see legend top right). Red circles on the topographic map indicate location of electrodes.*

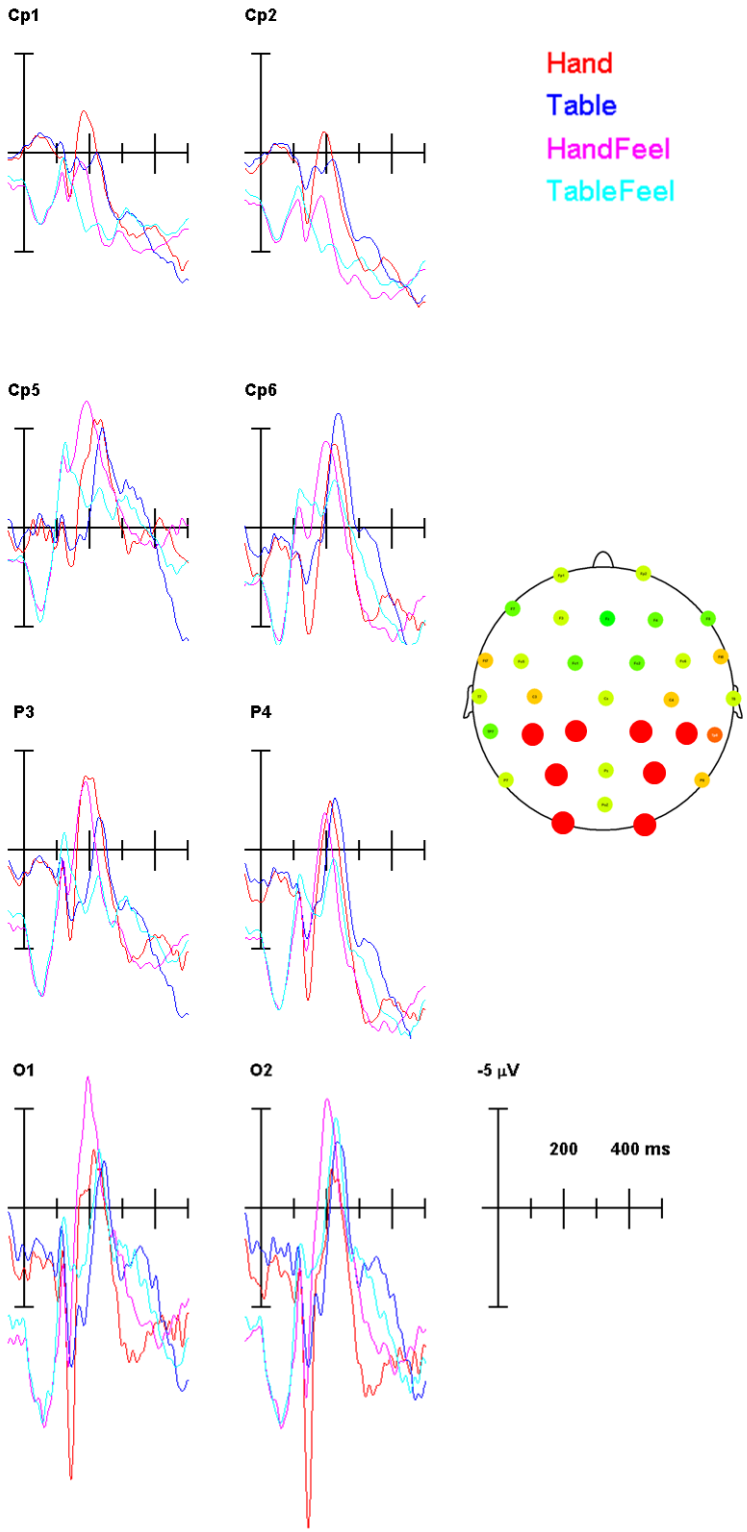

Figure 5.7.: *Grand average ERP per electrode: posterior electrodes. Time at 0ms corresponds to the presentation of stimulation. Each coloured trace shows the ERP for a given condition type (see legend top right). Red circles on the topographic map indicate location of electrodes.*

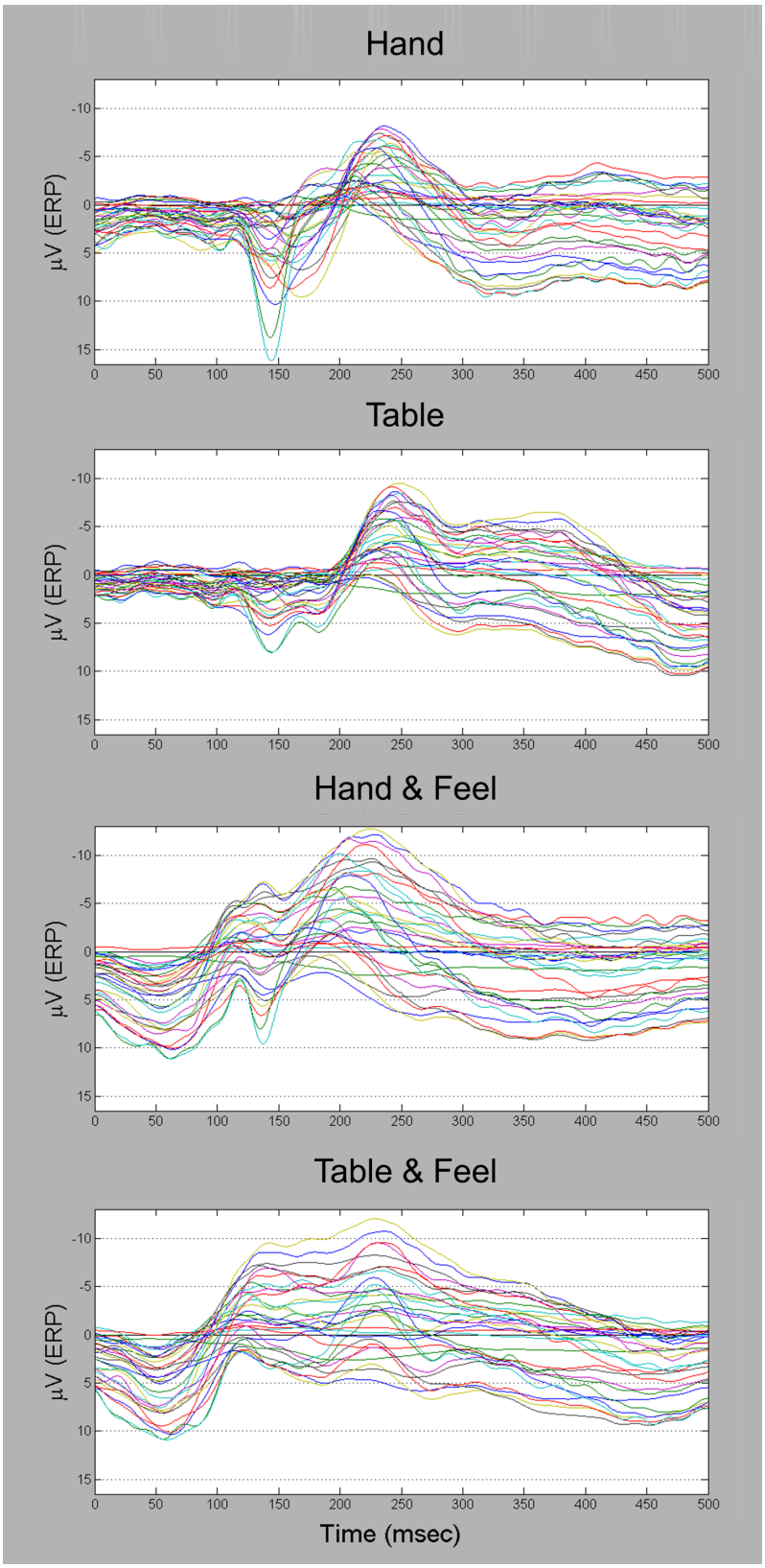

Figure 5.8.: *Grand average ERP of all channels per condition type. Each ERP plot shows the grand average for the condition indicated in the tile above the plot. Each coloured trace corresponds to ERP activity from a single electrode, averaged across all participants. Time at 0ms corresponds to the presentation of stimulation.*

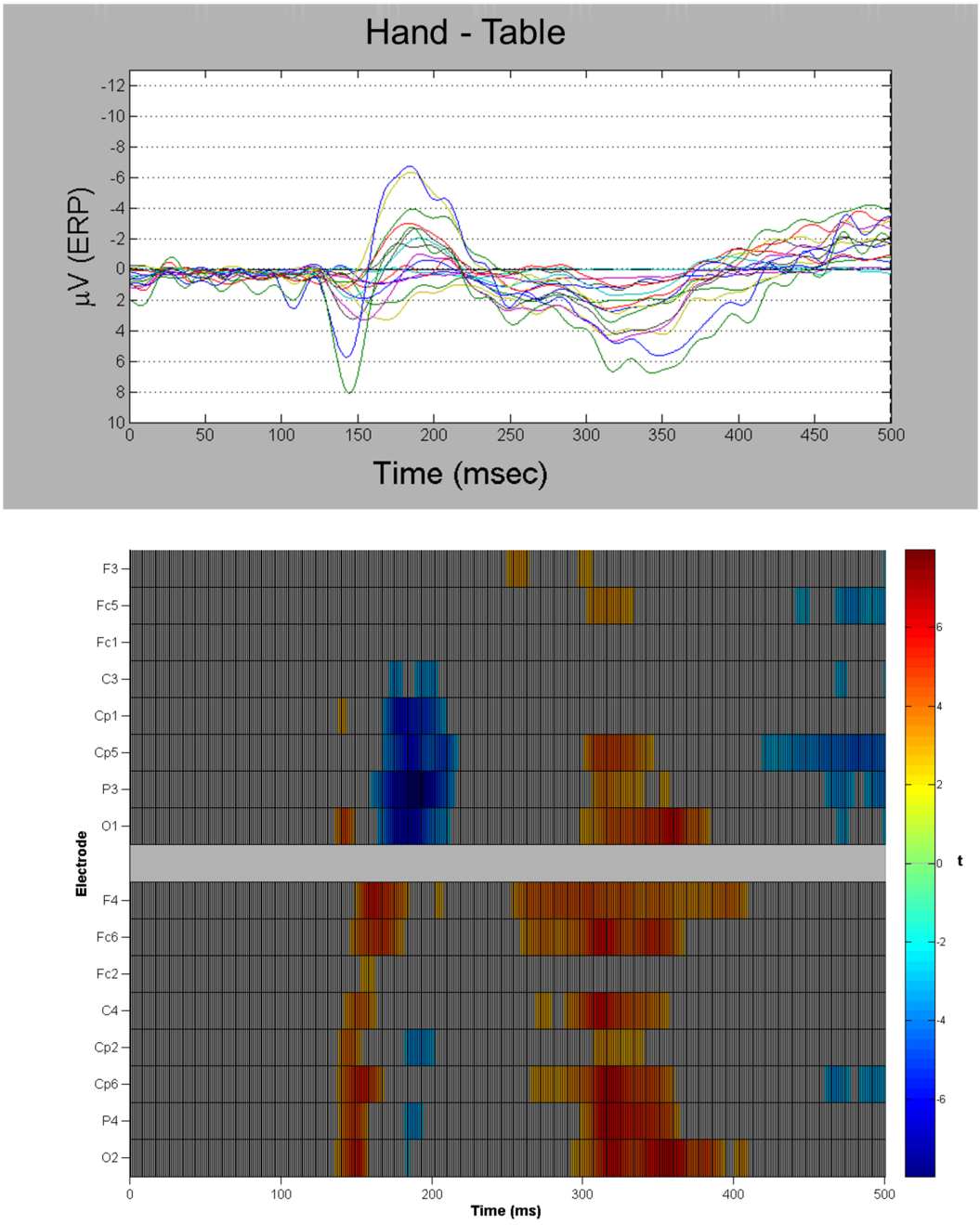

Figure 5.9.: *ERP component differences between the 'Hand' and 'Table' conditions. Top: Subtraction result of the 'Hand' - 'Table' ERP activities. Each coloured trace corresponds to ERP activity from a single electrode, averaged across all participants. Bottom: Raster plot indicating the timing and electrode where significant difference of the resulting ERP from the 0μV mean was detected. Red hues correspond to positive deviation from the mean, whereas blue hues correspond to negative difference. Only significant differences are shown in the raster plot: differences with a p value greater than 0.05 as corrected with the false detection rate method are shown in grey. Significant differences are detected at P200, P200b, and P400. Time at 0ms corresponds to the presentation of stimulation.*

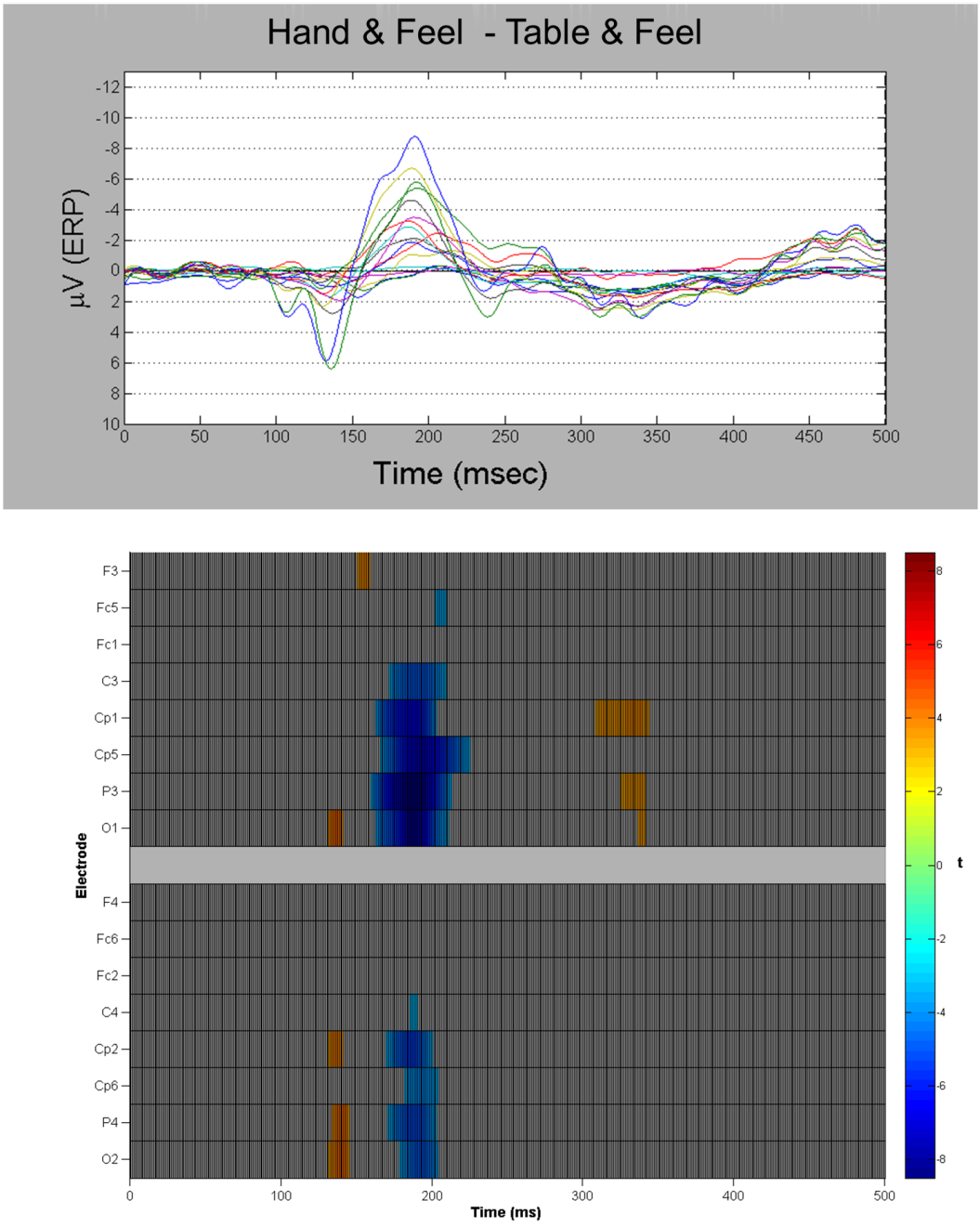

Figure 5.10.: *ERP component differences between the 'Hand & Feel' and 'Table & Feel' conditions. Top: Subtraction result of the 'Hand & Feel' - 'Table & Feel' ERP activities. Each coloured trace corresponds to ERP activity from a single electrode, averaged across all participant. Bottom: Raster plot indicating the timing and electrode where significant difference of the resulting ERP from the 0μV mean was detected. Red hues correspond to positive deviation from the mean, whereas blue hues correspond to negative difference. Only significant differences are shown in the raster plot: differences with a p value greater than 0.05 as corrected with the false detection rate method are shown in grey. Significant difference detected at N200. Time at 0ms corresponds to the presentation of stimulation.*

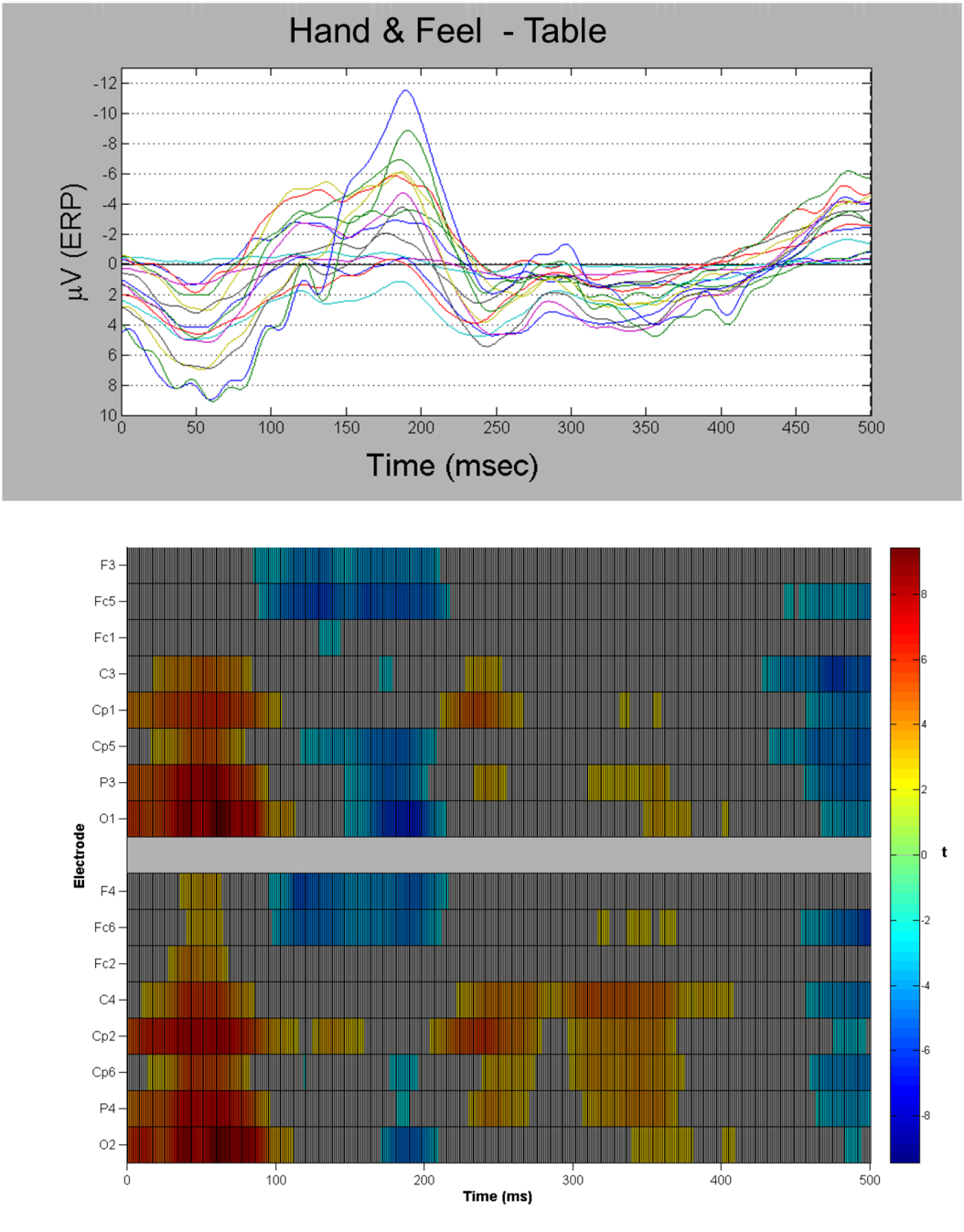

Figure 5.11.: *ERP component differences between the 'Hand & Feel' and 'Table' conditions. Top: Subtraction result of the 'Hand & Feel' - 'Table' ERP activities. Each coloured trace corresponds to ERP activity from a single electrode, averaged across all participant. Bottom: Raster plot indicating the timing and electrode where significant difference of the resulting ERP from the 0μV mean was detected. Red hues correspond to positive deviation from the mean, whereas blue hues correspond to negative difference. Only significant differences are shown in the raster plot: differences with a p value greater than 0.05 as corrected with the false detection rate method are shown in grey. Significant difference detected at P100, N200/P200b, and P400. Time at 0ms corresponds to the presentation of stimulation.*

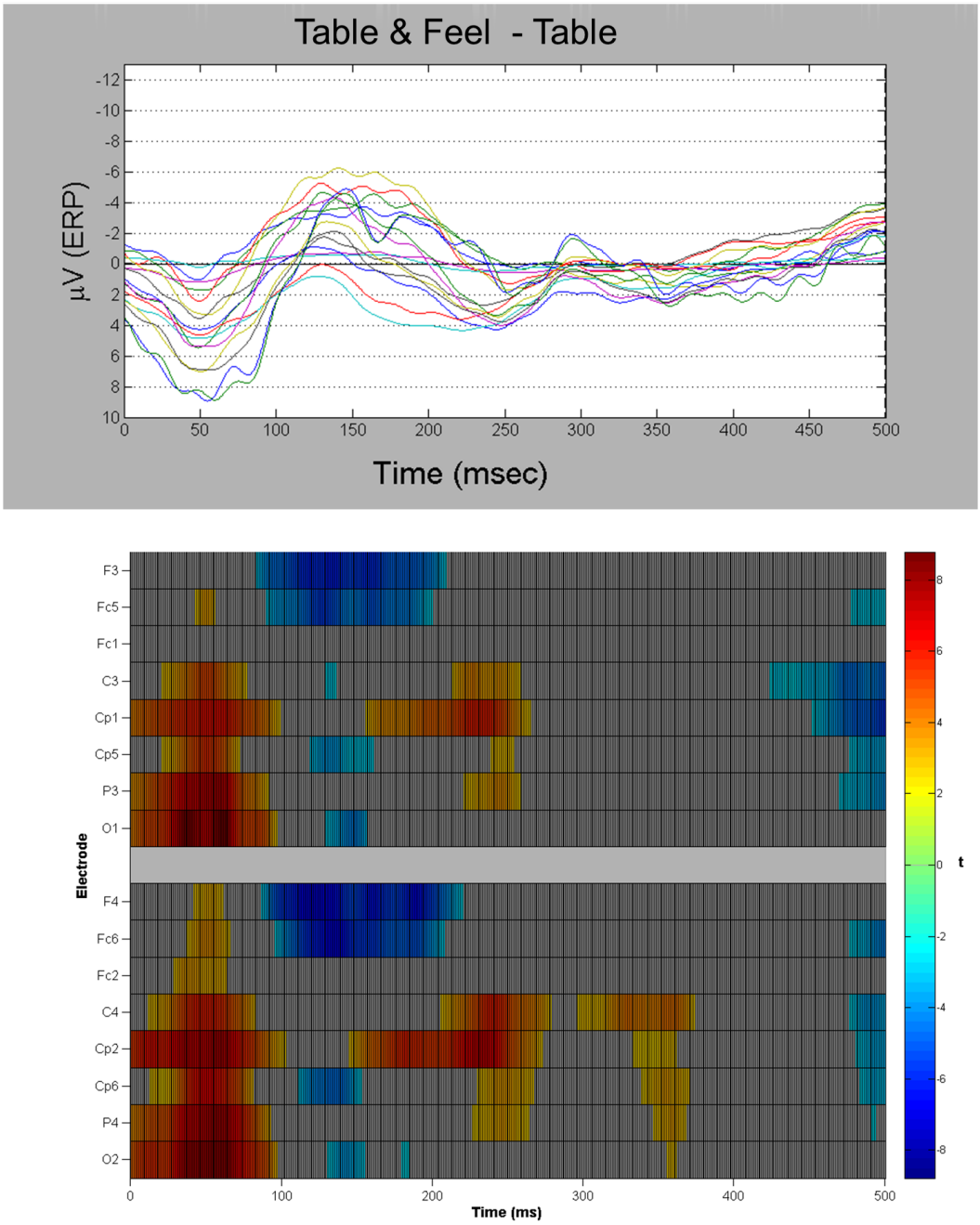

Figure 5.12.: *ERP component differences between the 'Table & Feel' and 'Table' conditions. Top: Subtraction result of the Table & Feel' - 'Table' ERP activities. Each coloured trace corresponds to ERP activity from a single electrode, averaged across all participant. Bottom: Raster plot indicating the timing and electrode where significant difference of the resulting ERP from the 0μV mean was detected. Red hues correspond to positive deviation from the mean, whereas blue hues correspond to negative difference. Only significant differences are shown in the raster plot: differences with a p value greater than 0.05 as corrected with the false detection rate method are shown in grey. Significant difference detected at P100, N200, and P400. Time at 0ms corresponds to the presentation of stimulation.*

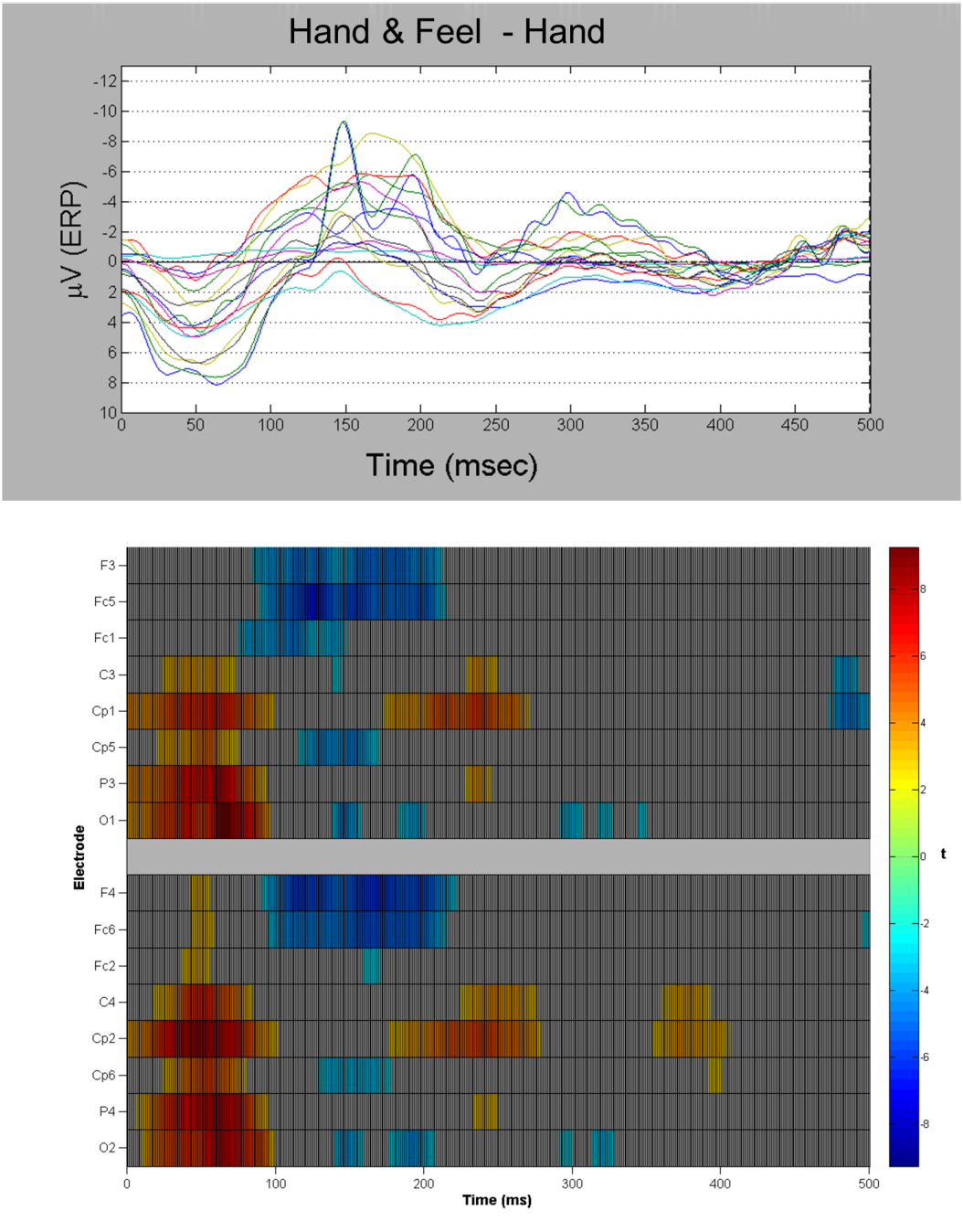

Figure 5.13.: *ERP component differences between the 'Hand & Feel' and 'Hand' conditions. Top: Subtraction result of the 'Hand & Feel' - 'Hand' ERP activities. Each coloured trace corresponds to ERP activity from a single electrode, averaged across all participant. Bottom: Raster plot indicating the timing and electrode where significant difference of the resulting ERP from the 0μV mean was detected. Red hues correspond to positive deviation from the mean, whereas blue hues correspond to negative difference. Only significant differences are shown in the raster plot: differences with a p value greater than 0.05 as corrected with the false detection rate method are shown in grey. Significant difference detected at P100, N200, and P400. Time at 0ms corresponds to the presentation of stimulation.*

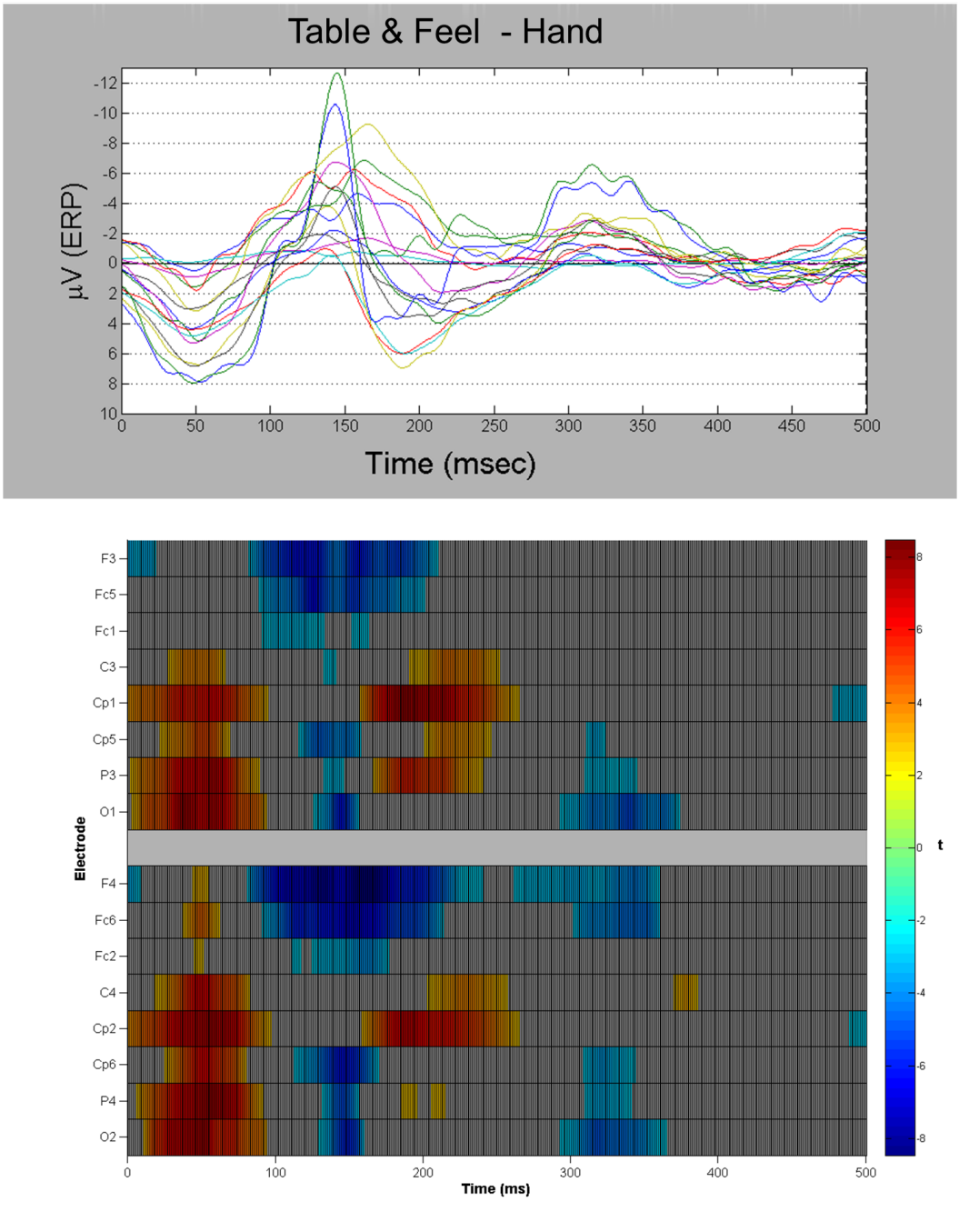

Figure 5.14.: *ERP component differences between the 'Table & Feel' and 'Hand' conditions. Top: Subtraction result of the 'Table & Feel' - 'Hand' ERP activities. Each coloured trace corresponds to ERP activity from a single electrode, averaged across all participant. Bottom: Raster plot indicating the timing and electrode where significant difference of the resulting ERP from the 0µV mean was detected. Red hues correspond to positive deviation from the mean, whereas blue hues correspond to negative difference. Only significant differences are shown in the raster plot: differences with a p value greater than 0.05 as corrected with the false detection rate method are shown in grey. Significant difference detected at P100, N200, and P400. Differences in the P400 between the 2 conditions are of larger amplitude than the differences between the 'Hand & Feel' and 'Hand' pair. Time at 0ms corresponds to the presentation of stimulation*

5.4. Discussion of behavioural results

5.4.1. Multisensory threat affects ownership

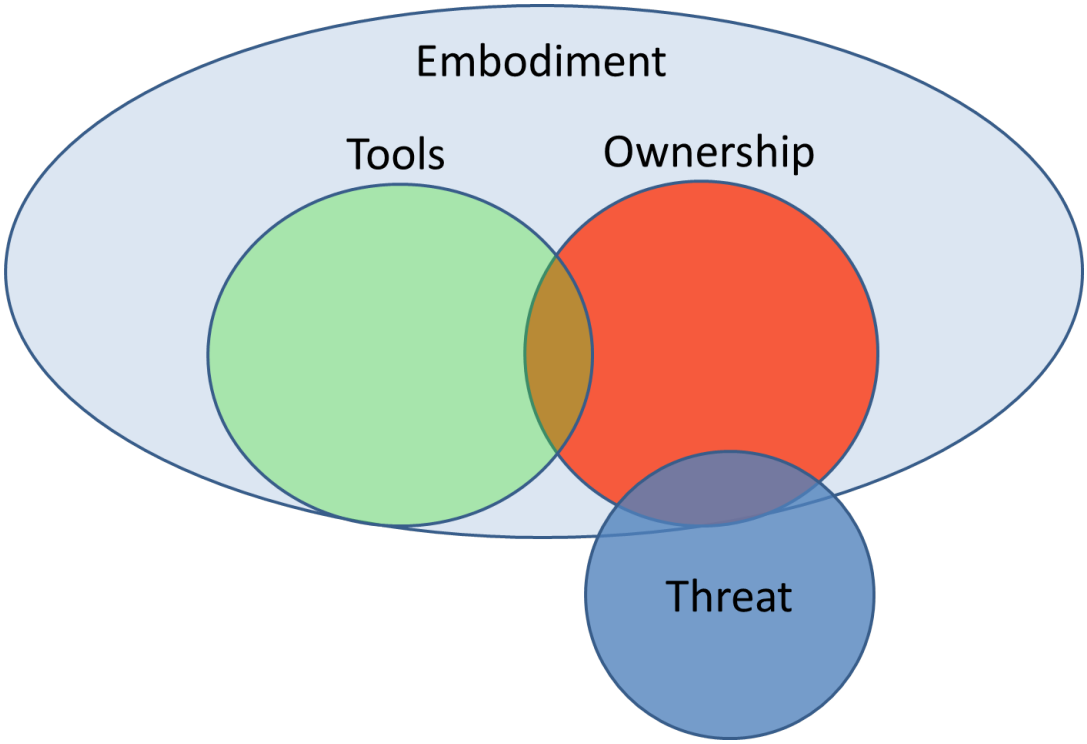

Figure 5.15.: *Venn diagram illustrating the introduction of threat perception in embodiment. In the questionnaire reports a separation of the perception of body ownership and bodily threat were observed. This could be due to distinct brain mechanisms responsible for eliciting the two senses. Threat outside the boundaries of embodiment corresponds to empathy Fan and Han (2008).*

The results from Experiment 1 showed that congruent visuo-tactile stimulation produced the highest perception of ownership and bodily threat. This was an expected result. As discussed in Chapter 3, body ownership is a result of multisensory convergence, and by introducing more congruent evidence supporting the illusion, a stronger BOI is achieved. Experiment 1 used two methods for presenting self-report questionnaires: a single question was presented after each trial and a full questionnaire was shown after a block of trials. Both methods reported similar results, as shown in the results from the threat perception (see Figure 5.3), and

the per trial method introduced an enhancement in the analysis of self-reports, which is discussed below.

Subjective reports showed that congruent visuo-tactile stimulation resulted in the highest threat perception, followed by conditions that presented only one threatening cue (visual or tactile), and finally the condition with no threatening cues. The threat results are consistent with studies on body ownership and threat: as previously discussed (see Section 3.2), presenting threatening stimulation on, or near, an illusory owned body part elicits feelings of threat and anxiety (Armel and Ramachandran, 2003; Ehrsson et al., 2007; González-Franco et al., 2014; Guterstam et al., 2011). Furthermore, the results were consistent with the study of González-Franco et al. (2014), in that no reports of threat were observed when the threatening stimulation was presented away from the hand ('Table' condition). In addition, the results presented confirm the expectations from Gonzalez-Franco et al., that congruent visuo-tactile stimulation enhances the effect observed in terms of threat and ownership.

These results expand on these previous studies, by specifically investigating the threat and ownership during single trials of a specific experimental condition, as found by self-report questionnaires. In contrast with Gonzalez-Franco et al., who captured the participants' feeling of ownership at the end of each block, Experiment 1 characterises reports of ownership and threat for individual trials. Interestingly, it was shown that reports of ownership and threat are not necessarily correlated: both the 'Hand' and 'Table & Feel' conditions which presented a threatening stimulation to the hand (visual, or tactile stimulation, respectively), resulted in reports of higher threat perception than the non-threatening 'Table' conditions, but also were associated with reports of significantly lower ownership. This is a novel result that separates ownership from bodily threat (see Figure 5.15); ownership and bodily harm have been correlated in previous studies, and used as

an example for dissociating the embodiment of tools and the embodiment of body parts (see Section 3.1.1.1). The difference between the feeling of ownership after a block and after a given trial can be explained as the difference between the average feeling of ownership during the experiment and the instantaneous feeling of ownership due to a single trial. During Experiment 1, the block average ownership report was positive, but not as high as the ownership reports after the congruent 'Hand & Feel' trials. Furthermore the per trial ownership reports after the 'Hand' and 'Table & Feel' conditions were lower than the average, with reports after the 'Table & Feel' trials reporting no ownership. This suggests that although overall the experiment elicited a strong BOI, the level of illusory ownership fluctuated during the course of the experiment based on the stimulation congruence of each trial.

The visuo-tactile stimulation incongruence in the 'Hand' and 'Table & Feel' trials may provide explanation for the diminished ownership; the absence of supporting tactile or visual cues, respectively, diminishes the effect of ownership in self-reports, but not enough to extinguish the feeling of bodily threat. This interpretation suggests body ownership as being a gradual experience; this theory of a non-binary basis for the sense of ownership is further expanded later (see Section 6.4.3). An alternative interpretation is that the feeling of bodily threat results through empathy from experiencing someone else's body being hurt (Meng et al., 2013), although, the dis-ownership self reports, and the self-referential nature of the threat questions (the questions specify harm towards the owned body) do not support this explanation.

5.4.2. Questionnaires and their efficacy as measure of introspection

All results presented in this chapter have been the subjective reports of participants. However, as noted in Section 3.2.1, questionnaires are not the most appropriate measures of cognitive processes such as body ownership (de Vignemont, 2011). For example, answers to the dis-ownership question, (see Q.2 Table 5.3) could be explained as a participant neither feeling embodiment over the presented virtual hand nor feeling that the virtual hand belongs to someone else. Despite the limited explanatory power of questionnaires, their simplicity to include in experiments, their consistency with biophysical results, and the absence of other widespread alternatives make them important experimental tools for the study of BOI. Furthermore, by adapting the experimental design with subjective questionnaires, novel results on ownership can be uncovered, such as those discussed in Section 5.4.1 for the dissociation of ownership and threat.

Nevertheless, reporting RHI using questionnaires has limitations and an objective measure from biophysical markers would be preferable for assessing the illusion strength and for confirming and expanding on the subjective results.

5.5. Discussion of biophysical results with respect to bodily threat and SI

5.5.1. SCR as a measure of threat

The results from Section 5.3.2 are consistent with the questionnaire reports of threat perception, discussed in Section 5.3.1, in that the 'Table' condition is shown to be the least threatening. However, the SCR responses and self-reports differ

in two accounts: i) SCR analysis showed no difference between the 'Hand & Feel' and 'Table & Feel' conditions, and ii) the 'Hand' condition is shown to have a significantly lower SCR response than the 'Table & Feel' condition. Furthermore, the amplitude of the SCR response appears to be modulated by the presentation of tactile cues: both conditions that deliver tactile stimulation result in a similar amplitude post-stimulus which is significantly higher than the two conditions that present visual-only stimuli. SCR was recorded from the right, stimulated hand of the participants due to the left hand being used to input the answers of the self-report questionnaires. By recording SCR on the hand that is not receiving stimulation, the ambiguity of the source of the SCR response can be mitigated. However, the timing of the SCR response suggests that it is unlikely for the amplitude change to be due to electrical noise, or coupling due to contact with the end-effector: if that were the case amplitude changes would be observed at the exact time contact with the skin was made. Moreover, the time evolution of the SCR response between all conditions is similar: a trough is observed around 1.5-2s with the SCR peaking around 3-3.5s. Taken together, these observations point to a physiological effect underlying the observed SCR responses, with tactile sensation modulating the amplitude of the SCR response by a greater amount than threat alone. Future studies should address this by recording SCR from the non stimulated hand of the participant.

5.5.2. Temporal and spatial characteristics of ERP reported threat

The ERP results from this experiment showed that perception of threat modulates the amplitude of the P400 component. This result is consistent with the results from the SCR and the questionnaires on threat perception, and confirms that no threat was perceived in the 'Table' condition. This was an expected result,

as previous studies have shown ERP responses (e.g. P3, P450) following visual presentation of threatening stimuli (Fan and Han, 2008; González-Franco et al., 2014; Li and Han, 2010; Meng et al., 2012,1). These studies have reported this component on EEG electrodes over the motor cortex (González-Franco et al., 2014; Li and Han, 2010), and over the visual cortex (Fan and Han, 2008; Meng et al., 2012,1). The result presented here suggest a functional divide for the activity in the two regions. P400 activity over the occipital lobe is correlated with visual threatening stimulation: this is observed in the difference in ERP activation on the posterior electrodes between the 'Table & Feel' and 'Hand' condition. Contrary, central (S1/motor cortex) P400 activity is correlated with both visual and tactile threat: little difference is detected in the central electrodes between the 'Hand' and the 'Hand & Feel' or 'Table & Feel' conditions. This result is further supported by the above studies on ERP and threat, which report that visually presented threatening stimulation induces activity of the motor cortex and the visual cortex.

The location of the P400 activity reported in this experiment is also consistent with the right-hemispheric model of body ownership discussed in Section 3.2.4. By combining the spatial location of the activity observed and the theory for central P400 activity being non-specific to sensory modality presented, discussed above, the following hypothesis can be made: the role of activity recorded from central electrodes (over motor cortex/S1) in threat perception is to respond to threatening stimuli towards body parts. This hypothesis is consistent with the models that assign the representation of the body schema to the motor cortex (e.g. Makin et al. (2008)). Furthermore, this theory is consistent with the subjective results for dissociating ownership and threat. This theory proposes a process for the perception of threat ownership at a separate level to that of ownership perception, which has been hypothesised to be located in the right insula (Tsakiris et al., 2010).

However, as source estimation, or clustering of the EEG activity has not been performed as part of the analysis for this experiment, conclusions on the brain regions responsible for activity are limited due volume conduction. Activity recorded on electrodes over the motor cortex could originate from a wide range of cortical sources, in proximity to the location of the EEG electrode. Further analysis of the data in terms of source localisation is necessary to provide stronger evidence for the role of the motor cortex in threat perception.

5.6. Chapter conclusion

This chapter discussed the subjective and biophysical data from the threat perception experiment. A novel observation was made that ownership and bodily threat perception are not necessarily correlated in BOI experiment. The chapter discussed the results obtained from SCR analysis, and the P400 ERP component, in terms of their consistency with the questionnaire reports; the biophysical results confirmed the reported level of perceived threat per condition as measured by the questionnaires. Particularly, it was shown that frequent reports, immediately after the presentation of a BOI condition can provide a more accurate narrative of the overall BOI induced during the experimental session. Furthermore, this chapter presented evidence for the distinct roles of the EEG activity recorded over central and occipital electrodes in the perception of threat, dependent on the sensory modality involved in perceiving the threatening stimulation. Activity in the occipital lobe is theorised to be sensitive to visual-only stimulation, whereas activity recorded over the central electrodes is sensitive to both visual and tactile stimulation as long as the object that is threatened is perceived to have a shape that matches a valid body representation. The integration of visual and tactile stimulus in threat perception over central electrodes confirms accounts of this

brain region as a centre of SI (discussed in Section 2.1.3.1 and Section 3.2.4). The following chapter will present and discuss the data from experiment 2, where the temporal effect of visuo-tactile stimulation is investigated.

6. Perception of stimulus onset asynchrony and its effect on body ownership

The second experiment that was conducted using the VR-BOI platform is described in this chapter: an investigation of the perception of the stimulation onset asynchrony in the BOI. The aims and hypothesis of this experiment are first discussed, and the behavioural and biophysical data analysis and discussion follows. In particular the relation of the ERP data with the results of the previous experiment is discussed, in terms of ERP as a predictor of BOI.

6.1. Aims and Hypothesis

This experiment investigated the effect of temporal delays on the strength of body ownership. Expanding on the experiments by Bekrater-Bodmann et al. (2014); Shimada et al. (2009) the experiment explored the range of stimulation delays between visuo-tactile sensory modalities that a human cannot detect as asynchronous. The aim was to quantify the effect of small temporal delays between visual and tactile stimulation on the perception and strength of the BOI. The experimental hypotheses were: 1) BOI would not be extinguished despite delays

in visuo-tactile stimulation, as measured by self-report questionnaires, and 2) the effects of those visuo-tactile temporal delays could be detected in the EEG activity, and provide evidence for the role of distinct brain regions in body ownership and SI.

6.2. Methods

6.2.1. Participants

Twenty seven healthy participants (7 females, age range: 18 - 28yr, mean age: 20yr) were recruited from the University of Reading. The experimental design was reviewed and approved by the University of Reading, School of System Engineering, Ethics Committee. All subjects gave written consent to participate in the study and were compensated £10 for their time. Participants were right handed with normal or corrected to normal vision.

6.2.2. Procedure

At the beginning of each session, the participants were briefed on the experiment and were given a demonstration of the virtual environment, servomotor and end-effector, and the input system for answering the questionnaire presented in the VR environment (see Figure 4.14, Figure 4.15). The questions were answered on a 7 point Likert scale ("strongly disagree" to "strongly agree") and were recorded on a scale of -3 to +3 corresponding to "strongly disagree" and "strongly agree" respectively, where 0 represented "neutral" (see Table 6.3). After the briefing, the participants were prepared for EEG, ECG, EMG and SCR recordings. The participants took part in two experiments: Experiment 1 discussed in the previous chapter, and Experiment 2 discussed here (see Chapter 6). Three participants

were excluded from Experiment 2 due to reporting no ownership during each experiment respectively. Each experiment lasted ~30min with a 5-10min break between the experiments. The order of the experiments was randomly chosen *a priori* and was counterbalanced to avoid order bias. The participant wore the Rift throughout both experiments, but during the break between experiments the HMD was switched off to avoid fatigue.

6.2.3. Stimuli

Experiment 2 followed the same procedure as the one outlined in Chapter 5. Each trial consisted of a 10s pre-stimulus preparation period and a stimulation period lasting ~45s during which the participant was tapped 20 times on the right hand. A tap had both a tactile cue (a plastic ball attached to the end-effector of the servomotor) and a visual cue (a virtual ball touching the hand, see Figure 6.1). Each tap lasted for 400ms with a random period of 800ms to 1100ms between taps. At the end of each trial the participant was asked to report their feeling of ownership, and their perception of simultaneity and temporal order of the visual and tactile stimulation (see Table 6.2). There were 7 conditions in the experiment derived by the delay onset between the visual and tactile stimulation of the hand. The first 5 conditions tested small delay values in the range of -128ms to +128ms with 64ms increments (-128ms, -64ms, 0ms, +64ms, +128ms)[1]. These increments were designed to prevent overlap between conditions based on the limitation imposed by the 16.6ms timing accuracy of co-stimulation (see Section 4.3.4). Negative values correspond to leading with visual stimulation, positive values correspond to tactile leading stimulation, and 0ms denotes the synchronous condition. The 6th condition was a negative control condition with a delay of +500ms. Finally,

[1]The stimulation delays are based on the 60Hz refresh rate of the Rift HMD. That means that the actual delays of those conditions are (+/-) 66.4ms and 132.8ms. For simplification, the delays of these conditions is rounded to the nearest multiple of 16.

in the 7th condition there was no fixed delay during the trial; for each tap, the delay between visual and tactile stimulation was randomly sampled from the pool of delays from the other conditions and could be positive, negative or synchronous. This condition aimed to to decrease the effect from sensory recalibration (Di Luca et al., 2009) by introducing a random stimulation pattern. All 7 conditions were randomly arranged and repeated once within a block of 7 trials, with the experiment lasting a total of 3 blocks. Originally, an 8th condition was designed, which was a further control condition with a delay of -500ms. However during the experimental period, an off-by-one coding error was found that resulted in the -500ms condition to have identical stimulation to the random condition. Since the +500ms control condition was shown to adequately extinguish the illusory ownership, experimentation continued without the second control and with the random condition being repeated twice. A summary of the experimental design is shown in Table 6.1.

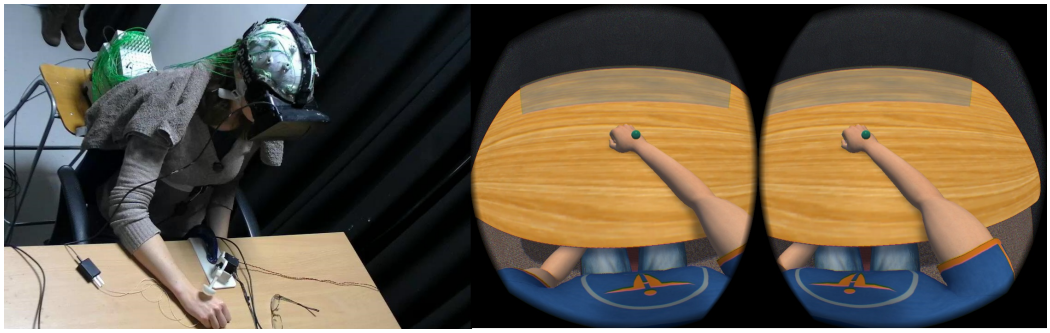

Figure 6.1.: *Experimental setup for experiment 2. The platform can accurately modulate visuo-tactile delays. Left: Participant during the experiment. The servomotor is equipped with the spherical end-effector. Right: The virtual environment from the point of view of the participant and the congruent visual cue.*

Table 6.1.: *Experimental design for experiment 2. On the left column, of each type of block of trials is listed. The right column gives a brief explanation of the SOA of each trial within the block.*

	Stimulus onset asynchrony
-500ms	Visual leading delay (control)
-128ms	Visual leading delay
-64ms	Visual leading delay
0ms	Synchronous condition
+64ms	Tactile leading delay
+128ms	Tactile leading delay
+500ms	Tactile leading delay (control)
Random	Each of the 20 stimulation delays are randomly chosen from the delays of the other conditions

Table 6.2.: *Questionnaire for experiment 2 (visuo-tactile delays experiment). Questions asked at the end of each trial of 20 visuo-tactile stimulations*

Virtual hand delays experiment questions
1. I felt as if the hand I saw in the virtual world might be my hand
2. The hand I saw was the hand of another person
3. The hand I saw resembles my own hand in terms of shape, skin tone, freckles, etc.
4. I felt the ball touch my hand at the SAME TIME as I saw the ball touch my hand
5. I felt the ball touch my hand BEFORE I saw the virtual ball touch my hand
6. I felt the ball touch my hand AFTER I saw the virtual ball touch my hand
7. I find it difficult to report the order of seeing and feeling the ball touch my hand

Table 6.3.: *Available answers for participants to choose from for answering each question. Participants saw the answers as the column on the left. Analysis of results herein is presented using the numerical equivalent on the right column.*

Answer	Numerical representation
Strongly disagree	-3
Disagree	-2
Somewhat disagree	-1
Neutral	0
Somewhat agree	+1
Agree	+2
Strongly agree	+3

6.2.4. Data analysis

The answers from the VR questionnaires were imported into R and were analyses using a linear mixed effect model. The eight conditions were defined as a fixed effect for the model with each block and participant being treated as a random effect to account for the repeated measure design of the experiment. Multiple comparison correction for P-values was performed post-hoc in using the Bonferroni method and the multcomp and lsmeans R packages (Hothorn et al., 2008; Lenth, 2016). SCR response was measured as the difference between the maximum and minimum peak post stimulus and was analysed using the same method in R. EEG data was first pre-process for analysis (see Section 4.3.3). Artefact-free EEG processing for ERP presentation and analysis was performed using the Mass Univariate ERP Toolbox, and statistical significance per time point was tested using the t-test false discovery rate method by Benjamini and Hochberg (1995).

6.3. Results

6.3.1. Perception of visuo-tactile delays

Experiment 2 asked participants to report their perceived order of the visuo-tactile simulation cues, after each trial of 20 visuo-tactile stimulations (see Table 6.1). Three questions (Q.4 - Q.6, see Table 6.2) were asked to assess the perceived order, with a further question aimed to assess the difficulty of reporting the order (Q.7, see Table 6.2). The three omnibus ANOVA for Q.4-Q.6 resulted in significance between conditions for the perception of the delays (Q.4: $F(6,426) = 158$, $P < 0.001$, Q.5: $F(6,426) = 81.3$, $P < 0.001$, Q.6 $F(6,426) = 50.4$, $P < 0.001$). Results on Q.4 (question on synchronous perception of cues) showed that visual leading cues ('-128ms' and '-64ms' conditions), synchronously presented cues ('0ms'

condition), and the '+64ms' leading tactile condition were all reported to be felt synchronously (median = +2 see Figure 6.2, top). Reports of stimulus synchrony during the '+128ms' tactile leading condition were significantly lower (median = +1, $P < 0.001$ compared to visual leading conditions, and conditions of smaller SOA). The same results were shown for Q.4 (question on perception of tactile stimulation as leading): the '+128ms' tactile leading delay showed significantly higher reports (median = +1, $P < 0.001$) than the conditions with SOA from -128ms to +64ms (see Figure 6.2, bottom). For the '+64ms' condition, although no significant difference was found in responses of Q.4 and Q.5, a wider range of responses compared to the synchronous and visually leading conditions was observed. Visual leading SOA were not perceived by participants: in Q.5 the median response of the fixed SOA condition was equal to -2 with no significant difference between conditions (see Figure 6.3, top). The random condition rejected the null hypothesis (Q.4 median = +1, $P = 0.0039$, $z = 2.8877$) that it was drawn from a 0 median distribution. Taken together, these results show that participants were susceptible to noticing tactile leading SOA but did not perceive the visual leading condition as asynchronous.

Participants reported little difficulty in reporting most delays (Q.7), with a median equal to -1 for most fixed SOA conditions ($F(6,426) = 14.13$, $P < 0.001$, see Figure 6.3, bottom). The '+128ms' conditions showed significantly higher responses for difficulty to report the SOA from the synchronous condition ($P < 0.05$, see Figure 6.3, bottom). The random condition was the only other condition with significantly higher responses on difficulty to report SOA. The reports on Q.7 support the result that the visual leading conditions were not perceived by the participants as asynchronous during the experiment.

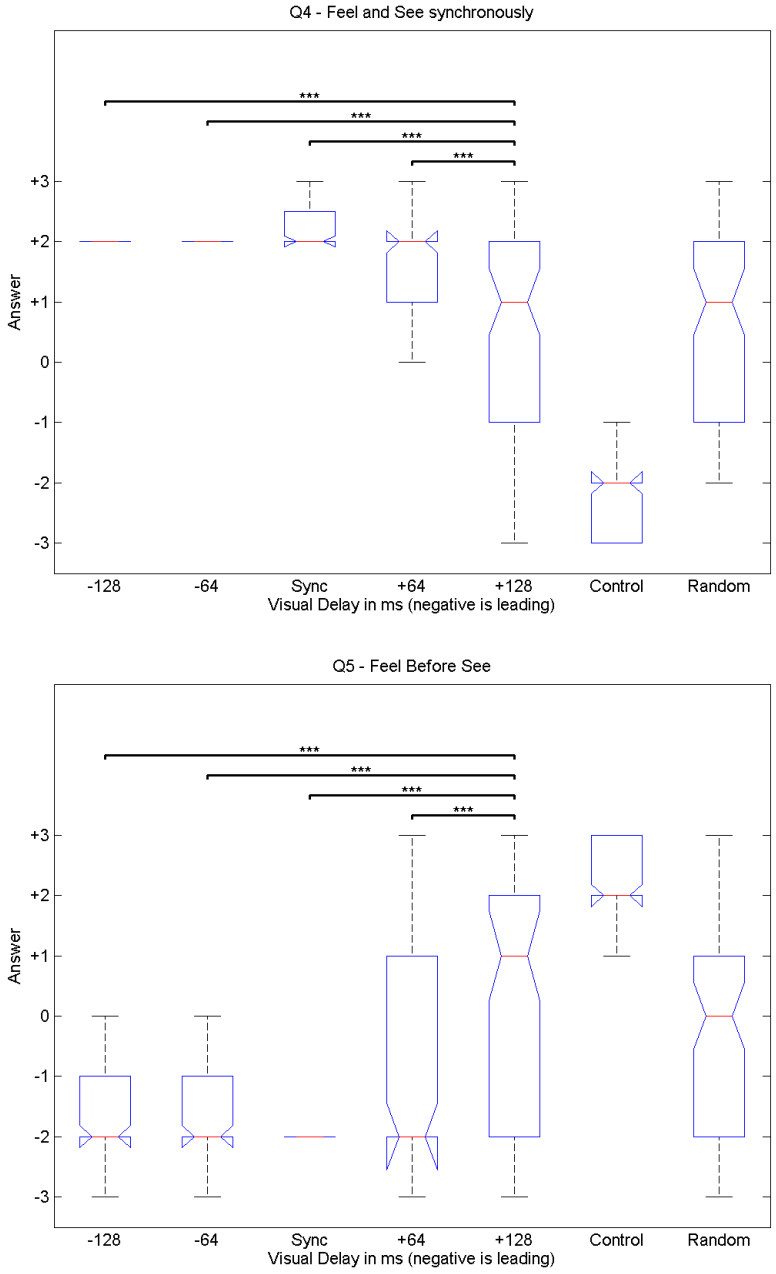

Figure 6.2.: *Temporal order judgement and synchrony of stimulation I. Top: Responses to synchronous stimulation. Results for conditions with tactile leading stimulation show that participants were significantly more likely to notice a difference. Bottom: Responses to feeling the tactile cue before the visual. Answer values -3 to +3 correspond to 7 point Likert answers "strongly disagree" to "strongly agree". Negative conditions denote visual leading stimulation. Sync: Synchronous ('0ms') condition. Control: negative control (+500ms delay). Random: Random condition, each tap during the trial assigned randomly from all other available delays. * , **, *** : corresponding to p-values at 0.05, 0.01 and 0.001 significant level, respectively. Significance not shown for the control condition (significance against all conditions) and Random condition (significance against all but the '+128ms' condition). Red line is the median, top and bottom of boxes are the 75th and 25th percentile, respectively, whiskers correspond to approximately 99%.*

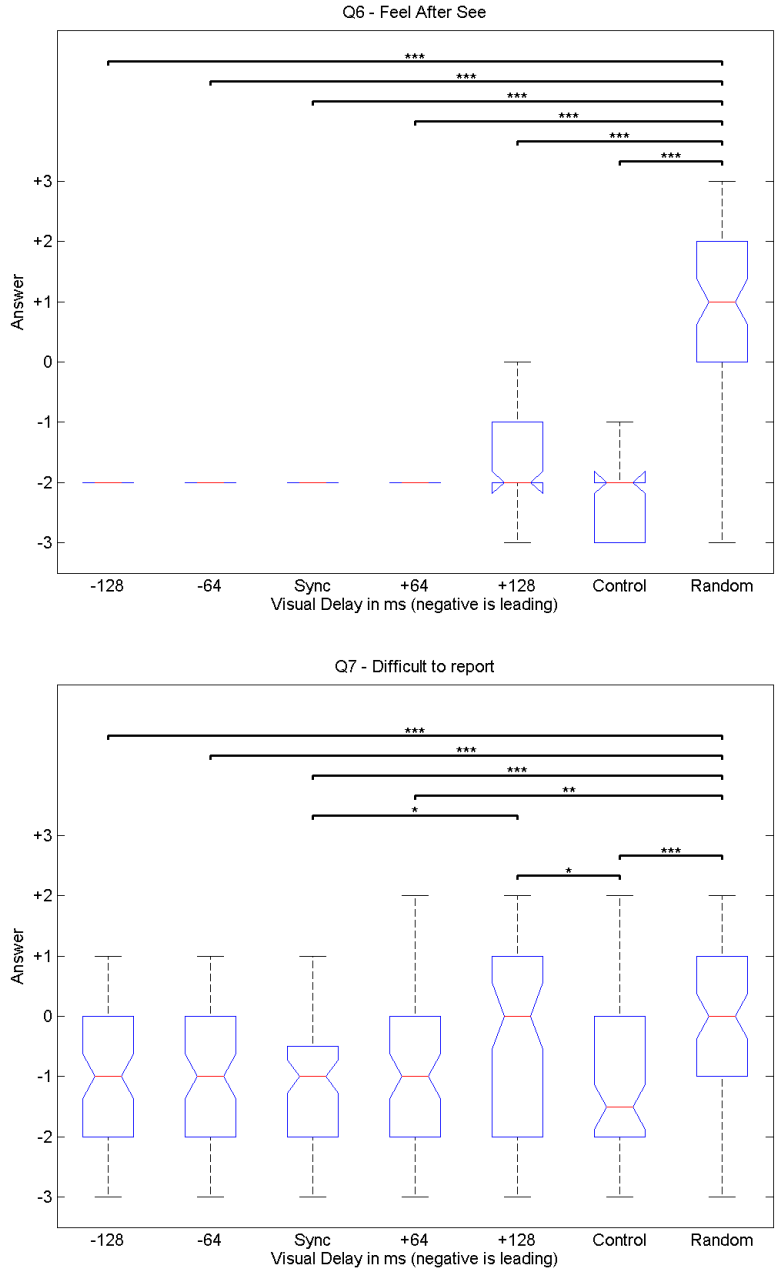

Figure 6.3.: *Temporal order judgement and synchrony of stimulation II. Top: Responses to feeling the tactile cue after the visual cue. Participants did not report seeing visual leading stimulation for fixed SOA conditions. Bottom: Difficulty to respond to Q.4-Q.6. Answer values -3 to +3 correspond to 7 point Likert answers "strongly disagree" to "strongly agree". Negative conditions denote visual leading stimulation. Sync: Synchronous condition (0ms delays). Control: negative control (+500ms delay). Random: Random condition, each tap during the trial assigned randomly from all other available delays. * , **, *** : corresponding to p-values at 0.05, 0.01 and 0.001 significant level, respectively. Red line is the median, top and bottom of boxes are the 75th and 25th percentile, respectively, whiskers correspond to approximately 99%.*

6.3.2. Ownership under delayed visuo-tactile cues

The effect of the different SOA was also investigated in terms of affecting the self-reports of ownership (Q.1 and Q.2). The omnibus ANOVA showed that the SOA condition had a significant effect in the responses to the ownership questions (Q.1: $F(6,426) = 39.25$, $P < 0.001$, Q.2: $F(6,426) = 16.1$, $P < 0.001$). Specifically, reports of ownership were also compared against conditions of different SOA. Ownership reports showed that conditions with SOA in the range of -128ms to +128ms resulted in significantly higher perception of ownership than the control condition ($P < 0.001$ for all conditions versus control, see Figure 6.4, top). Interestingly, a significant different was found between the +128ms tactile leading condition versus the synchronous condition ($P = 0.0173$). In addition, the +128ms approached significance against the -64ms visual leading condition ($P = 0.0522$).

The random condition resulted in significantly lower perceptions of ownership than the visual leading and synchronous stimulation conditions, and also in higher ownership perception than the control condition. The questionnaire reports on disownership are symmetric to the reports on ownership (see Figure 6.4, bottom), and follow the same trend that was observed between these same questions in Experiment 1 (see Section 5.3.1).

To further investigate the effect of the perception of delays on ownership, a post-hoc comparison of ownership perception was made within the '+128ms' condition between trials with low perception of delay (answer to Q.4 < 0) and those with a high perception of delay (answers to Q.4 > 0). Trials from the two groups were then compared on their reported level of ownership (Q.1). It was found that trials in which the participant could identify the temporal delay had a significantly different response of ownership level compared to trials during which participants had low perception of the delay ($P < 0.01$, Figure Figure 6.5). Furthermore, a

Pearson's correlation analysis showed that in the +128ms condition, responses to ownership are negatively correlated to perception of delay (ρ = -0.37, P = 0.0014).

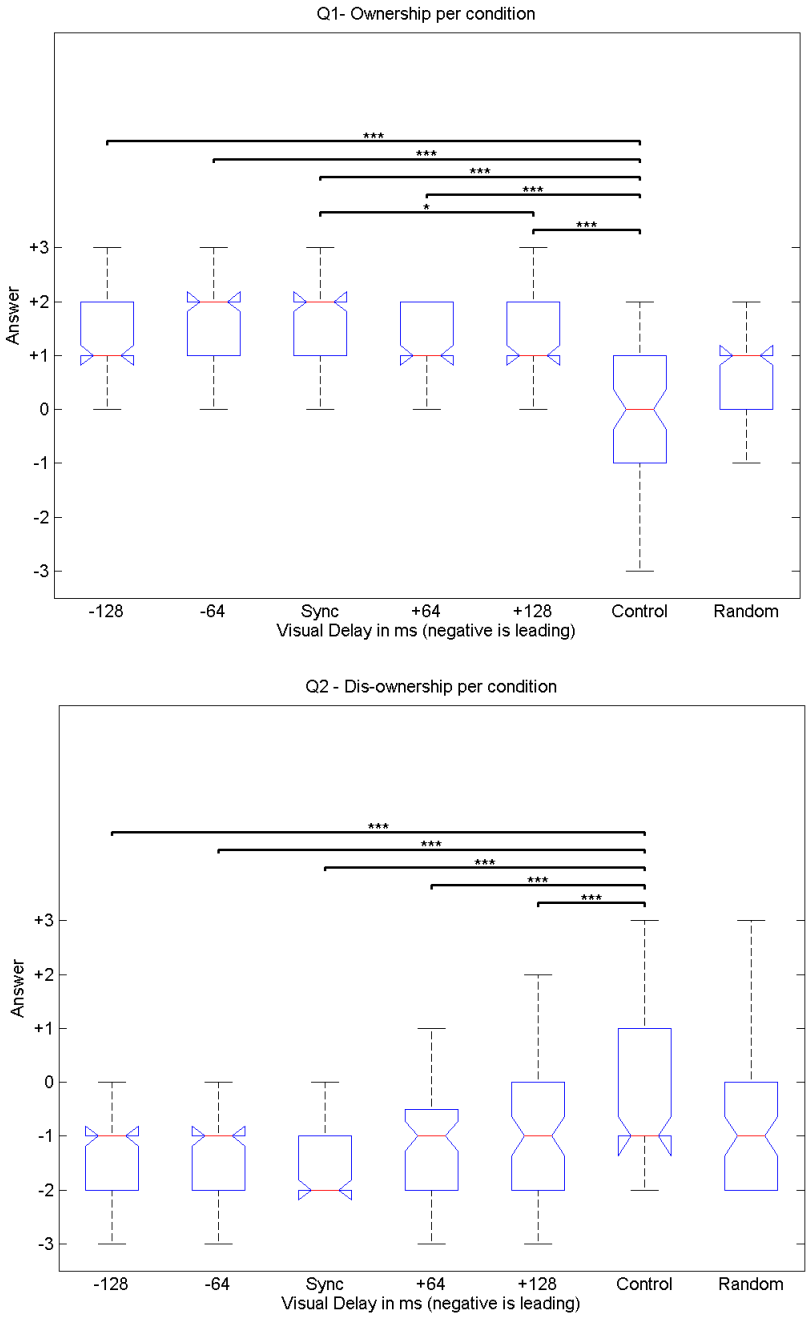

Figure 6.4.: *Ownership and dis-ownership reports. Top: Reports of ownership. Tactile leading stimulation by 128ms produces significantly weaker illusion than the synchronous condition (P = 0.0173). Bottom: Reports of dis-ownership of the hand. The experiment was successful in evoking RHI. * , **, *** : corresponding to p-values at 0.05, 0.01 and 0.001 significant level respectively. Significance not shown for the control (top, significance against all conditions, bottom significance against '-128ms' to '+64ms' conditions), and random condition (top, significance against '-128ms' to 'Sync', bottom, significance against '-64ms' and 'Sync' conditions). Red line is the median, top and bottom of boxes are the 75th and 25th percentile respectively, whiskers correspond to approximately 99%.*

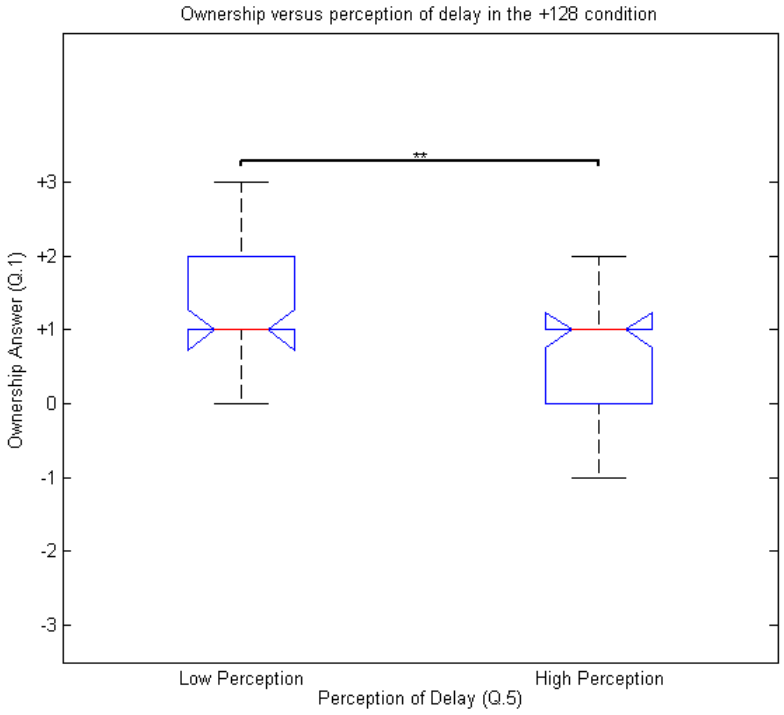

Figure 6.5.: *Effect on ownership from trials with high and low perception of delays. Using data from the +128ms condition trials were split by the subjects' response of Q5; below "neutral" was grouped in low perception and above was grouped in high perception. The response on the level of the illusion is significantly lower for the group that perceived the delay. This supports the hypothesis that the perception of a delay between the visual and tactile stimulation has an effect on the reported level on ownership. Red line is the median, top and bottom of boxes are the 75th and 25th percentile, respectively, whiskers correspond to approximately 99%. ** corresponds to a p-value of 0.01*

6.3.2.1. Event related potentials - ownership and perception of delays

ERP activity recorded from this was analysed for differences due to the perception of delays and the strength of BOI elicited. Throughout all conditions 3 main ERP components were identified: i) a P100 (60ms post-stimulus) immediately following the tactile stimulation, ii) a visual P200 after the visual stimulation, and iii) a N200 time-locked to the tactile stimulation. These components were observed twice per visuo-tactile stimulation: once when the ball end-effector touched the participant's hand, and once when the ball was lifted.

To identify ERP activity differences due to the level of ownership, individual trials were grouped according to their originating block: a) the 'fixed delay' group were trials from a block with fixed delay, and b) the random delay group were trials that were presented during the random delay block. As discussed in Section 6.4.2 the perception of ownership, as recorded at the end of a block of trials, was stronger in the fixed delay conditions ('-128ms', '-64ms' , and '0ms') than in the random block. The ERP activity from trials of the same visuo-tactile delay were compared between the two groups (see Figure 6.6). Across all pairs of trials of the same delay, no significant difference was detected.

ERP activity was also compared in relation to the questionnaire reports. In Chapter 5, it was discussed that after the '+128ms' tactile leading condition, participants reported significantly higher perception of the delays. Furthermore, trials in which participants perceived the delay, resulted in significantly lower scores of BOI. ERP activity from trials of the '+128ms' condition[2] were compared using as a grouping factor: a) the reported delay perception (see Figure 6.7) , and b) the reported strength of BOI (see Figure 6.8). In both comparisons, no statistical significance was observed between the groups.

[2]Comparison of ERP activity from other conditions based on the reported ownership or delay perception was not possible due to one group having too few members for statistical analysis to be carried out.

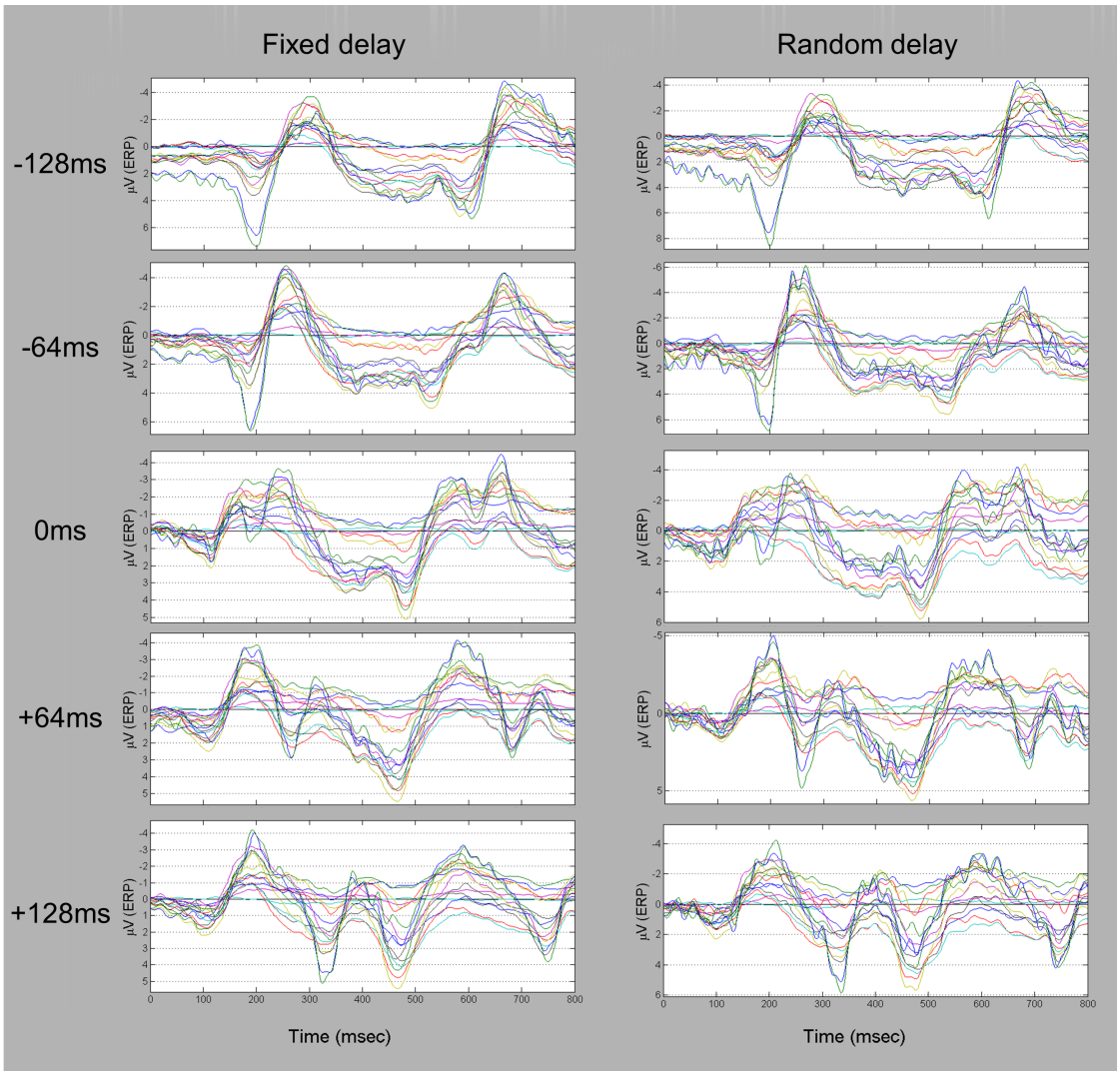

Figure 6.6.: *Comparison of ERP data originating from a fixed-delay or random-delay block of trials. Each row shows trials of a specific visuo-tactile delay. In the left column trials were presented in a fixed delay block. In the right column the trials were presented in a block of trials with random delays. All conditions resulted in the P100, P200, and N200 components, time locked to the presentation of visual and tactile stimulation. No significant difference was found between any pair fixed/random delays. Each coloured trace corresponds to ERP activity from a single electrode, averaged across all trials. Positive delay condition correspond to tactile leading stimulation, negative delays indicate visual leading stimulation. Time at 0ms corresponds to the presentation of stimulation: for tactile leading conditions time at 0ms is when the tactile stimulation is presented, for the synchronous (0ms) and visual leading conditions time 0ms corresponds to visual cue presentation.*

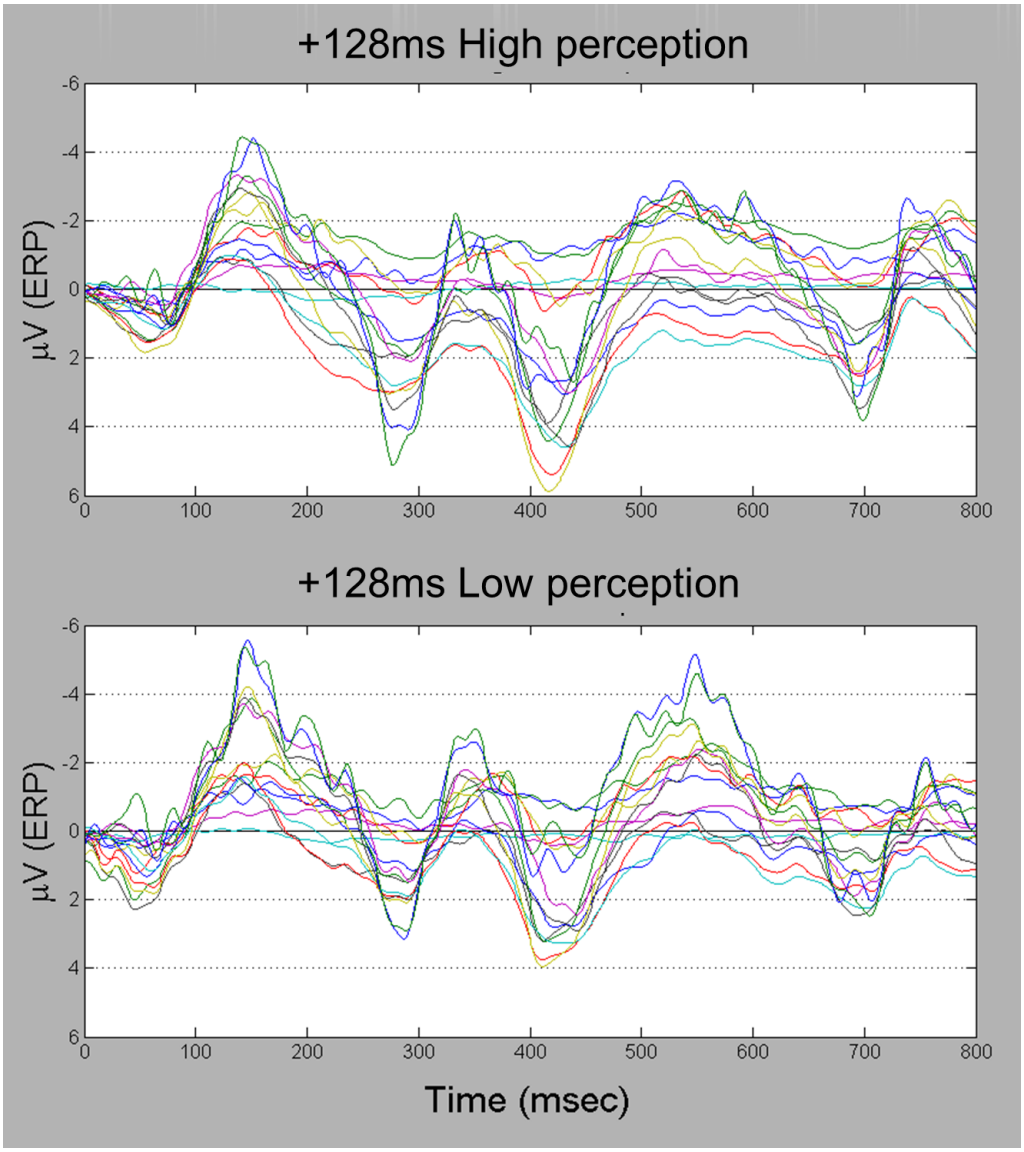

Figure 6.7.: *ERP activity comparison between trials where participants correctly perceived a tactile-leading delays and trials were participants did not notice the delay. All trials are sampled from the '+128ms' tactile leading condition. Top: Grand average ERP from trials with participant reports of tactile leading delays. Bottom: ERP from trials with negative reports of a tactile leading delay. No significant difference was found between the two groups. Each coloured trace corresponds to ERP activity from a single electrode, averaged across all trials. Time at 0ms corresponds to the presentation of tactile stimulation.*

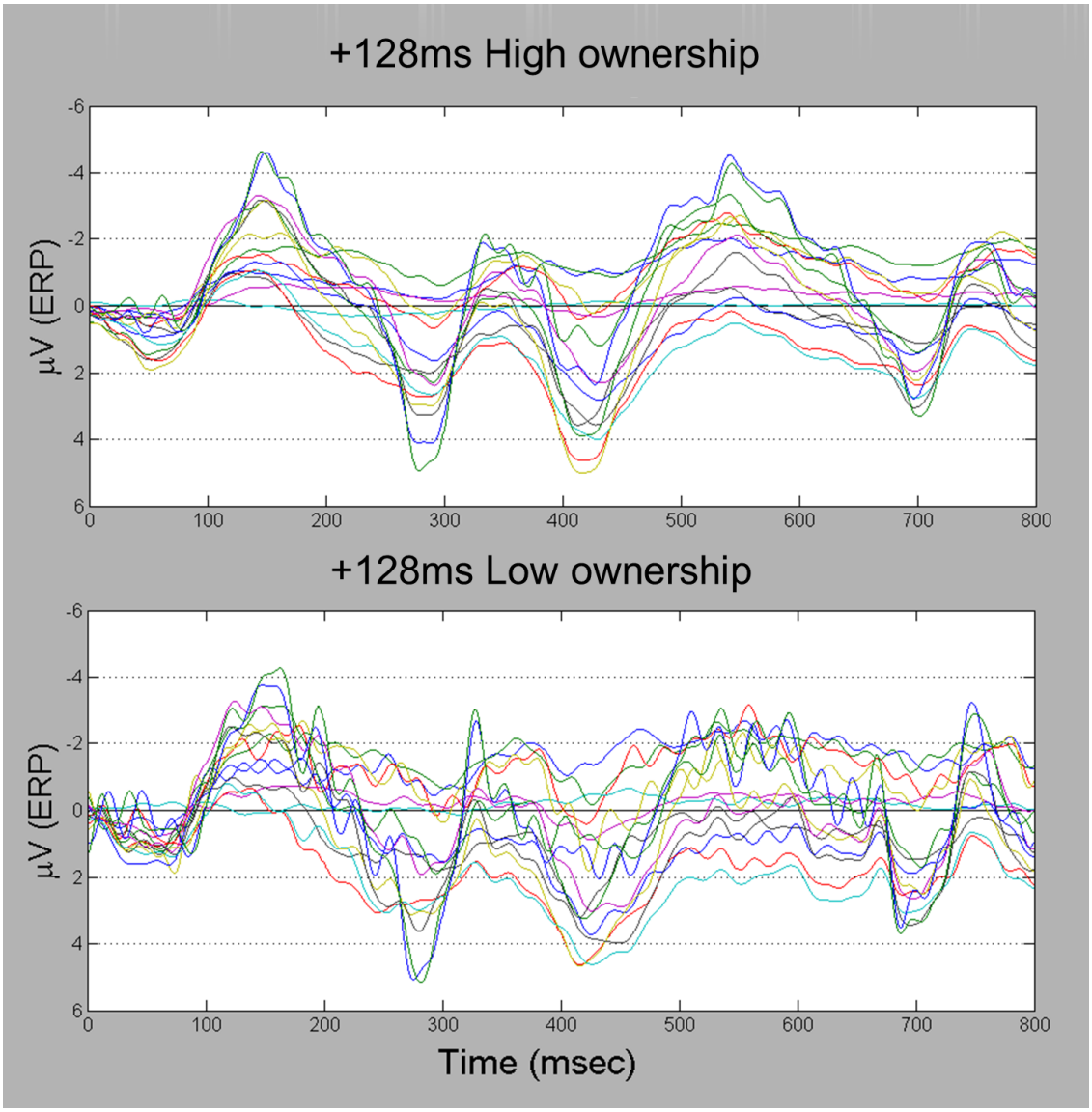

Figure 6.8.: *ERP activity comparison between trials where participants reported high BOI for the virtual hand versus trials with low reports of BOI. All trials are sampled from the '+128ms' tactile leading condition. Top: Grand average ERP from trials that scored high for BOI. Bottom: ERP from trials with low reports of BOI. No significant difference was found between the two groups. Each coloured trace corresponds to ERP activity from a single electrode, averaged across all trials. Time at 0ms corresponds to the presentation of tactile stimulation*

6.4. Discussion of behavioural results

6.4.1. Temporal order affects perception of synchrony

Confirming observations from the literature on audio-visual and audio-tactile temporal order (Fink et al., 2006; Kanabus et al., 2002; Keetels and Vroomen, 2012; Levitin, 2000), the results from Experiment 2 suggest that perception of multisensory synchrony has a larger temporal window of SOA when vision is leading. As shown in Figure 6.2, no condition for which the visual stimulation is leading is perceived significantly differently from the synchronous stimulation condition. Conversely, the '+128ms' tactile lead condition is reported to be significantly different than the synchronous stimulation condition.

It is important to note that conditions with significantly different responses between them can have little differnce in the median reported level of questionnaire. One possible explanation is that the small SOA do not outright extinguish the BOI, however, they produce a diminished level of the illusion to a sub-population of the subjects, especially to those subjects who are sensitive to perceiving the small delays. Following this explanation, the significant difference in the reports of simultaneity perception between conditions of different SOA can be explained due to the varying temporal perception sensitivity between participants. The change in the range of responses and the trend seen in the data suggests that the window for failing to notice small asynchronies is much larger when vision is leading versus when tactile stimulation is leading. Furthermore, the higher variation in responses shows that as the delay between the visual and tactile stimulation increases, a larger population of subjects will perceive the asynchrony for tactile leading conditions. On the one hand, the similarities in temporal perception between conditions can be explained as an effect of sensory recalibration: the repeated nature of the experiment, necessary in order to generate the RHI, could produce a sensory recal-

ibration effect further pushing the perception towards synchrony (Di Luca et al. (2009); Keetels and Vroomen (2008); Vroomen et al. (2004), see Section 2.3.3).

6.4.2. Effect of delays on ownership

The results showed that the order of the stimulation not only has an effect on the window of asynchrony detection, but also on the perceived strength of the illusion. The small delays, although not sufficient to abolish illusory ownership, significantly decreased the perceived strength of the illusion. When delays of different SOA were grouped together within a single block in random order (i.e. the 'random' condition), ownership perception was significantly lower than the highest ownership perception recorded (during the synchronous stimulation condition), but also higher than the ownership perception reported in the control condition. This suggests the possibility that the sense of ownership is not necessarily an all-or-none phenomenon, but rather it may be a graded experience (see Section 6.4.3). The possibility of different levels of ownership is further shown when looking at the responses of ownership within the '+128ms' condition. In this condition those participants who could correctly identify the delay reported a lower level of ownership versus those who could not. Furthermore, the theory of a graded ownership has support from previous studies by Ismail and Shimada (2016); Shimada et al. (2009), that looked at the effect of a range of SOA to the perceived ownership. In their studies delays of 300ms resulted in significant changes in the perception of ownership, however, the perception of ownership was extinguished for delays equal or greater than 500ms. An alternative explanation could be that difference of reported levels of ownership correspond to individual participants having a specific tolerance for detecting SOA. However, this does not explain the difference in the reported level of ownership between the control con-

dition which extinguishes BOI and the conditions that show diminished reports of BOI but do not outright extinguish the illusion.

An important note is on the size of the effects reported in Experiment 2. In the comparison between the synchronous and '+128ms' conditions on the ownership questions (Q.1, see Table 6.2) there is a small effect size (Cliff's d = 0.2549), while a medium effect is seen in the comparison between high and low delay perception (Cliff's d = 0.4214). The small effect size could be explained by sensory recalibration; within a trial, a subject's perception of the time between the stimulation cues gets recalibrated to perceive the two cues as synchronous, hence the perceived difference between the conditions becomes smaller. Another possible explanation is that ownership is the result of the integration of many senses (Blanke, 2012; Ehrsson, 2012); small inconsistencies within a subset of the responsible senses for ownership are compensated for by agreement from the remaining set of the senses (e.g. a visual - proprioceptive agreement). The recent studies from Maselli et al. (2016) and Costantini et al. (2016), showed results that are compatible with the view that small delays have an effect on ownership which is dependent on the participant's ability to perceive inter-stimulus delays. In both of these studies the perception of delays was correlated with the self-reports of body ownership, and reported SOA $<$ 200ms to have an effect on ownership.

On the importance of the order of presentation of visual and tactile cues, a previous study by Bekrater-Bodmann et al. (2014) found no difference on ownership as a result of the order of sensory stimulation. In their experiment visual leading and tactile leading stimulation of 300ms were compared with no significant difference found. A possible explanation for the discrepancy between that study and the results presented here is the magnitude of the stimulation delays. As discussed earlier (see Section 6.4.1), visual leading delays of 128ms are not perceived by the participants. However a larger visual leading delay of 300ms would be perceived

(Kanabus et al., 2002; Levitin, 2000). If the perception of delay is necessary to affect the level of ownership, as discussed above, no significant effect would be observed between delays of +/-300ms. Conversely, the order of stimulation would play a more significant role for delays of +/-128ms due to the difference induced by the order of stimulation on the perception of the delays. However, a study by Costantini et al. (2016), which investigated visuo-tactile SOA in the region of +/- 400ms, did not report an effect of TOJ on ownership. Crucially, in the same study, a TOJ shift towards visual-leading cues was not observed; this could be due to the nature of the stimulation, as discussed in Section 2.3.2. For example, the vibration and light cues delivered in the case of the RHI are not an ecologically valid stimuli, whereas the ball/touch cues used in Experiment 2 are, and ecological validity has been shown to affect the PSS (Levitin, 2000). No effect on the PSS was reported in the study by Constantini et al., due to the order of visuo-tactile cue presentation: this, coupled with the expectation that ownership is only affected by perceived stimulation discrepancies, can explain the absence of results in their study showing that the stimulus temporal order affect ownership reports.

Further exploration of delays in the range of +/- 300ms could provide more evidence on the asymmetric boundary of perception of the delays and hence on the effect of stimulation order on the level of ownership.

6.4.3. Graded ownership within the philosophical framework of embodiment

Previous sections discuss ownership as a continuum of states of embodiment (see Section 5.4.1 and Section 6.4.2). This theory of graded ownership can be connected to the philosophical framework of embodiment as set by de Vignemont (see Section 3.1.1.1). A healthy real hand has maximal embodiment as it fulfils all

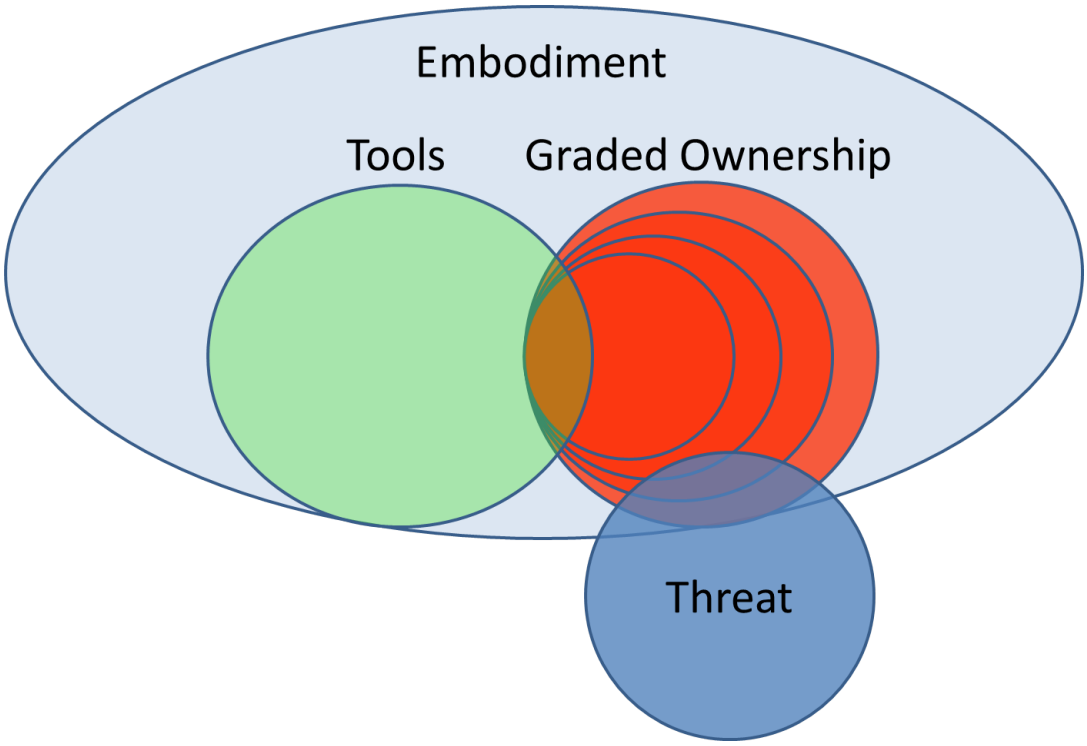

Figure 6.9.: *Venn diagram of graded ownership within the concept of embodiment. Body ownership is not a binary experience, but instead, it is a graded experience that depends on the number and weight of the embodiment criteria that are fulfilled by the owned body part. The stronger the body ownership, the more it is embodied as a real body part. In the case of BOI, stimulation incongruence results in a weaker sense of ownership through the loss of embodiment criteria. Note that threat is separate to ownership as discussed earlier (see Section 5.4.1)*

of the criteria of an embodied limb. A rubber (or virtual) hand, embodies some of the criteria of a real hand. Introducing incongruence between the visuo-tactile cues presented on the rubber hand, some of the rubber hand's criteria for embodiment are lost. The number and weight[3] of the criteria of an embodied limb that are shared with the rubber hand, are correlated with the level of stimulus congruence: small stimulus incongruence results in a smaller loss of the sense of embodiment than larger stimulus incongruence (see Figure 6.9). For example, in Experiment 2, the control condition introduces a large temporal asynchrony and

[3]Different embodiment criteria could have different weights in the perception of ownership. For example, the embodiment criterion for an embodied object to be included in the internal representation of body size (shared by both tool embodiment and ownership) could have a smaller impact on the perception of ownership than the embodiment criterion for feeling threat over the embodied object.

eliminates the criteria for embodiment, whilst the '128ms' condition removes fewer embodiment criteria, diminishing the reported ownership but maintaining a sense of embodiment. Results from Experiment 1 (see Chapter 5) on the dissociation of ownership and threat can also be explained through this theory: the 'Hand' and 'Table & Feel' conditions introduce visuo-tactile incongruence which removes some of the criteria for embodying the virtual hand. However, the incongruence is not sufficiently significant to completely abolish embodiment, and embodiment properties of the virtual hand that are associated with bodily threat are maintained. Hence a bodily threat is perceived but ownership reports are diminished. Contrary, in the 'Table' condition, no incongruence is introduced, thereby increasing the reported body ownership without necessarily eliciting a feeling of threat (due to the absence of threatening stimuli).

6.5. ERP as a measure of BOI

Experiments 1 discussed in the previous chapter failed to detect any ERP component modulation from the strength of the BOI. The results shown in Figure 5.9 and Figure 5.10 are not connected although they appear similar, but are instead generated by distinct causes: the 'Hand' / 'Table' difference at 200ms is due to the P200b present in the 'Table' condition, whereas the 'Hand & Feel' / 'Table & Feel' difference at the same time, is due to the N200 activity occurring earlier in the 'Hand & Feel' condition than in the 'Table & Feel' condition. If the activity was correlated to the same factor (e.g. strength of BOI) it would be expected that the ERP activity of the two conditions would share polarity, however, this is not the case for this activity. In Experiment 2, when comparing trials with high reports of BOI versus trials that elicited weak BOI, no difference in ERP is detected.

Although previous studies have reported that ERP amplitude (e.g. N140) is modulated by the BOI (Press et al., 2008), this contrasts with the results generated from Experiments 1 and 2. One potential explanation is that ERP is modulated by the strength of the BOI, as reported elsewhere (Press et al., 2008), however, only large changes of BOI strength, or complete extinction of the illusion result in a detectable change in ERP amplitude. According to this hypothesis, if Experiments 1 and 2 did not sufficiently reduce ownership, no change in ERP would be observed. To further test this hypothesis, Experiments 1 and 2 would need to be expanded with non-realistic body representations and/or orientations. Whether ERP components do not correlate with ownership, or ERP components can capture only the larger differences in the perception of ownership, the ERP results from this and the previous chapter are evidence that ERP components are not an appropriate measure for comparing the strength of illusory ownership between BOI experiments.

In Experiment 2, direct comparison between conditions of different temporal delays was not possible due to time locked ERP components: ERP of trials from different conditions would have components originating from the same type of stimulus in distinct locations. By aligning the single trials with respect to the presentation of a given stimulus (e.g. visual), ERP components due to the other stimulus (e.g. tactile) would be misaligned. An alternative method that expands the ERP analysis would consider the time progression of the ERP activity and define the evolving temporal features for a given trial. Methods that analyse temporal dynamics, would allow trials with different temporal progression to be compared through common features, identified in the temporal progression of the brain activity. Furthermore, other EEG analysis techniques, such techniques that employ spectral dynamics, and Bayesian causal methods, which have been successfully employed in previous studies (Kanayama et al., 2016; Kilteni et al., 2015; Zeller et al., 2016)

could be used for the investigation of neural mechanisms that can be identified through different neural activity patterns.

6.6. Chapter conclusion

This chapter discussed the effect of delay perception in terms of self-report questionnaires and EEG data. Results from this experiment showed that small delays have a negative effect on the strength of the RHI when tactile stimulation precedes the visual cue. This was shown to be due to the tactile leading delays being perceived by the participants: when the SOA is perceived, a lower strength BOI is reported. This suggests that where inter-modal stimulation delays are unavoidable in a situation in which illusory ownership is desirable, stimulation with leading visual cues is preferable due to the stimulation onset differences being less likely to be perceived. Furthermore, results from Experiment 1 of the previous chapter, and Experiment 2 discussed here have suggested the theory that the sense of ownership is not an all-or-nothing experience where one can either feel ownership or not; instead, the sense of ownership is a graded experience, and experiments of BOI elicit body ownership within a spectrum of illusory ownership strengths. This theory of a graded ownership is discussed for its fit within the philosophical context of embodiment as discussed earlier (see Section 3.1.1.1).

This chapter further discussed the experimental evidence presented in this chapter as well as the previous which failed to find support for using ERP as a measure of ownership: in neither Experiment 1 nor 2, no ERP component was shown to be correlated with ownership. However, it was discussed that a more comprehensive investigation for ERP is necessary to address to what extent ERP represents ownership, in terms of the body schema, or the body image as evidence in other lit-

erature has hinted. To that effect, the next chapter will outline future experiments that can be conducted in the VR-BOI which could address these concerns.

7. Future experiments

The last two chapters discussed the results from the two experiments conducted, showing novel outputs in terms of behavioural results and neural patterns for SI. However, a number of limitations with the experimental design were uncovered and the discussion of the results provided further questions that can be investigated in future experiments. This chapter will outline two follow-up experiments that can address these new research avenues.

7.1. Threat: Dissociation of empathy and bodily threat

In experiment 1 (see Chapter 5), perception of bodily threat and the strength of BOI were shown that could be dissociated. However, the roles of body image and body schema in the perception of the threat over the virtual body could not be separated. Other research has shown that the neural activity associated with threat (P400) can be generated through images of body threat, when viewed without any body ownership imposed (e.g. through pictures of body parts being harmed that belonged to someone else) (Meng et al., 2013).

7.1.1. Aims and scope

The aim of this experiment is to dissociate the effect of body image and body schema in the experience of threat. In addition it aims to consider the effect of tactile and visual threatening sensation towards body ownership and bodily threat and to provide a more complete picture of the differentiation, or not, between the strength of BOI and threat perception. The hypothesis of this experiment is that body image plays a more important role in threat perception, showing a stronger P400 response in the conditions where the human looking body part is threatened versus the condition where harm is presented to an object that does not comply to body image.

7.1.2. Procedure

The VR-BOI platform will be used to conduct this experiment providing the visual and tactile stimulation necessary to deliver the BOI, in a similar way to what is described in Chapter 5. Additional to the virtual environment would be a second avatar, viewed from the 3-rd person perspective, seated in the opposite side of the desk. Furthermore, both avatars would have an option to make the stimulated arm disappear and replaced with a brick, on a trial-to-trial basis. Given these modification the experimental procedure would be a 3x4 factorial design. Stimulation pattern (3 factors) would be one variable, changing in terms of visual only, tactile only, and visual and tactile stimulation. The threatened object (4 factors) variable would vary in where the threatening stimulation is applied: own virtual hand, brick in place of own hand, other virtual person's arm, brick in place of other person's arm. The experimental design is summarised in Table 7.1

Table 7.1.: *Experimental design (3x4) for follow up threat experiment.*

		Threatened object			
		Own hand	'Own' brick	Other's hand	'Other's brick
Stimulation pattern	Tactile stimulation				
	Visual stimulation				
	Visual and Tactile stimulation				

7.2. SOA outside the temporal binding window

Experiment 2 investigated the effects of the visuo-tactile stimulation temporal asynchronies on the strength of BOI. Results from this experiment showed that it is the perception of the delay that can have an effect on the strength of the BOI, with the temporal order of the stimulation playing a role in the illusion due to its effect on delay perception. This experiment also showed that ERP was not correlated with the strength of the illusion, with condition that had elicited stronger BOI having no significantly different ERP components to the control conditions. However, due to the variability of the simultaneity perception between participants, the critical time window during which the perception of the stimulus delay occurs was under-represented in the study. This shortcoming can be addressed by following procedure that was discussed in Chapter 6 (Costantini et al., 2016; Maselli et al., 2016).

7.2.1. Aims and scope

This experiment aims to concentrate at the point where temporal incongruence become noticeable by the participants and to investigate the effect of perceived,

short and long stimulus onset asynchronies in the BOI. Furthermore it aims to investigate to what extent ERP is modulated by the strength of the illusion, taking into account the effect of body schema and body image in the BOI. Finally, using a concrete base for controlling the strength of the illusion, based on the individual tolerance, this experiment aims to investigate further biophysical markers which could relay objective information for the strength of BOI, such as event-related spectral perturbations and network analysis methodologies which have also shown correlation with the strength of BOI (Zeller et al., 2016,1) . The hypothesis of this experiment is that ERP will not be correlated with small changes in the the strength of BOI (following from the results presented in Chapter 6), however, ERP is hypothesised to be modulated either by larger changes in the strength of BOI, or by changes in the body image represented by the virtual avatar, to explain the ERP results observed by Press et al. (2008).

7.2.2. Procedure

The experimental procedure is expanded from the one discussed earlier in Chapter 6 to account for the effect of body image and body schema. Furthermore the changes in experimental procedure account for the inter-participant differences in stimulus simultaneity judgement, producing equal group sizes between conditions which were perceived as asynchronous and conditions which were perceived simultaneous. The experimental procedure is split into two tasks. The first task aims to identify the participant-specific temporal binding window: the timing period during which the participant perceives the visuo-tactile stimulation as simultaneous. During this task a temporal order judgement task will be presented to the participants, showing a visual and tactile stimulation occuring at varying SOA between trials, with the participant having to decide if the visuo-tactile stimulus was synchronous or not during that trial. This task would provide further evidence

on the asymmetry of the point of subjective simultaneity, which was observed to be biased towards visual-first stimulation.

In the second task, the two dimensions of variability in BOI that were defined earlier will be investigated: delay perception and body image/body schema. To achieve this, a 3x4 factorial experimental design will be followed for task 2. The first variable, temporal congruity of visuo-tactile stimulation, will be modulated in four steps: synchronous (point of subjective simultaneity, as found by task 1), just noticeable difference (JND), JND + 100ms, and JND + 500ms. The second variable, pertaining to body image/body schema, will be the presentation of the avatar's arm in three possible visual states: realistic, hand-shaped but low resolution/pixelated, and unrealistic (using a brick in place of the arm, as defined in the procedure of the previous experiment, see Section 7.1.2). The timings used for the SOA variables will ensure a range of BOI strengths, which would provide evidence of the gradient effect of the BOI strength, and could be used as a metric for the objective measure of BOI, as derived by EEG measures. On the other hand, the visual image of the virtual arm and its resemblance to the internal body image would provide results that could dissociate markers of BOI related to body image and body schema. Furthermore, it could provide a new dimension for the gradient of the BOI, in terms of visual representation to accompany the timing dimension proposed in this project. Finally, the control cases where a non-body shaped object (brick) is stimulated entirely out of phase (JND + 500ms) would provide a stark difference in BOI, effectively extinguishing the illusion and provide an adequate metric for comparing between conditions.

Table 7.2.: *Experimental design (3x4) for follow up SOA experiment - Task 2.*

		Stimulus onset asynchrony			
		Simultaneous	Just noticeable difference (JND)	JND + 100ms	JND + 500
Visual fidelity of avatar's arm	Realistic				
	Pixelated / Low resolution				
	Unrealistic (Brick)				

7.3. Conclusions

This chapter discussed the follow up experiments that were designed based on the findings presented in Chapters 5 and 6. It provided a framework for further experimentation of SI, using the VR-BOI platform designed as part of this project. These follow up experiments aim to: (i) explore the relation between threat, empathy and the P400 ERP component, (ii) conduct a more thorough investigation on the effect of noticeable delays in the strength of BOI, (iii) investigate the dichotomy between body image and body schema, and its effect on EEG markers, and finally (iv) provide a concrete template with strong control for further testing objective, biophysical markers for the strength of BOI. The next chapter will summarise the content of this body of work discussed in the thesis and will frame the future research avenues in a more general

8. Summary

8.1. Summary of research outcomes

The aim of this research project was to identify brain mechanisms of SI through the use of the BOI. To achieve this, a VR-BOI platform was developed that was capable of eliciting a strong BOI using visuo-tactile stimulation. Furthermore, the VR-BOI platform could accurately control the temporal presentation of visuo-tactile stimuli so that specialised research experiments could be performed. Using the developed platform, two experiments were conducted: i) an experiment on threat perception that investigated the behavioural and biophysical effects of visuo-tactile threatening stimulation, and ii) an experiment that investigated temporal congruency of visuo-tactile stimulation to assess the effect of small but perceptible delays on the strength of BOI.

The results from the experiments can be divided into two categories: a) those derived from the subjective perception reports of the participants, and b) those obtained from the biophysical signals recorded. Results from the subjective reports demonstrated that threat perception does not necessarily correlate with the strength of the BOI. This was, in part, verified by the biophysical data: the condition with the lowest threat perception as measured by questionnaires and the biophysical recordings, scored the second highest reports of ownership. Furthermore, the results from the questionnaires suggested a variable strength of BOI

depending on the congruency of the most recent stimulation. Through these results of Experiment 1, it is proposed that by collecting frequent subjective reports, an accurate account of the per trial strength of BOI can be derived, rather than the average strength of BOI throughout the whole experiment. Another outcome from the subjective questionnaires was that when small delays between visuotactile stimulation are perceived, the strength of the BOI is negatively affected, however, they do not result in a total extinction of the illusion. This result led to the proposal that the sense of body ownership is a gradual experience. This theory of a continuum of levels of body ownership was framed within the context of embodiment proposed by de Vignemont (2011).

Analysis of the biophysical recording identified a potential differentiation in ERP activity correlated with threat perception: activity recorded from occipital electrodes correlated to presentation of visual-only cues, whereas, ERP activity recorded over central electrodes (above the sensorimotor cortices) was observed during body threatening stimulations, regardless of the sensory modality. By combining the results of this study, with the results from the literature on the perception of pain, and models of body ownership, the ERP activity recorded over central electrodes was hypothesised to be elicited due to the perceived harm of a valid representation of a body part. This is consistent with existing body ownership brain models and also provides a potential example for the theory of body ownership as a gradual experience. If bodily threat can be perceived independently from the sense of ownership, as the subjective and biophysical results of this study suggest, a partial embodiment is implied.

These findings have significant implications for the scientific understanding of SI and body ownership, and have a clear impact for both the experimental, and technological, practical applications of BOI. This project's contribution to scientific knowledge is twofold: 1) the proposed model of a graded sense of body owner-

ship presents a novel perspective that expands the dimensionality of ownership from a binary to a continuous scale, and 2) the separation of activity pertaining to threat perception between the occipital and central regions can inform existing anatomical models of body ownership. With regards the practical impacts for experimental paradigms, two important findings were made within this research: 1) frequent, per-trial, self-report questionnaires more accurately represent the strength of BOI, versus the traditional 'end of experiment' questionnaires, which instead represent an overall BOI throughout the experiment, and 2) ERP analysis is not a suitable metric for comparing the strength of BOI elicited during an experiment. These findings also demonstrate a technological application as the results demonstrate that a visual leading stimulus is preferred in order to maintain a high perception of BOI. Thus in practical situations or experimental paradigms where BOI is a necessary goal, but the visuo-tactile stimulation that invokes the BOI has unavoidable delays between information streams, a visual leading stimulus is a more robust method to maintain the illusion, compared to its tactile-leading counterpart. This is especially relevant in VR settings used for entertainment purposes, in rehabilitation systems that use VR and robotics, and for any experimental research using visuo-tactile stimulation to investigate body ownership.

8.2. Future research avenues

This project has provided a novel perspective, and enhanced techniques, for investigating the mechanisms underlying body ownership and sensory integration. Further experimentation is required to validate and expand the proposals introduced in this work. First, extended analysis could address the source localisation of the EEG activity; in particular surface Laplacian, current source estimation,

and activity clustering techniques could improve localisation of activity. Accurate localisation of ERP activity could inform which specific brain areas are involved in multisensory threat perception. Furthermore, by employing methods that investigate the temporal development of the biophysical signal, it would be possible to investigate the temporal evolution of the neural correlates of SI/body ownership. This would permit comparisons between experimental conditions that are not possible to make using the techniques employed in this study. Such enhanced EEG analysis methods could provide evidence of neural correlates of body ownership, which this project did not observe through ERP analysis alone. Experimentation using an extended range of delays, sensory stimuli, and/or visual body representations will enhance the results of the current study, and provide new evidence to support or disprove the hypotheses proposed based on the findings of this study.

I would like to acknowledge several individuals who have provided considerable help either directly, or indirectly, towards the completion of this thesis. First, I would like to thank my supervisors, Prof. S. Nasuto, Prof. W.Harwin and Dr. Y. Hayashi for their tremendous help, support, and guidance throughout this PhD project. Your influence has been instrumental in growing my passion and skills in science. I would also like to thank Dr. N. Holmes and Prof. D. Saddy, for their vital input in the conception and funding of this project. I would also like to thank the many members of staff and colleagues of the School of Systems Engineering and the School of Biological sciences (Dr. Hwang, Dr. Janko, Ms White, Mr Minchinton, Prof Holderbaum, Dr. Armengol, Mr. Gurr, Mr. Laird, Mr. Gould, Mr. Dove, Dr. Portelli, Dr. Cave-Ayland, Dr. Daly, Dr. Weaver, Ms Oguntosin, Ms Wairagkar, Mr Sainz-Martinez, Dr. Dubuc, Dr. Sforza, but to name a few with apologies to the many that I have mistakenly left out) that directly and indirectly helped me through various stages to complete this PhD project. I would also like to thank my examiners, Dr. Roesch and Dr. Newport for their input and insights that lead to this final version of my thesis.

I would also like to thank my family, Dora, Dimitris, Matina, Kai, and Dimitris-William for being an awesome family and for supporting me financially and emotionally through the long years of academia. I would also like to acknowledge the support of my many friends both in the UK and Overseas, for all the good times that kept me going (with special mention to Rob, Thodoris, Natasa, Thanos, Alex, Vicky, Pauline, Andi, and Karl). Special thanks to Gay, Andrew, Robert, and Liam for having me at the last and most stressful stages of the write-up.

Last but not least I would like to thank Orla Fannon, I would have not been able to have done any of this without you. Thank you for your patient and support and for putting up with me through the write-up. Thank you. A billion-googolplex thank you.

Appendices

A. Mathematical model of pneumatic vibrations

A.1. System model

The pneumatic/hydraulic vibration system is comprised of a piston (pneumatic or hydraulic cylinder) actuated by a motor, a pipe to transfer the energy in the fMRI room and an elastic end-effector to deliver the vibration on the test subject, as shown in figure Figure A.1

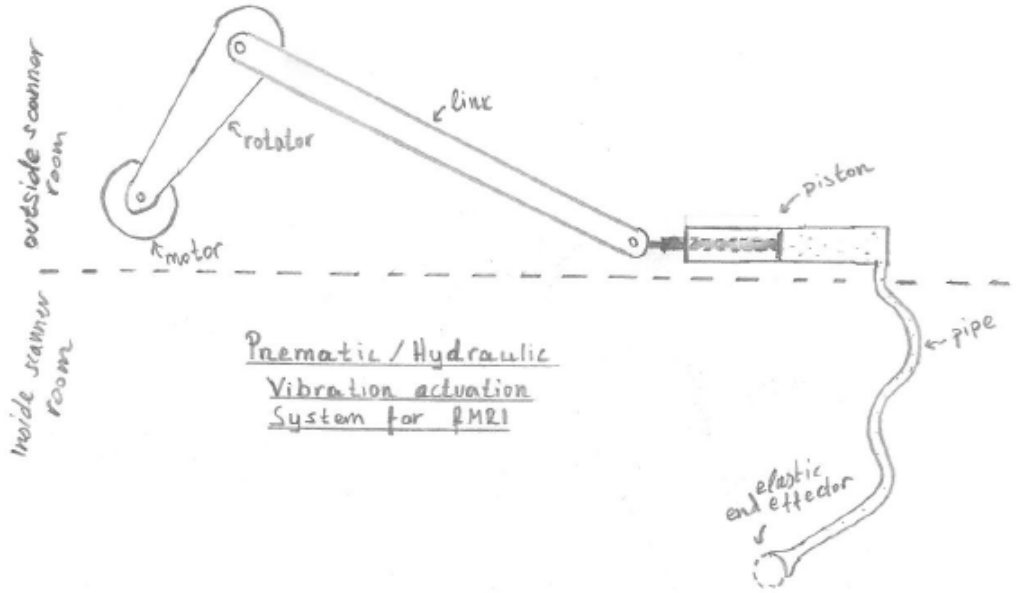

Figure A.1.: *Schematic of the actuation system proposed to create vibration in the fMRI room. Top part is the part of the mechanism that lies outside of the shielded room and bottom part lies in the fMRI scanner.*

A.2. Equivalent system - Boyle's law

Using Boyle's law, the pressure and volume of gas inside the piston can be translated as a pressure and volume exerted by an imaginary piston inside the tube in order to simplify the modelling of the system. The conversion to the equivalent system using Boyle's law is shown in the upper part of figure Figure A.2

A.3. Hagen - Poiseuille law

The Hagen - Poiseuille law states that:

$$q = \frac{\pi r^4 (P_1 - P_2)}{8\eta l} \tag{A.1}$$

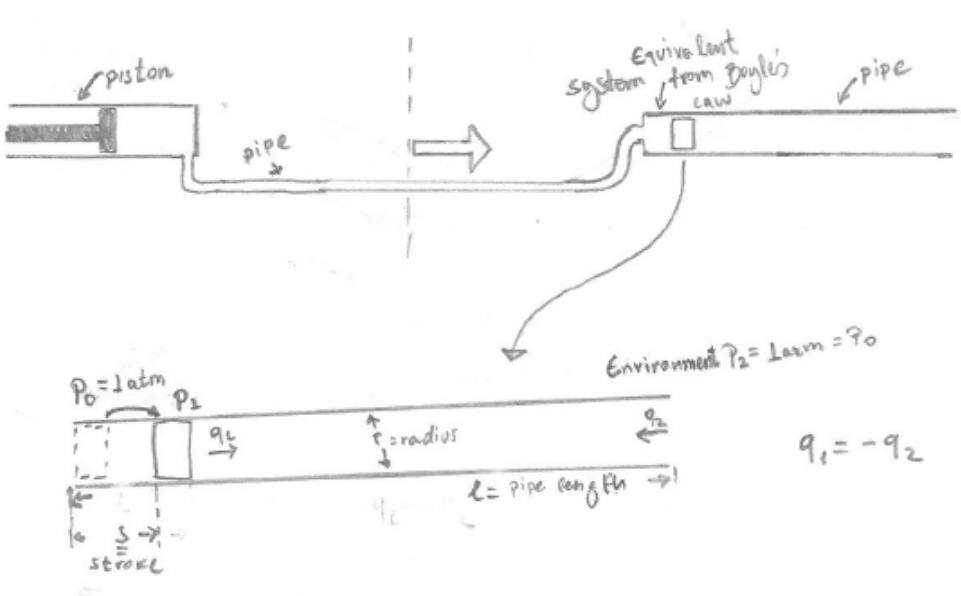

Figure A.2.: *Equivalent system using Boyle's law. Top left is the piston situated outside of the fMRI room. Top right shows the equivalent system when applying Boyle's law of gases. Finally bottom part of the picture illustrates the variables used for modelling.*

where q is the flow, r is the radius of the pipe, $P_1$is the inlet pressure, P_2 is the outlet pressure, η is the viscosity and$l$ the length of the pipe, as shown in the lower part of figure 2.

The flow can also be defined as:

$$q = \frac{2\Delta \mathrm{x} \pi r^2}{t} \tag{A.2}$$

where Δx is the displacement of the medium in the pipe and t is the time that it took for the medium to be displaced by Δx.

By equating Equation (A.1) and Equation (A.2) the difference in pressure is set as:

$$P_1 - P_2 = \frac{16\Delta x l \eta}{r^2 t} \tag{A.3}$$

from Boyle's law P_1can be found:

$$P_1 = P_0 \frac{l}{l-2} \tag{A.4}$$

By using Equation (A.4), Equation (A.3), and $P_2 = P_0$ and solving for Δx :

$$\boxed{\Delta x = \frac{P_o r^2 t s}{16\eta l(l-s)}} \tag{A.5}$$

Which can be used to calculate the displacement of an incompressible medium in laminar flow.

A.4. Compressibility correction factor

Equation (A.5) is not accurate for compressible flow. To correct for compressibility for using air as a medium a correction factor $\frac{P_1^2 - P_0^2}{P_o}$ can be used in Equation (A.1) so that Δx for compressible flow can be computed as:

$$\boxed{\Delta x = \frac{t r^2 P_o^2 (l^2 - (l-s)^2)}{32\eta P_o l(l-s)^2}} \tag{A.6}$$

A.5. Energy of the air

The kinetic energy of the displacement of the medium can be found by getting the mass of the medium:

$$m = Vd = \pi r^2 \Delta x d \tag{A.7}$$

where m is the mass, V is the volume and d is density of the medium.

The velocity u of the mass of the medium can be found as:

$$u = \frac{2\Delta x}{t} \tag{A.8}$$

Then using Equation (A.7) and Equation (A.8) the kinetic energy $E_k$is:

$$E_k = \frac{1}{2}mu^2 = \frac{2\pi r^2 \Delta x^3 d}{t^2} \tag{A.9}$$

Assuming lossless transfer of energy from the medium to the elastic material of the end effector$E_k = E_u$, with $E_u$being the elastic energy the final amplitude of vibration of the elastic end effector, Δ_{act} can be derived:

$$\boxed{\Delta_{act} = \frac{2E_k}{k}} \tag{A.10}$$

where k is the spring constant of the elastic material of the end effector.

A.6. Theoretical results

The above system was coded in Matlab® (The MathWorks, Inc.), a mathematical modelling software. One of the important insights of the mathematical model is that by increasing the radius of the pipe an increase in the end effector amplitude is expected, as can be seen in figure Figure A.3. Also the effects of modulating the frequency and length of the pipe can be seen in figure Figure A.4 and Figure A.5 accordingly.

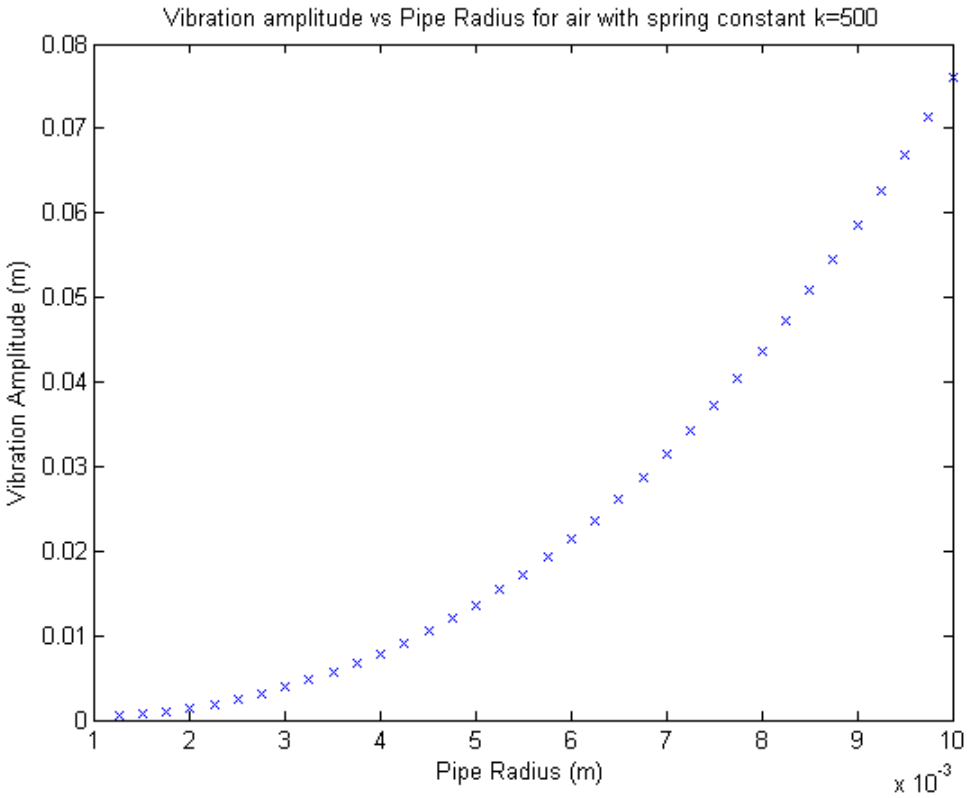

Figure A.3.: *Graph showing the change of the end effector vibration amplitude when using pipes of different radius. The model predicts that the greater the radius of the pipe the greater the resulting amplitude is. Pipe radius range of values is selected to reflect a realistic choice for pipes so that they can fit through the cable opening at the fMRI room wall.*

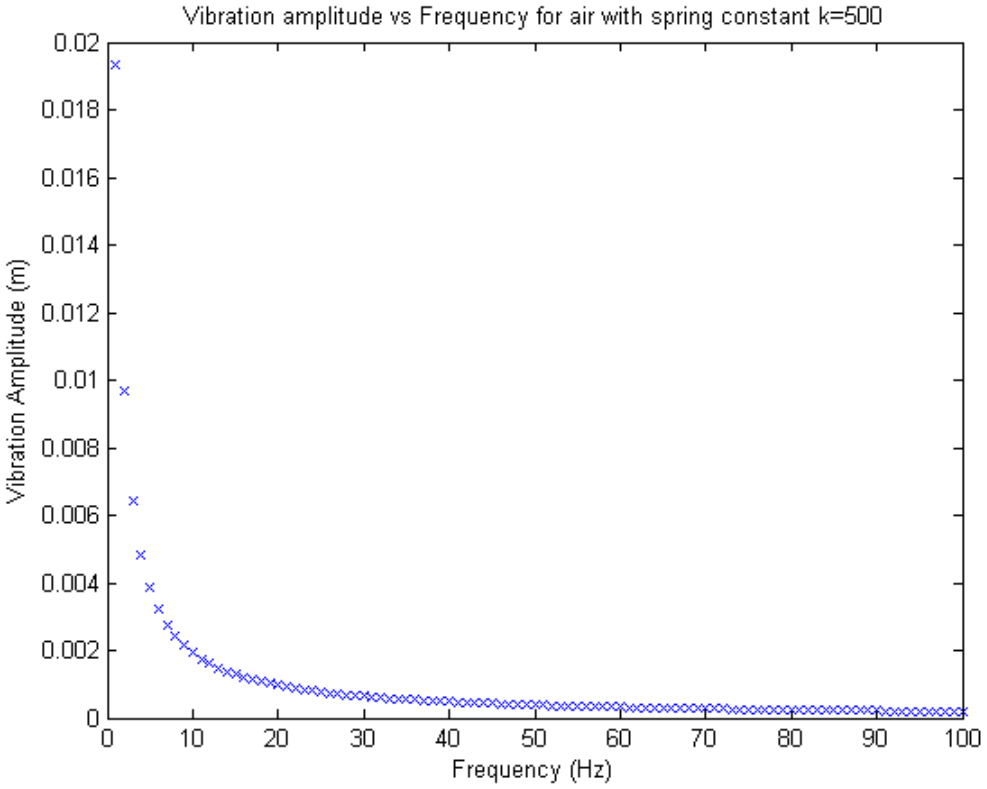

Figure A.4.: *Graph showing change of end effector amplitude with the change of input frequency of piston strokes.*

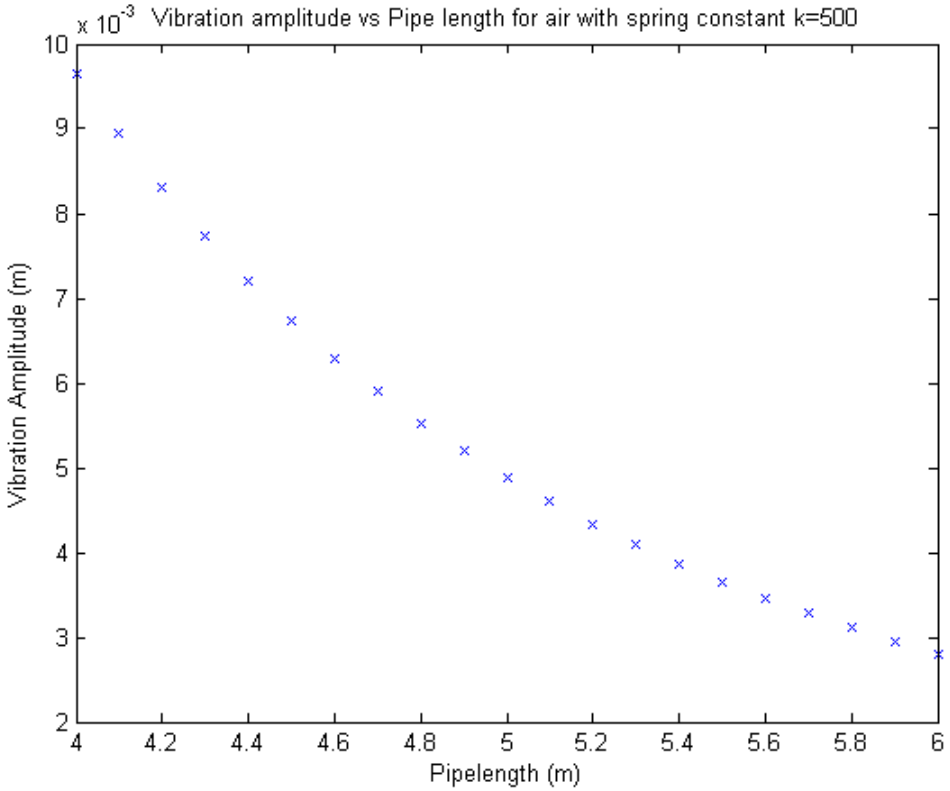

Figure A.5.: *Change of end effector amplitude as an effect of changing the length of the pipe. Pipe lengths are selected from a range of +/- 1m of the measured minimum length required to reach to the centre of the fMRI coil from the control room outside.*

Bibliography

Aflalo, T., Kellis, S., Klaes, C., Lee, B., Shi, Y., Pejsa, K., Shanfield, K., Hayes-Jackson, S., Aisen, M., Heck, C., Liu, C., and Andersen, R. A. (2015). Decoding motor imagery from the posterior parietal cortex of a tetraplegic human. *Science*, 348(6237):906–910.

Alitto, H. J. and Usrey, W. M. (2003). Corticothalamic feedback and sensory processing. *Current Opinion in Neurobiology*, 13(4):440–445.

Allman, B. L., Bittencourt-Navarrete, R. E., Keniston, L. P., Medina, A. E., Wang, M. Y., and Meredith, M. A. (2008). Do Cross-Modal Projections Always Result in Multisensory Integration? *Cerebral Cortex*, 18(9):2066–2076.

Allman, B. L., Keniston, L. P., and Meredith, M. A. (2009). Not Just for Bimodal Neurons Anymore: The Contribution of Unimodal Neurons to Cortical Multisensory Processing. *Brain Topography*, 21(3-4):157–167.

Angelaki, D. E., Gu, Y., and DeAngelis, G. C. (2009). Multisensory integration: psychophysics, neurophysiology, and computation. *Current Opinion in Neurobiology*, 19(4):452–458.

Apps, M. A. J., Tajadura-Jimenez, A., Sereno, M., Blanke, O., and Tsakiris, M. (2015). Plasticity in Unimodal and Multimodal Brain Areas Reflects Multisensory Changes in Self-Face Identification. *Cerebral Cortex*, 25(1):46–55.

Arizono, N., Ohmura, Y., Yano, S., and Kondo, T. (2016). Functional Connectivity Analysis of NIRS Data under Rubber Hand Illusion to Find a Biomarker of Sense of Ownership. *Neural Plasticity*, 2016:1–9.

Armel, K. C. and Ramachandran, V. S. (2003). Projecting sensations to external objects: evidence from skin conductance response. *Proceedings of the Royal Society of London. Series B: Biological Sciences*, 270(1523):1499 LP – 1506.

Arumana, J. M. (2012). *Integration of EEG-FMRI in an Auditory Oddball Paradigm Using Joint Independent Component Analysis*. PhD thesis, Marquette University.

Aspell, J. E., Palluel, E., and Blanke, O. (2012). Early and late activity in somatosensory cortex reflects changes in bodily self-consciousness: an evoked potential study. *Neuroscience*, 216:110–22.

Bai, O., Lin, P., Vorbach, S., Li, J., Furlani, S., and Hallett, M. (2007). Exploration of computational methods for classification of movement intention during human voluntary movement from single trial EEG. *Clinical neurophysiology : official journal of the International Federation of Clinical Neurophysiology*, 118(12):2637–55.

Bai, O., Rathi, V., Lin, P., Huang, D., Battapady, H., Fei, D.-Y., Schneider, L., Houdayer, E., Chen, X., and Hallett, M. (2011). Prediction of human voluntary movement before it occurs. *Clinical Neurophysiology*, 122(2):364–372.

Banakou, D., Groten, R., and Slater, M. (2013). Illusory ownership of a virtual child body causes overestimation of object sizes and implicit attitude changes. *Proceedings of the National Academy of Sciences of the United States of America*, 110(31):12846–51.

Banakou, D., H, P., and Slater, M. (2016). Virtual Embodiment of White People in a Black Virtual Body Leads to a Sustained Reduction in their Implicit Racial Bias. *Frontiers in Human Neuroscience*, 10:601.

Bear, M. F., Connors, B. W., and Paradiso, M. A. (2001). *Neuroscience: Exploring the Brain*. Lippincott Williams & Wilkins, 2nd edition.

Beauchamp, M. S. (2005). Statistical Criteria in fMRI Studies of Multisensory Integration. *Neuroinformatics*, 3(2):93–113.

Beauchamp, M. S., Yasar, N. E., Frye, R. E., and Ro, T. (2008). Touch , sound and vision in human superior temporal sulcus. 41:1011–1020.

Bekrater-Bodmann, R., Foell, J., Diers, M., Kamping, S., Rance, M., Kirsch, P., Trojan, J., Fuchs, X., Bach, F., Çakmak, H. K., Maaß, H., and Flor, H. (2014). The Importance of Synchrony and Temporal Order of Visual and Tactile Input for Illusory Limb Ownership Experiences - An fMRI Study Applying Virtual Reality. *PLoS ONE*, 9(1):e87013.

Benjamini, Y. and Hochberg, Y. (1995). Controlling the False Discovery Rate: A Practical and Powerful Approach to Multiple Testing. *Journal of the Royal Statistical Society. Series B (Methodological)*, 57(1):289–300.

Berger, C. C. and Ehrsson, H. H. (2014). The Fusion of Mental Imagery and Sensation in the Temporal Association Cortex. *Journal of Neuroscience*, 34(41):13684–13692.

Blakemore, S. J., Wolpert, D. M., and Frith, C. D. (2002). Abnormalities in the awareness of action. *Trends in cognitive sciences*, 6(6):237–242.

Blanchard, C., Roll, R., Roll, J.-P., and Kavounoudias, A. (2011). Combined contribution of tactile and proprioceptive feedback to hand movement perception. *Brain research*, 1382:219–29.

Blanchard, C., Roll, R., Roll, J.-P., and Kavounoudias, A. (2013). Differential contributions of vision, touch and muscle proprioception to the coding of hand movements. *PloS one*, 8(4):e62475.

Blanke, O. (2012). Multisensory brain mechanisms of bodily self-consciousness. *Nature reviews. Neuroscience*, 13(July):556–71.

Blanke, O., Slater, M., and Serino, A. (2015). Behavioral, Neural, and Computational Principles of Bodily Self-Consciousness. *Neuron*, 88(1):145–166.

Botvinick, M. and Cohen, J. (1998). Rubber hands 'feel' touch that eyes see. *Nature*, 391(6669):756.

Boucsein, W., Fowles, D. C., Grimnes, S., Ben-Shakhar, G., Roth, W. T., Dawson, M. E., and Filion, D. L. (2012). Publication recommendations for electrodermal measurements. *Psychophysiology*, 49(8):1017–34.

Brang, D., McGeoch, P. D., and Ramachandran, V. S. (2008). Apotemnophilia: a neurological disorder. *Neuroreport*, 19(13):1305–1306.

Breitwieser, C., Daly, I., Neuper, C., and Muller-Putz, G. R. (2012). Proposing a standardized protocol for raw biosignal transmission. *IEEE transactions on bio-medical engineering*, 59(3):852–859.

Briggs, F. and Usrey, W. M. (2008). Emerging views of corticothalamic function. *Current Opinion in Neurobiology*, 18(4):403–407.

Brozzoli, C., Gentile, G., Petkova, V. I., and Ehrsson, H. H. (2011). fMRI Adaptation Reveals a Cortical Mechanism for the Coding of Space Near the Hand. *Journal of Neuroscience*, 31(24):9023–9031.

Buzsaki, G., Anastassiou, C. A., and Koch, C. (2012). The origin of extracellular fields and currents - EEG, ECoG, LFP and spikes. *Nature Reviews Neuroscience*, 13(6):407–420.

Cappe, C., Morel, A., Barone, P., and Rouiller, E. M. (2009). The thalamocortical projection systems in primate: An anatomical support for multisensory and sensorimotor interplay. *Cerebral Cortex*, 19(9):2025–2037.

Cappe, C., Rouiller, E. M., and Barone, P. (2012). Cortical and Thalamic Pathways for Multisensory and Sensorimotor Interplay. In Murray, M. and Wallace, M. T., editors, *The Neural Bases of Multisensory Processes*, number Calvert 2001, chapter 2, pages 13–28.

CRC Press/Taylor & Francis, Boca Raton (FL).

Cappe, C., Thut, G., Romei, V., and Murray, M. M. (2010). Auditory-Visual Multisensory Interactions in Humans: Timing, Topography, Directionality, and Sources. *J Neurosci*, 30(38):12572–12580.

Cardinali, L., Frassinetti, F., Brozzoli, C., Urquizar, C., Roy, A. C., and Farnè, A. (2009). Tool-use induces morphological updating of the body schema. *Current Biology*, 19(12):R478–R479.

Carriere, B. N., Royal, D. W., Perrault, T. J., Morrison, S. P., Vaughan, J. W., Stein, B. E., and Wallace, M. T. (2007). Visual Deprivation Alters the Development of Cortical Multisensory Integration. *Journal of Neurophysiology*, 98(5):2858–2867.

Cheyne, D. and Ferrari, P. (2013). MEG studies of motor cortex gamma oscillations: evidence for a gamma "fingerprint" in the brain? *Frontiers in human neuroscience*, 7(September):575.

Chin, Z. Y., Ang, K. K., Wang, C., and Guan, C. (2010). Online performance evaluation of motor imagery BCI with augmented-reality virtual hand feedback. *Conference proceedings : ... Annual International Conference of the IEEE Engineering in Medicine and Biology Society. IEEE Engineering in Medicine and Biology Society. Conference*, 2010:3341–4.

Clemo, H. R., Keniston, L. P., and Meredith, M. A. (2012). Structural Basis of Multisensory Processing. In Murray, M. M. and Wallace, M. T., editors, *The Neural Bases of Multisensory Processes*, chapter 1, pages 3–14. CRC Press/Taylor & Francis, Boca Raton (FL).

Costantini, M., Robinson, J., Migliorati, D., Donno, B., Ferri, F., and Northoff, G. (2016). Temporal limits on rubber hand illusion reflect individuals' temporal resolution in multisensory perception. *Cognition*, 157:39–48.

Cudeiro, J. and Sillito, A. M. (2006). Looking back: corticothalamic feedback and early visual processing. *Trends in Neurosciences*, 29(6):298–306.

Darvas, F., Scherer, R., Ojemann, J. G., Rao, R. P., Miller, K. J., and Sorensen, L. B. (2010). High gamma mapping using EEG. *NeuroImage*, 49(1):930–8.

David, N. (2012). New frontiers in the neuroscience of the sense of agency. *Frontiers in human neuroscience*, 6(June):161.

de Vignemont, F. (2011). Embodiment, ownership and disownership. *Consciousness and cognition*, 20(1):82–93.

de Vignemont, F. (2013). The mark of bodily ownership. *Analysis*, 73(4):643–651.

de Vignemont, F. (2014). A multimodal conception of bodily awareness. *Mind*, pages 1–43.

de Vignemont, F. and Farnè, A. (2010). Widening the body to rubber hands and tools: what's the difference? *Revue de Neuropsychologie, Neurosciences Cognitives*, 2(3):203–211.

Delorme, A. and Makeig, S. (2004). EEGLAB: an open source toolbox for analysis of single-trial {EEG} dynamics including independent component analysis. *Journal of Neuroscience Methods*, 134(1):9–21.

Desmurget, M. (2013). Searching for the neural correlates of conscious intention. *Journal of cognitive neuroscience*, 25(6):830–833.

Desmurget, M. and Sirigu, A. (2009). A parietal-premotor network for movement intention and motor awareness. *Trends in Cognitive Sciences*, 13(10):411–419.

Desmurget, M. and Sirigu, A. (2012). Conscious motor intention emerges in the inferior parietal lobule. *Current Opinion in Neurobiology*, 22(6):1004–1011.

Di Luca, M., Machulla, T.-K., and Ernst, M. O. (2009). Recalibration of multisensory simultaneity: cross-modal transfer coincides with a change in perceptual latency. *Journal of vision*, 9(12):7.1–16.

Dieguez, S., Mercier, M. R., Newby, N., and Blanke, O. (2009). Feeling numbness for someone else's finger. *Current Biology*, 19(24):R1108 – R1109.

Ehrsson, H. (2012). The Concept of Body Ownership and Its Relation to Multisensory Integration. In Calvert, G. A., Spence, C., and Stein, B. E., editors, *The New Handbook of Multisensory Processes*, chapter 43, pages 775–792. MIT Press, Cambridge, Massachusetts.

Ehrsson, H. H. (2007). The experimental induction of out-of-body experiences. *Science*, 317(5841):1048.

Ehrsson, H. H. (2009). How many arms make a pair? Perceptual illusion of having an additional limb. *Perception*, 38(2):310–312.

Ehrsson, H. H., Holmes, N., and Passingham, R. E. (2005a). Touching a Rubber Hand: Feeling of Body Ownership Is Associated with Activity in Multisensory Brain Areas. *Journal of Neuroscience*, 25(45):10564–10573.

Ehrsson, H. H., Kito, T., Sadato, N., Passingham, R. E., and Naito, E. (2005b). Neural substrate of body size: illusory feeling of shrinking of the waist. *PLoS biology*, 3(12):e412.

Ehrsson, H. H., Rosen, B., Stockselius, A., Ragno, C., Kohler, P., and Lundborg, G. (2008). Upper limb amputees can be induced to experience a rubber hand as their own. *Brain*, 131(12):3443–3452.

Ehrsson, H. H., Wiech, K., Weiskopf, N., Dolan, R. J., and Passingham, R. E. (2007). Threatening a rubber hand that you feel is yours elicits a cortical anxiety response. *Proceedings of the National Academy of Sciences*, 104(23):9828–9833.

Einevoll, G. T., Kayser, C., Logothetis, N. K., and Panzeri, S. (2013). Modelling and analysis of local field potentials for studying the function of cortical circuits. *Nat Rev Neurosci*, 14(11):770–785.

Evans, N. and Blanke, O. (2013). Shared electrophysiology mechanisms of body ownership and motor imagery. *NeuroImage*, 64:216–28.

Fabre-Thorpe, M., Delorme, a., Marlot, C., and Thorpe, S. (2001). A limit to the speed of processing in ultra-rapid visual categorization of novel natural scenes. *Journal of Cognitive Neuroscience*, 13(2):171–180.

Fan, Y. and Han, S. (2008). Temporal dynamic of neural mechanisms involved in empathy for pain: An event-related brain potential study. *Neuropsychologia*, 46(1):160–173.

Farmer, H., Tajadura-Jiménez, A., and Tsakiris, M. (2012). Beyond the colour of my skin: How skin colour affects the sense of body-ownership. *Consciousness and Cognition*, 21(3):1242–1256.

Farrow, T. F. D., Johnson, N. K., Hunter, M. D., Barker, A. T., Wilkinson, I. D., and Woodruff, P. W. R. (2012). Neural correlates of the behavioral-autonomic interaction response to potentially threatening stimuli. *Frontiers in Human Neuroscience*, 6:349.

Feinberg, T. E., Venneri, A., Simone, A. M., Fan, Y., and Northoff, G. (2010). The neuroanatomy of asomatognosia and somatoparaphrenia. *Journal of neurology, neurosurgery, and psychiatry*, 81(3):276–81.

Felch, D. L., Khakhalin, A. S., and Aizenman, C. D. (2016). Multisensory integration in the developing tectum is constrained by the balance of excitation and inhibition. *eLife*, 15600(401).

Ferri, F., Chiarelli, A. M., Merla, A., Gallese, V., and Costantini, M. (2013). The body beyond the body: expectation of a sensory event is enough to induce ownership over a fake hand. *Proceedings. Biological sciences / The Royal Society*, 280(1765):20131140.

Fink, M., Ulbrich, P., Churan, J., and Wittmann, M. (2006). Stimulus-dependent processing of temporal order. *Behavioural processes*, 71(2-3):344–52.

First, M. B. (2005). Desire for amputation of a limb: paraphilia, psychosis, or a new type of identity disorder. *Psychological medicine*, 35(6):919–928.

Friston, K. J., Fletcher, P., Josephs, O., Holmes, A., Rugg, M. D., and Turner, R. (1998). Event-Related fMRI: Characterizing Differential Responses. *NeuroImage*, 7(1):30–40.

Fuentes-Santamaria, V., Alvarado, J. C., Stein, B. E., and McHaffie, J. G. (2008). Cortex contacts both output neurons and nitrergic interneurons in the superior colliculus: Direct and indirect routes for multisensory integration. *Cerebral Cortex*, 18(7):1640–1652.

Fuster, J. M. (2001). The Prefrontal Cortex - An Update: Time Is of the Essence. *Neuron*, 30(2):319–333.

Fuster, J. M., Bodner, M., and Kroger, J. K. (2000). Cross-modal and cross-temporal association in neurons of frontal cortex . *Nature*, 405(6784):347–351.

Gallagher, I. (2000). Philosophical conceptions of the self: implications for cognitive science. *Trends in cognitive sciences*, 4(1):14–21.

Gallese, V. and Lakoff, G. (2005). The Brain's concepts: the role of the Sensory-motor system in conceptual knowledge. *Cognitive Neuropsychology*, 22(3-4):455–479.

Gentile, G., Björnsdotter, M., Petkova, V. I., Abdulkarim, Z., and Ehrsson, H. H. (2015). Patterns of neural activity in the human ventral premotor cortex reflect a whole-body multisensory percept. *NeuroImage*, 109:328–40.

Gentile, G., Guterstam, A., Brozzoli, C., and Ehrsson, H. H. (2013). Disintegration of Multisensory Signals from the Real Hand Reduces Default Limb Self-Attribution: An fMRI Study. *Journal of Neuroscience*, 33(33):13350–13366.

Gentsch, A., Kathmann, N., and Schutz-Bosbach, S. (2012). Reliability of sensory predictions determines the experience of self-agency. *Behavioural brain research*, 228(2):415–422.

Ghazanfar, A. A. (2009). The multisensory roles for auditory cortex in primate vocal communication. *Hearing Research*, 258(1-2):113–120.

Ghazanfar, A. A. and Schroeder, C. E. (2006). Is neocortex essentially multisensory? *Trends in Cognitive Sciences*, 10(6):278–285.

Giard, M. H. and Peronnet, F. (1999). Auditory-visual integration during multimodal object recognition in humans: a behavioral and electrophysiological study. *J Cogn Neurosci*, 11(5):473–490.

González-Franco, M., Peck, T. C., Rodríguez-Fornells, A., and Slater, M. (2014). A threat to a virtual hand elicits motor cortex activation. *Experimental Brain Research*, 232(3):875–887.

Goodwin, G. M., McCloskey, D. I., and Matthews, P. B. (1972). The contribution of muscle afferents to kinaesthesia shown by vibration induced illusions of movement and by the

effects of paralysing joint afferents. *Brain : a journal of neurology*, 95(4):705–48.

Gray, H. (1918). *Anatomy of the human body*. Lea & Febiger, Philadelphia, 20th edition.

Graziano, M. S. (2011). New insights into motor cortex. *Neuron*, 71(3):387–388.

Graziano, M. S. a. and Aflalo, T. N. (2007). Mapping behavioral repertoire onto the cortex. *Neuron*, 56(2):239–251.

Grill-Spector, K. (2006). Selectivity of Adaptation in Single Units: Implications for fMRI Experiments. *Neuron*, 49(2):170–171.

Grill-Spector, K. and Malach, R. (2001). fMR-adaptation: a tool for studying the functional properties of human cortical neurons. *Acta psychologica*, 107(1-3):293–321.

Grivaz, P., Blanke, O., and Serino, A. (2017). Common and distinct brain regions processing multisensory bodily signals for peripersonal space and body ownership. *NeuroImage*, 147:602–618.

Groppe, D. M., Urbach, T. P., and Kutas, M. (2011). Mass univariate analysis of event-related brain potentials/fields I: A critical tutorial review. *Psychophysiology*, 48(12):1711–1725.

Guterstam, A. (2016). *Multisensory mechanisms of body ownership and self-location*. PhD thesis, Karolinska Institutet.

Guterstam, A., Björnsdotter, M., Gentile, G., and Ehrsson, H. H. (2015). Posterior Cingulate Cortex Integrates the Senses of Self-Location and Body Ownership. *Current Biology*, 25(11):1416–1425.

Guterstam, A., Petkova, V. I., and Ehrsson, H. H. (2011). The illusion of owning a third arm. *PLoS ONE*, 6(2):e17208.

Haggard, P. (2008). Human volition: towards a neuroscience of will. *Nat Rev Neurosci*, 9(12):934–946.

Hägni, K., Eng, K., Hepp-Reymond, M.-C., Holper, L., Keisker, B., Siekierka, E., and Kiper, D. C. (2008). Observing Virtual Arms that You Imagine Are Yours Increases the Galvanic Skin Response to an Unexpected Threat. *PLOS ONE*, 3(8):1–6.

Hebb, T. D. O., Ramachandran, V. S., and Hirstein, W. (1998). The perception of phantom limbs. pages 1603–1630.

Henschke, J. U., Noesselt, T., Scheich, H., and Budinger, E. (2015). Possible anatomical pathways for short-latency multisensory integration processes in primary sensory cortices. *Brain structure & function*, 220(2):955–977.

Holmes, N. P., Snijders, H. J., and Spence, C. (2006). Reaching with alien limbs: Visual exposure to prosthetic hands in a mirror biases proprioception without accompanying illusions of

ownership. *Perception & psychophysics*, 68(4):685–701.

Holmes, N. P. and Spence, C. (2005). Multisensory integration: Space, time, & superadditivity. *Current biology : CB*, 15(18):R762–R764.

Horn, G. and Hill, R. (1966). Responsiveness to sensory stimulation of units in the superior colliculus and subjacent tectotegmental regions of the rabbit. *Experimental Neurology*, 14(2):199–223.

Hothorn, T., Bretz, F., and Westfall, P. (2008). Simultaneous Inference in General Parametric Models. *Biometrical Journal*, 50(3):346–363.

Ionta, S., Martuzzi, R., Salomon, R., and Blanke, O. (2014). The brain network reflecting bodily self-consciousness: a functional connectivity study. *Social cognitive and affective neuroscience*.

Ismail, M. A. F. and Shimada, S. (2016). 'Robot' Hand Illusion under Delayed Visual Feedback: Relationship between the Senses of Ownership and Agency. *PLOS ONE*, 11(7):1–9.

Jay, M. F. and Sparks, D. L. (1984). Auditory receptive fields in primate superior colliculus shift with changes in eye position. *Nature*, 309(5966):345–347.

Jeannerod, M. (1994). The representing brain: Neural correlates of motor intention and imagery. *Behavioral and Brain Sciences*, 17(02):187–245.

Jeannerod, M. (1995). Mental imagery in the motor context. *Neuropsychologia*, 33(11):1419–1432.

Jeannerod, M. (2001). Neural Simulation of Action: A Unifying Mechanism for Motor Cognition. *NeuroImage*, 14(1):S103 – S109.

Jeannerod, M. (2003). The mechanism of self-recognition in humans. *Behavioural Brain Research*, 142(1-2):1–15.

Jenkinson, P. M., Haggard, P., Ferreira, N. C., and Fotopoulou, A. (2013). Body ownership and attention in the mirror: Insights from somatoparaphrenia and the rubber hand illusion. *Neuropsychologia*, 51(8):1453–1462.

Johnson, J. A. and Zatorre, R. J. (2005). Attention to Simultaneous Unrelated Auditory and Visual Events: Behavioral and Neural Correlates. *Cerebral Cortex*, 15(10):1609–1620.

Johnson, J. A. and Zatorre, R. J. (2006). Neural substrates for dividing and focusing attention between simultaneous auditory and visual events. *NeuroImage*, 31(4):1673–1681.

Jones, L. a. (1988). Motor illusions: what do they reveal about proprioception? *Psychological bulletin*, 103(1):72–86.

Kaiser, J. and Naumer, M. J. (2010). Cortical Oscillations and Multisensory Interactions in Humans. In Kaiser, J. and Naumer, M. J., editors, *Multisensory Object Perception in the Primate Brain*, chapter 5, pages 71–82. Springer New York, New York, NY.

Kajikawa, Y. and Schroeder, C. E. (2011). How Local Is the Local Field Potential? *Neuron*, 72(5):847–858.

Kalckert, A. and Ehrsson, H. H. (2012). Moving a Rubber Hand that Feels Like Your Own: A Dissociation of Ownership and Agency. *Frontiers in Human Neuroscience*, 6(March):1–14.

Kalckert, A. and Ehrsson, H. H. (2014). The moving rubber hand illusion revisited: Comparing movements and visuotactile stimulation to induce illusory ownership. *Consciousness and Cognition*, 26:117–132.

Kanabus, M., Szelag, E., Rojek, E., and Poppel, E. (2002). Temporal order judgement for auditory and visual stimuli. *Acta Neurobiol Exp (Wars)*, 62(4):263–270.

Kanayama, N., Morandi, A., Hiraki, K., and Pavani, F. (2016). Causal Dynamics of Scalp Electroencephalography Oscillation During the Rubber Hand Illusion. *Brain Topography*, pages 1–14.

Kanayama, N., Sato, A., and Ohira, H. (2009). The role of gamma band oscillations and synchrony on rubber hand illusion and crossmodal integration. *Brain and cognition*, 69(1):19–29.

Kanayama, N., Tamè, L., Ohira, H., and Pavani, F. (2012). Top down influence on visuo-tactile interaction modulates neural oscillatory responses. *NeuroImage*, 59(4):3406–17.

Kavounoudias, A., Roll, J.-P., Anton, J. L., Nazarian, B., Roth, M., and Roll, R. (2008). Proprio-tactile integration for kinesthetic perception: an fMRI study. *Neuropsychologia*, 46(2):567–75.

Kayser, C., Petkov, C. I., and Logothetis, N. K. (2008). Visual Modulation of Neurons in Auditory Cortex. *Cerebral Cortex*, 18(7):1560–1574.

Keetels, M. and Vroomen, J. (2008). Temporal recalibration to tactile-visual asynchronous stimuli. *Neuroscience Letters*, 430(2):130–134.

Keetels, M. and Vroomen, J. (2012). Perception of Synchrony between the Senses. In Murray, M. and Wallace, M. T., editors, *The Neural Bases of Multisensory Processes*, chapter Chapter 9. CRC Press/Taylor & Francis.

Keysers, C., Kohler, E., Umiltà, M. A., Nanetti, L., Fogassi, L., and Gallese, V. (2003). Audiovisual mirror neurons and action recognition. *Experimental Brain Research*, 153(4):628–636.

Kilteni, K., Maselli, A., Kording, K. P., and Slater, M. (2015). Over my fake body: body ownership illusions for studying the multisensory basis of own-body perception. *Frontiers in Human Neuroscience*, 9(March).

Kilteni, K., Normand, J. M., Sanchez-Vives, M. V., and Slater, M. (2012). Extending body space in immersive virtual reality: A very long arm illusion. *PLoS ONE*, 7(7):e40867.

Klemen, J. and Chambers, C. D. (2012). Current perspectives and methods in studying neural mechanisms of multisensory interactions. *Neuroscience & Biobehavioral Reviews*, 36(1):111–133.

Kokkinara, E., Slater, M., and López-Moliner, J. (2015). The Effects of Visuomotor Calibration to the Perceived Space and Body, Through Embodiment in Immersive Virtual Reality. *ACM Trans. Appl. Percept.*, 13(1):3:1—-3:22.

Kondo, T., Saeki, M., Hayashi, Y., Nakayashiki, K., and Takata, Y. (2015). Effect of instructive visual stimuli on neurofeedback training for motor imagery-based brain-computer interface. *Human Movement Science*, 43:239–249.

Kothe, C., Medine, D., and Grivich, M. (2016). Lab streaming layer.

Lakatos, P., Chen, C.-M., O'Connell, M. N., Mills, A., and Schroeder, C. E. (2007). Neuronal Oscillations and Multisensory Interaction in Primary Auditory Cortex. *Neuron*, 53(2):279–292.

Lederman, S. J. and Jones, L. A. (2011). Tactile and Haptic Illusions. 4(4):273–294.

Lenggenhager, B., Halje, P., and Blanke, O. (2011). Alpha band oscillations correlate with illusory self-location induced by virtual reality. *The European journal of neuroscience*, 33(10):1935–43.

Lenggenhager, B., Tadi, T., Metzinger, T., and Blanke, O. (2007). Video Ergo Sum: Manipulating BodilySelf-Consciousness. *Science (New York, N.Y.)*, 317(5841):1–5.

Lenth, R. V. (2016). Least-Squares Means: The {R} Package {lsmeans}. *Journal of Statistical Software*, 69(1):1–33.

Levitin, D. J. (2000). The perception of cross-modal simultaneity (or "the Greenwich Observatory Problem" revisited). In *AIP Conference Proceedings*, volume 517, pages 323–329. AIP.

Li, W. and Han, S. (2010). Perspective taking modulates event-related potentials to perceived pain. *Neuroscience Letters*, 469(3):328–332.

Libet, B., Gleason, C. A., Wright, E. W., and Pearl, D. K. (1983). Time of conscious intention to act in relation to onset of cerebral activity (readiness-potential). The unconscious initiation of a freely voluntary act. *Brain : a journal of neurology*, 106 (Pt 3):623–642.

Linares, D. and Holcombe, A. O. (2014). Differences in perceptual latency estimated from judgments of temporal order, simultaneity and duration are inconsistent. *i-Perception*, 5(6):559–571.

Longo, M. R., Long, C., and Haggard, P. (2012). Mapping the invisible hand: a body model of a phantom limb. *Psychological science*, 23(7):740–2.

Longo, M. R., Schuur, F., Kammers, M. P. M., Tsakiris, M., and Haggard, P. (2008). What is embodiment? A psychometric approach. *Cognition*, 107(3):978–998.

Luck, S. J. (2014). *An Introduction to the Event-Related Potential Technique, Second Edition*. MIT Press, Cambridge, Massachusetts, 2nd edition.

Macdonald, J. and McGurk, H. (1978). Visual influences on speech perception processes. *Perception {&} Psychophysics*, 24(3):253–257.

Makeig, S. (1993). Auditory event-related dynamics of the EEG spectrum and effects of exposure to tones. *Electroencephalography and clinical neurophysiology*, 86(4):283–293.

Makeig, S., Debener, S., Onton, J., and Delorme, A. (2004). Mining event-related brain dynamics. *Trends in Cognitive Sciences*, 8(5):204–210.

Makin, T. R., Holmes, N. P., and Ehrsson, H. H. (2008). On the other hand: Dummy hands and peripersonal space. *Behavioural Brain Research*, 191(1):1–10.

Maselli, A., Kilteni, K., López-Moliner, J., and Slater, M. (2016). The sense of body ownership relaxes temporal constraints for multisensory integration. *Scientific Reports*, 6:30628.

Maselli, A. and Slater, M. (2013). The building blocks of the full body ownership illusion. *Frontiers in Human Neuroscience*, 7:83.

Maselli, A. and Slater, M. (2014). Sliding perspectives: dissociating ownership from self-location during full body illusions in virtual reality. *Frontiers in Human Neuroscience*, 8:693.

McFarland, D. J., Miner, L. a., Vaughan, T. M., and Wolpaw, J. R. (2000). Mu and beta rhythm topographies during motor imagery and actual movements. *Brain topography*, 12(3):177–186.

Meier, J. D., Aflalo, T. N., Kastner, S., and Graziano, M. S. A. (2008). Complex Organization of Human Primary Motor Cortex: A High-Resolution fMRI Study. *Journal of Neurophysiology*, 100(4):1800–1812.

Meng, J., Hu, L., Shen, L., Yang, Z., Chen, H., Huang, X., and Jackson, T. (2012). Emotional primes modulate the responses to others' pain: an ERP study. *Experimental Brain Research*, 220(3):277–286.

Meng, J., Jackson, T., Chen, H., Hu, L., Yang, Z., Su, Y., and Huang, X. (2013). Pain perception in the self and observation of others: An {ERP} investigation. *NeuroImage*, 72:164–173.

Meredith, M. A., Nemitz, J. W., and Stein, B. E. (1987). Determinants of multisensory integration in superior colliculus neurons. I. Temporal factors. *The Journal of neuroscience : the official journal of the Society for Neuroscience*, 7(10):3215–29.

Meredith, M. A. and Stein, B. E. (1986). Visual, auditory, and somatosensory convergence on cells in superior colliculus results in multisensory integration. *Journal of Neurophysiology*, 56(3):640–662.

Mesulam, M. M. (1998). From sensation to cognition. *Brain*, 121(6):1013–1052.

Millar, S. and Al-Attar, Z. (2002). The Müller-Lyer illusion in touch and vision: Implications for multisensory processes. *Perception {&} Psychophysics*, 64(3):353–365.

Miller, K. J., Hermes, D., Honey, C. J., Hebb, A. O., Ramsey, N. F., Knight, R. T., Ojemann, J. G., and Fetz, E. E. (2012). Human Motor Cortical Activity Is Selectively Phase-Entrained on Underlying Rhythms. *PLoS Comput Biol*, 8(9):1–21.

Miller, L. M. (2005). Perceptual Fusion and Stimulus Coincidence in the Cross-Modal Integration of Speech. *Journal of Neuroscience*, 25(25):5884–5893.

Montant, M., Romaiguère, P., and Roll, J.-P. (2009). A new vibrator to stimulate muscle proprioceptors in fMRI. *Human brain mapping*, 30(3):990–7.

Morgan, M., Hole, G., and Glennerster, A. (1990). Biases and sensitivities in geometrical illusions. *Vision Research*, 30(11):1793–1810.

Muller-Putz, G. R., Breitwieser, C., Cincotti, F., Leeb, R., Schreuder, M., Leotta, F., Tavella, M., Bianchi, L., Kreilinger, A., Ramsay, A., Rohm, M., Sagebaum, M., Tonin, L., Neuper, C., and Millan, J. D. R. (2011). Tools for Brain-Computer Interaction: A General Concept for a Hybrid BCI. *Frontiers in neuroinformatics*, 5:30.

Nagel, S. K., Carl, C., Kringe, T., Märtin, R., and König, P. (2005). Beyond sensory substitution–learning the sixth sense. *Journal of neural engineering*, 2(4):R13–26.

Nam, C. S., Jeon, Y., Kim, Y. J., Lee, I., and Park, K. (2011). Movement imagery-related lateralization of event-related (de)synchronization (ERD/ERS): Motor-imagery duration effects. *Clinical Neurophysiology*, 122(3):567–577.

Newport, R. and Gilpin, H. R. (2011). Multisensory disintegration and the disappearing hand trick. *Current biology : CB*, 21(19):R804–5.

Newport, R. and Jackson, S. R. (2006). Posterior parietal cortex and the dissociable components of prism adaptation. 44:2757–2765.

Newport, R., Pearce, R., and Preston, C. (2010). Fake hands in action: Embodiment and control of supernumerary limbs. *Experimental Brain Research*, 204(3):385–395.

Niazi, I. K., Jiang, N., Tiberghien, O., Nielsen, J. F., Dremstrup, K., and Farina, D. (2011). Detection of movement intention from single-trial movement-related cortical potentials. *Journal of neural engineering*, 8(6):066009.

Nunez, P. L. (1974). The brain wave equation: a model for the EEG. *Mathematical Biosciences*, 21(3):279–297.

Ogawa, S., Lee, T. M., Kay, A. R., and Tank, D. W. (1990). Brain magnetic resonance imaging with contrast dependent on blood oxygenation. *Proceedings of the National Academy of Sciences of the United States of America*, 87(24):9868–9872.

Palluel, E., Aspell, J. E., and Blanke, O. (2011). Leg muscle vibration modulates bodily self-consciousness: integration of proprioceptive, visual, and tactile signals. *Journal of neurophysiology*, 105(5):2239–47.

Pasalar, S., Ro, T., and Beauchamp, M. S. (2010). TMS of posterior parietal cortex disrupts visual tactile multisensory integration. *European Journal of Neuroscience*, 31(10):1783–1790.

Pérez, A. (2011). Influence of the Learnt Direction of Reading on Temporal Order Judgments. *Psychology*, 02(2):103–108.

Perez-Marcos, D., Sanchez-Vives, M. V., and Slater, M. (2012). Is my hand connected to my body? The impact of body continuity and arm alignment on the virtual hand illusion. *Cognitive Neurodynamics*, 6(4):295–305.

Perez-Marcos, D., Slater, M., and Sanchez-Vives, M. V. (2009). Inducing a virtual hand ownership illusion through a brain-computer interface. *Neuroreport*, 20(6):589–594.

Petkova, V. I. (2011). *Do I need a body to know who I am? Neural mechanisms of body ownership*. PhD thesis, Karolinska Institutet.

Petkova, V. I. and Ehrsson, H. H. (2008). If I were you: Perceptual illusion of body swapping. *PLoS ONE*, 3(12):e3832.

Petkova, V. I., Zetterberg, H., and Ehrsson, H. H. (2012). Rubber hands feel touch, but not in blind individuals. *PLoS ONE*, 7(4):e35912.

Petrini, K., Russell, M., and Pollick, F. (2009). When knowing can replace seeing in audiovisual integration of actions. *Cognition*, 110(3):432–439.

Pfurtscheller, G. (1977). Graphical display and statistical evaluation of event-related desynchronization (ERD). *Electroencephalography and clinical neurophysiology*, 43(5):757–760.

Pfurtscheller, G. and Lopes da Silva, F. H. (1999). Event-related EEG/MEG synchronization and desynchronization: basic principles. *Clinical neurophysiology : official journal of the International Federation of Clinical Neurophysiology*, 110(11):1842–57.

Pfurtscheller, G. and Neuper, C. (2001). Motor imagery and direct brain-computer communication. *Proceedings of the IEEE*, 89(7):1123–1134.

Pinheiro, J., Bates, D., DebRoy, S., Sarkar, D., and R Core Team (2017). *{nlme}: Linear and Nonlinear Mixed Effects Models*.

Press, C., Heyes, C., Haggard, P., and Eimer, M. (2008). Visuotactile Learning and Body Representation: An ERP Study with Rubber Hands and Rubber Objects. *Journal of Cognitive Neuroscience*, 20(2):312–323.

Rigoni, D., Brass, M., Roger, C., Vidal, F., and Sartori, G. (2013). Top-down modulation of brain activity underlying intentional action and its relationship with awareness of intention: an ERP/Laplacian analysis. *Experimental brain research. Experimentelle Hirnforschung. Experimentation cerebrale*, (2008).

Rohde, M., Di Luca, M., and Ernst, M. O. (2011). The Rubber Hand Illusion: Feeling of Ownership and Proprioceptive Drift Do Not Go Hand in Hand. *PLoS ONE*, 6(6):e21659.

Roll, J.-P., Albert, F., Thyrion, C., Ribot-Ciscar, E., Bergenheim, M., and Mattei, B. (2009). Inducing any virtual two-dimensional movement in humans by applying muscle tendon vibration. *Journal of neurophysiology*, 101(2):816–23.

Romano, D., Pfeiffer, C., Maravita, A., and Blanke, O. (2014). Illusory self-identification with an avatar reduces arousal responses to painful stimuli. *Behavioural brain research*, 261:275–81.

Romanski, L. M. (2007). Representation and Integration of Auditory and Visual Stimuli in the Primate Ventral Lateral Prefrontal Cortex.

Romanski, L. M., Bates, J. F., and Goldman-Rakic, P. S. (1999). Auditory belt and parabelt projections to the prefrontal cortex in the Rhesus monkey. *The Journal of Comparative Neurology*, 403(2):141–157.

Romo, R. and De Lafuente, V. (2013). Conversion of sensory signals into perceptual decisions. *Progress in Neurobiology*, 103:41–75.

RUTSCHMANN, J. and LINK, R. (1964). PERCEPTION OF TEMPORAL ORDER OF STIMULI DIFFERING IN SENSE MODE AND SIMPLE REACTION TIME. *Perceptual and motor skills*, 18:345–352.

Sanchez-Vives, M. V., Spanlang, B., Frisoli, A., Bergamasco, M., and Slater, M. (2010). Virtual hand illusion induced by visuomotor correlations. *PLoS ONE*, 5(4):e10381.

Schutz, M. and Kubovy, M. (2007). Causality and audio-visual integration. *Journal of Experimental Psychology: Human Perception and Performance*, 123:3412.

Schutz, M. and Lipscomb, S. (2007). Hearing gestures, seeing music: vision influences perceived tone duration. *Perception*, 36(6):888–897.

Seibold, V. C., Fiedler, A., and Rolke, B. (2011). Temporal attention shortens perceptual latency: A temporal prior entry effect. *Psychophysiology*, 48:708–717.

Seizova-Cajic, T., Smith, J. L., Taylor, J. L., and Gandevia, S. C. (2007). Proprioceptive movement illusions due to prolonged stimulation: reversals and aftereffects. *PloS one*, 2(10):e1037.

Senkowski, D., Schneider, T. R., Foxe, J. J., and Engel, A. K. (2008). Crossmodal binding through neural coherence: implications for multisensory processing. *Trends in neurosciences*, 31(8):401–409.

Senna, I., Maravita, A., Bolognini, N., and Parise, C. V. (2014). The Marble-Hand Illusion. *PloS one*, 9(3):e91688.

Seth, A. K. (2013). Interoceptive inference, emotion, and the embodied self. *Trends in cognitive sciences*, 17(11):565–73.

Sharott, A. (2013). *Local Field Potential, Methods of Recording*, pages 1–3. Springer New York, New York, NY.

Shibata, E. and Kaneko, F. (2013). Kinesthetic perception based on integration of motor imagery and afferent inputs from antagonistic muscles with tendon vibration. *Neuroscience letters*, 541:24–8.

Shimada, S., Fukuda, K., and Hiraki, K. (2009). Rubber Hand Illusion under Delayed Visual Feedback. *PLoS ONE*, 4(7):e6185.

Shimada, S., Hiraki, K., and Oda, I. (2005). The parietal role in the sense of self-ownership with temporal discrepancy between visual and proprioceptive feedbacks. *NeuroImage*, 24(4):1225–32.

Siegel, M., Donner, T. H., and Engel, A. K. (2012). Spectral fingerprints of large-scale neuronal interactions. *Nature Reviews Neuroscience*, 13(February):20–25.

Slater, M. and Garau, M. (2007). The Use of Questionnaire Data in Presence Studies: Do Not Seriously Likert. *Presence: Teleoperators and Virtual Environments*, 16(4):447–456.

Slater, M., Perez-Marcos, D., Ehrsson, H. H., and Sanchez-Vives, M. V. (2008). Towards a digital body: the virtual arm illusion. *Frontiers in human neuroscience*, 2(August):6.

Slater, M., Perez-Marcos, D., Ehrsson, H. H., and Sanchez-Vives, M. V. (2009). Inducing illusory ownership of a virtual body. *Frontiers in neuroscience*, 3(2):214–220.

Slater, M., Spanlang, B., Sanchez-Vives, M. V., and Blanke, O. (2010). First person experience of body transfer in virtual reality. *PLoS ONE*, 5(5):e10564.

Spence, C., Nicholls, M. E., and Driver, J. (2001a). The cost of expecting events in the wrong sensory modality. *Perception & psychophysics*, 63(2):330–336.

Spence, C. and Parise, C. (2010). Prior-entry: A review. *Consciousness and Cognition*, 19(1):364–379.

Spence, C., Shore, D. I., and Klein, R. M. (2001b). Multisensory prior entry. *Journal of experimental psychology. General*, 130(4):799–832.

Stein, B. E. and Stanford, T. R. (2008). Multisensory integration: current issues from the perspective of the single neuron. *Nature reviews. Neuroscience*, 9(4):255–266.

Stekelenburg, J. J. and Vroomen, J. (2007). Neural correlates of multisensory integration of ecologically valid audiovisual events. *Journal of cognitive neuroscience*, 19(12):1964–1973.

Stevenson, R. a., Ghose, D., Fister, J. K., Sarko, D. K., Altieri, N. a., Nidiffer, A. R., Kurela, L. R., Siemann, J. K., James, T. W., and Wallace, M. T. (2014). Identifying and Quantifying Multisensory Integration: A Tutorial Review. *Brain Topography*, 27(6):707–730.

Sugihara, T., Diltz, M. D., Averbeck, B. B., and Romanski, L. M. (2006). Integration of Auditory and Visual Communication Information in the Primate Ventrolateral Prefrontal Cortex.

Sutton, S., Braren, M., Zubin, J., and John, E. R. (1965). Evoked-Potential Correlates of Stimulus Uncertainty. *Science*, 150(3700):1187–1188.

Tamè, L., Johnstone, T., and Holmes, N. P. (2012). Inter-hemispheric interaction of touches at the fingers: A combined psychophysics and TMS approach. *Seeing and Perceiving*, 25(0):163.

Thyrion, C. and Roll, J.-P. (2009). Perceptual integration of illusory and imagined kinesthetic images. *The Journal of neuroscience : the official journal of the Society for Neuroscience*, 29(26):8483–92.

Thyrion, C. and Roll, J.-P. (2010). Predicting any arm movement feedback to induce three-dimensional illusory movements in humans. *Journal of neurophysiology*, 104(2):949–59.

Tsakiris, M. (2011). The Sense of Body Ownership. In Gallagher, S., editor, *The Oxford Handbook of the Self*, number December.

Tsakiris, M., Hesse, M. D., Boy, C., Haggard, P., and Fink, G. R. (2007). Neural Signatures of Body Ownership: A Sensory Network for Bodily Self-Consciousness. *Cerebral Cortex*, 17(10):2235–2244.

Tsakiris, M., Longo, M. R., and Haggard, P. (2010). Having a body versus moving your body: Neural signatures of agency and body-ownership. *Neuropsychologia*, 48(9):2740–2749.

Tsuji, T., Yamakawa, H., Yamashita, A., Takakusaki, K., Maeda, T., Kato, M., Oka, H., and Asama, H. (2013). Analysis of electromyography and skin conductance response during rubber hand illusion. *2013 IEEE Workshop on Advanced Robotics and its Social Impacts*, pages 88–93.

Uffmann, K., Grote, W., Abicht, C., Quick, H. H., and Ladd, M. E. (2002). A Piezoelectric Actuator for MR Elastography. In *International Society for Magnetic Resonance in Medicine*, volume 10, pages 359–362, Honolulu.

Valdes-Sosa, P. a., Roebroeck, A., Daunizeau, J., and Friston, K. (2011). Effective connectivity: influence, causality and biophysical modeling. *NeuroImage*, 58(2):339–61.

van Eijk, R. L. J., Kohlrausch, A., Juola, J. F., and van de Par, S. (2008). Audiovisual synchrony and temporal order judgments: effects of experimental method and stimulus type. *Perception & psychophysics*, 70(6):955–968.

Vatakis, A. and Spence, C. (2008). Evaluating the influence of the 'unity assumption' on the temporal perception of realistic audiovisual stimuli. *Acta Psychologica*, 127(1):12–23.

Vesia, M. and Davare, M. (2011). Decoding action intentions in parietofrontal circuits. *The Journal of neuroscience : the official journal of the Society for Neuroscience*, 31(46):16491–3.

Vroomen, J., Keetels, M., de Gelder, B., and Bertelson, P. (2004). Recalibration of temporal order perception by exposure to audio-visual asynchrony. *Cognitive Brain Research*, 22(1):32–35.

Wairagkar, M., Zoulias, I., Oguntosin, V., Hayashi, Y., and Nasuto, S. (2016). Movement intention based Brain Computer Interface for Virtual Reality and Soft Robotics rehabilitation using novel autocorrelation analysis of EEG. In *2016 6th IEEE International Conference on Biomedical Robotics and Biomechatronics (BioRob)*, page 685.

Wallace, M. T. (2004). The development of multisensory processes. *Cognitive Processing*, 5(2):69–83.

Wallace, M. T. and Stein, B. E. (1997). Development of multisensory neurons and multisensory integration in cat superior colliculus. *The Journal of neuroscience : the official journal*

of the Society for Neuroscience, 17(7):2429–2444.

Weeks, S. R., Anderson-Barnes, V. C., and Tsao, J. W. (2010). Phantom limb pain: theories and therapies. *The neurologist*, 16(5):277–86.

Williams, J. J., Rouse, A. G., Thongpang, S., Williams, J. C., and Moran, D. W. (2013). Differentiating closed-loop cortical intention from rest: building an asynchronous electrocorticographic BCI. *Journal of neural engineering*, 10(4):046001.

Yu, N., Hollnagel, C., Blickenstorfer, A., Kollias, S., and Riener, R. (2009). fMRI-Compatible Robotic Interfaces with Fluidic Actuation. In Oliver, B., Jeff, T., and Ramos, F., editors, *Robotics: Science and Systems*, pages 199–205, Zurich. The MIT Press.

Yu, N., Murr, W., Blickenstorfer, A., Kollias, S., and Riener, R. (2007). An fMRI compatible haptic interface with pneumatic actuation. 00(c).

Zeller, D., Friston, K. J., and Classen, J. (2016). Dynamic causal modeling of touch-evoked potentials in the rubber hand illusion. *NeuroImage*, 138:266–273.

Zeller, D., Litvak, V., Friston, K. J., and Classen, J. (2014). Sensory Processing and the Rubber Hand Illusion - An Evoked Potentials Study. *Journal of Cognitive Neuroscience*, 27(3):573–582.

Zoulias, I., Wairagkar, M., and Oguntosin, V. (2016a). Hybrid neuro-rehabilitation system using Brain Computer Interface, Virtual Reality and Soft Robotics. In *Eurohaptics 2016*.

Zoulias, I. D., Harwin, W. S., Hayashi, Y., and Nasuto, S. J. (2016b). *Milliseconds Matter: Temporal Order of Visuo-tactile Stimulation Affects the Ownership of a Virtual Hand*, pages 479–489. Springer International Publishing, London.

Zoulias, I. D., Hayashi, Y., Harwin, W. S., and Nasuto, S. J. (2015). Visual Stimulation by the Oculus Rift ® HMD to detect stronger motion imagery ERD. In *7th International IEEE/EMBS Conference on Neural Engineering*, Montpellier.